9-2011

Autoimmune Responses to Atherosclerotic Lipids: A Study in Murine Models of Atherosclerosis and Obesity

hanjing wu

12-2011

AUTOIMMUNE RESPONSES TO ATHEROSCLEROTIC

hanjing wu

AUTOIMMUNE RESPONSES TO ATHEROSCLEROTIC LIPIDS: A STUDY IN MURINE MODELS OF ATHEROSCEROSIS AND OBESITY

by

Hanjing Wu, Bachelor of Medicine, Master of Medicine

APPROVED:

_____
Supervisory Professor: Yong-Jian Geng (M.D., Ph.D.)

_____
Marie-Francoise Doursout. Ph.D.

_____
Yangxin Li, Ph.D.

_____
Sudhir Paul, Ph.D.

_____
Michael Wassler, Ph.D.

APPROVED:

_____
Dean, The University of Texas
Graduate School of Biomedical Science at Houston

AUTOIMMUNE RESPONSES TO ATHEROSCLEROTIC LIPIDS: A STUDY IN MURINE MODELS OF ATHEROSCEROSIS AND OBESITY

A

DISSERTATION

Presented to the Faculty of

The University of Texas

Health Science Center at Houston

and

The University of Texas

M.D. Anderson Cancer Center

Graduate School of Biomedical Science

In Partial Fulfillment

of the Requirments

for the Degree of

Doctor of Philosophy

By

Hanjing Wu, M.B., M.Med

Houston, Texas

September 2011

Acknowledgements

[redacted]

[redacted]

Autoimmune Responses to Atherosclerotic Lipids: A Study in Murine Models of Atherosclerosis and Obesity

Publication No._____

Hanjing Wu, M.B, M.Med
Supervisory Professor: Yong-Jian Geng, M.D., Ph.D.

Atherosclerosis is a chronic, complex arterial disease characterized by intimal lipid accumulation and inflammation. A unique lipid-binding molecule, namely cluster of differentiation 1d (CD1d), may impact atherosclerosis. Structurally, CD1d acts as a nonpolymorphic cell-surface receptor, resembling the major histocompatibility complex-I (MHC-I). While MHC-I restricts peptide antigen presentation to T cells, CD1d presents lipid antigens to T cells named CD1d-restrictedd T cells. Although increased expression of CD1d has been found in human plaques, the exact nature of CD1d-recognized lipids in atherosclerosis remains to be determined. Three groups of lipids may undergo oxidation in atherosclerosis producing atherogenic lipids: phospholipids, fatty acids, and cholesterol. The central hypothesis is that CD1d recognizes and present oxidative lipids to activate CD1d-restricted T cells, and trigger proinflammatory signal transduction

In the first part of this study, oxidative phospholipids were identified and characterized as potential autoantigen for CD1d-restricted T cells. Derived from phospholipid 1-palmitoyl-2-arachidonoyl-sn-glycero-3-phosphorylcholine by oxidization, 1-palmitoyl-2-glutaryl-sn-glycero-3-phosphocholine (PGPC) is

commonly found in atherosclerotic plaques. Upon stimulation with PGPC, spleen-derived CD1d-restricted T cells produced higher levels of cytokines and proliferated at higher rates than those without PGPC stimulation. CD1d deficiency compromised the PGPC-triggered T cell activation, suggesting that PGPC may function as a potentially novel autoantigen for T cells in atherosclerosis.

In the second part of this study, CD1d-mediated proinflammatory signaling was evaluated in murine models. Enhanced CD1 expression occurred in spleens of db/db mice with hyperlipidemia. Tumor necrosis factor-alpha (TNF-α) was increased in db/db spleen, while TNF-α receptor expression augmented in the db/db murine heart, in comparison with those in normal mice. The nuclear factor-κ B (NF-κB) expression was enhanced in the db/db heart, whereas CD1d-null mice showed lower NF-κB, implying the involvement of CD1d in inflammation of the spleen and heart tissues in the mice with hyperlipidemia.

The current study has identified PGPC as a novel lipid antigen recognized by CD1d-restricted T cells in atherosclerosis. The animal study has also provided evidence that CD1d regulates NF-κB-mediated proinflammatory signaling. Hence, CD1d-restricted T cell responses to autolipid antigen and mediated inflammatory signal may represent a new molecular pathway that triggers cardiovascular tissue injury in atherosclerosis and hyperlipidemia.

Table of Contents

List of Figures xii

List of Tables xv

Abbreviations and Terms used xvi

Chapter 1: Background 1

1. Inflammation in atherosclerosis **1**

2. Cluster of Differentiation 1 (CD1) family **4**

2.1 Architecture and groups of CD1 proteins 4

2.2 Characteristics of CD1 binding groove and CD1 family ligands 6

2.3 Tissue distribution of CD1 and expression in disease 8

3. CD1-restricted T cells 9

3.1 Group 1 versus Group 2 CD1-restricted T cells 9

3.2 Subgroups of CD1d-restricted T cells 10

3.3 Activation of CD1d-restricted T cells by microbial or self lipid antigens 10

4. Oxidized Phospholipids 13

4.1 Origin and structure of oxidized phospholipids 13

4.2 Receptors for OxPLs 13

4.3 OxPLs and atherosclerosis 16

Chapter 2: Hypothesis and Specific Aims 19

1. Autoantigens and atherosclerosis 19

2. CD1 and atheroslcerosis 21

3. CD1-restricted T cells related inflammation in atherosclerosis **22**

4. Inflammation in atherosclerosis with obesity and hyperlipidemia **23**

Hypothesis **26**

Specific Aims **26**

Chapter 3: Methods and Materials **28**

1. Hypothetic prediction of lipid-CD1d interaction by computer stimulation **28**

2. Gas-chromatography (GC) /mass-spectrometry (MS) of lipids **28**

3. Cell lines and culture **28**

3.1 Culture of mCD1-HEK293 cells and HeLa cells 29

3.2 Culture of MOLT-4 cells 31

3.3 Culture of DN32.D3 cells 31

3.4 Culture of Peripheral Blood Mononuclear Cells (PBMC) 31

3.5 Isolation and culture of mouse spleen cells 32

4. cDNA cloning and transfection 33

4.1 Generation of hCD1d cDNA 33

4.2 cDNA subcloning and plasmid construction 34

4.3 Plasmid transfection and stable cell line establshment 38

5. Analysis of cell proliferation **38**

5.1 Thymidine incorporation into DNA 38

5.2 Proliferation assay of splenocytes 39

6. Lipids binding assays **40**

6.1 Lipid preparation and storage 40

6.2 Lipid binding assay 40

7. Fluorescent detection of lipid loaded cells **41**

8. Measurement of cytokine production **42**

9. Induction and detection of CD1d expression in PBMCs **43**

10. Flow cytometry **44**

10.1 Intracellular IFN-γ immunostaining 44

10.2 Flow cytometric staining 44

10.3 CD1d expression detection by flow cytometry 47

11. Reverse-transcription polymerase chain reaction

(RT-PCR) for detection of T-cell receptor (TCR) mRNA **47**

11.1 T-cell repertoire analysis 47

11.2 RT-PCR for detection of TCR mRNA 47

12. Murine models for atherosclerosis and obesity **48**

12.1 Apolipoproetin-E-deficient (ApoE -/-) Mice 48

12.2 db/db Mice 48

12.3 Blood lipid and glucose analysis 49

12.4 Tissue preparation and histochemistry 50

12.5 RNA isolation and RT-PCR analysis 51

12.6 Electrophoretic Mobility Shift Assays (EMSA) 52

12.7 Immunoblotting of p65 NF-κB subunits 52

13. Statistical Analysis **53**

Chapter 4: Results 54

1. Prediction of lipid ligands for CD1d by computer stimulation **54**

2. Detection of lipids by GS/MS in murine plasma **60**

3. Biology analysis of potential lipid ligands to CD1d by lipid binding assay **62**

4. CD1d-mediated lipid accumulation in spleen derived macrophages and human CD1d transfected Hela cells (hCD1d-Hela) incubated with PGPC **64**

5. PGPC as potential ligand for CD1d stimulating CD1d-restricted T cells **70**

5.1 Stimulation of mCD1d-restricted T cells by PGPC 70

5.2 Induction of CD1d expression in natural CD1d+ antigen presenting cells 72

6. CD1d-mediated splenocytes responses to oxidized phospholipids **74**

7. Detection of cell type producing IFN-γ stimulated with PGPC **81**

8. Presence of PGPC reacting CD1-restricted T cells in ApoE-/- mice and WT mice **84**

9. Analysis of TCR repertoire **86**

10. Development of hyperlipidemia and hyperglycemia in db/db mice **88**

11. Different expression of CD1d between db/db and C57BL6 spleen cells **90**

12. Increased TNFα expression in db/db spleen cells and

TNFα receptor1 in cardiac cells **94**

13. Lipid accumulation and NF-kB activity in hearts of db/db mice **97**

Chapter 5: Discussion **104**

1. Identification of ligands for CD1d in atherosclerosis **104**

2. CD1d mediated immune reactions in atherosclerosis **109**

3. CD1d expression and impact on heart injured by hyperlipdemia **114**

3.1 CD1d-mediated NF-κB signaling 114

3.2 CD1d induced inflammation in atherosclerosis and NF-κB activation 115

Reference 118

Vita 135

List of Figures

Figure 1. Schematic representation of oxidized lipid-activated T lymphocyte immune responses in atherosclerosis 2

Figure 2. Diagram of CD1d-lipid complex on antigen-presenting cell (APC) 5

Figure 3. Localization of CD1 genes in human and mouse chromosome 7

Figure 4. Activation of CD1d-restricted T cells by foreign or self lipid antigens 12

Figure 5. Chemical structures of oxidized phospholipids formed during oxidation of PAPC 15

Figure 6. Activation of NF-κB by the TNF-α pathway 25

Figure 7. Chemical structures of lipids commonly found in atherosclerotic lesions 30

Figure 8. Construction of CD1d-pEGFP-N3 plasmid 36

Figure 9. Verification of CD1d cDNA sequence in hCD1d-pEGFP- N3 plasmid 37

Figure 10. CD1d tetramer preparation 46

Figure 11. Predicted CD1d capacity binding to three groups of lipids by running SYBYL program 55

Figure 12. Prediction of interaction between CD1d and lipid 58

Figure 13. Presence of PGPC, PAPC, 7K and Chol in the plasma of balb/c mice 61

Figure 14. ^{3}H-7-K-Cho binding to CD1d in the presence or absence of PGPC and free cholesterol 63

Figure 15. Expression of hCD1d-GFP fusion protein in Hela cells transfected with hCD1d-GFPN3 66

Figure 16. Nile red fluorescence in CD1+/+ mouse splenocytes and hCD1d-Hela cells incubated with or without PGPC 68

Figure 17. **C**omparison of lipid activation between 293 and mCD1-293 71

Figure 18. Western- Blotting assay for CD1d and GAPDH in lipid treated PBMCs 73

Figure 19. Comparison of lipid activation between CD1-/- balb/c and balb/c splenic cells by 3H thymidine uptake 75

Figure 20. The response of PGPC was CD1d mediated 78

Figure 21. Responder T cells in lipid treated balb/c spleen cells 83

Figure 22. Flow cytometry of CD1d-tetramers loaded with PGPC stained CD3+T cells 85

Figure 23. RT-PCR analysis of TCR repertoire in ApoE-/- and WT C57BL/6 mice 87

Figure 24. Comparsion of CD1 expression in db/db and WT mice spleen 91

Figure 25. Expression of TNFαin db/db and WT spleen,

TNFαR1 in db/db and WT heart 95

Figure 26. Lipid accumulation in hearts of db/db 98

Figure 27. NF-κB activity in hearts of db/db mice 101

List of Tables

Table 1. Assessment of CD1d binding to three groups of lipids by computer molecular stimulation 56

Table 2. Key binding sites between CD1d and lipids 59

Table 3. Lipid profiles and glucose levels in serum of db/db C57BL/6J and C57BL/6J mice 89

Abbreviations

ApoE-/- ---- Apolipoprotein E -/-

APCs---- antigen presenting cells

ATCC---- American Type Culture Collection

α-GC----α-galactosylceramide

BW----body weight

β2M----β2-microglobulin

CD1----cluster of differentiation 1

CD4---- cluster differentiation 4

CD8---- cluster differentiation 8

CD36---- cluster of differentiation 36

CHD---- coronary heart disease

cDNA---- complementary DNA

DMEM---- Dulbecco's Modified Eagle's Medium

DCs---- dendritic cells

ECs---- endothelial cells

FBS---- fetal bovine serum

GPCRs---- G-protein-coupled receptors

HSP---- heat shock protein

HDL---- high density lipoprotein

^{3}H-7-K-Cho----^{3}H-7-K-Cholesterol

HAEC---- human aortic endothelial cells

HexPC---- hexadecyl Arachidonyl PC

hCD1d---- human CD1d

HW----heart weight

IL-2---- interleukin-2

IL-4---- interleukin-4

IL-6---- interleukin-6

IL-8---- interleukin-8

IL-10---- interleukin-10

IkB---- inhibitor of kappa B

IFN-γ---- interferon-γ

IKK---- inhibitor of kappa B kinase

iNKT---- invariant natural killer T

IFN-γ---- interferon-gamma

ICAM-1---- inter- cellular adhesion molecule 1

LDL---- low-density lipoproteins

mRNA---- messenger RNA

MHC----major histocompatibility complex

MIP-1α---- macrophage inflammatory protein-1 alpha

MIP-1β---- macrophage inflammatory protein-1 beta

MM-LDL---- minimally modified low density lipoprotein

mCD1-HEK293---- mouse CD1 transfected HEK293

NaOH---- sodium hydroxide

NF-kB---- nuclear factor-kappa B

NKT---- natural killer T

OxPAPC---- oxidized PAPC

OxPLs ----oxidized phospholipids

OxLDL---- oxidized low density lipoprotein

OCT---- optimal-cutting-temperature

PC---- phosphatidylcholine

PAPC----1-palmitoyl-2-arachidonoyl-sn-glycero-3-phosphrylcholine

POVPC----1-palmitoyl-2-(5-oxovaleroyl)-sn-glycero-3-phosphatidylcholine

PGPC----1-palmitoyl-2-glutaroyl-sn-glycero-3-phosphatidylcholine

PEIPC----1-palmitoyl-2-(5,6-epoxyisoprostane E2)-sn-glycero-3-phosphatidylcholine

PPARs---- peroxisome proliferator-activated receptors

POVPC----1-palmitoyl-2-(5-oxovaleroyl)-sn-glycero-phosphocholine

PDB---- protein databank

PBMCs---- Peripheral Blood Mononuclear Cells

PE---- phycoerythrin

PGPC----1-palmitoyl-2-glutaryl-*sn*-glycero-3-phosphocholine

PCR---- Polymerase Chain Reaction amplification

PTY---- phosphatidylethanolamine

PC---- protein C

PBS---- phosphate-buffered saline

qRT-PCR---- quantitative real time polymerase chain reaction amplification

SDS---- sodium dodecyl sulfate

SPNA1---- spectrin alpha 1; spherocytosis

SPTA1---- spectrin alpha erythrocytic 1

SMCs---- smooth muscle cells

TNF-α---- tumor necrosis factor alpha

TLRs---- Toll-like-receptors

TCA---- trichloroacetic acid

TCR---- T cell receptor

VLDLs---- very low-density lipoproteins

VCAM-1---- vascular cell adhesion molecule 1

Chapter 1: Background

1. Inflammation in atherosclerosis

Atherosclerosis is characterized by inflammation that occurred mainly in large- or medium-sized arteries. The initial phase is monocytes/macrophages activation, which is followed by effector T cells activation in response to antigens presented by antigen presenting cells (APCs). As the consequence of T cells activation, elevated levels of cytokines, as well as other pro-inflammatory mediators are detected (Figure 1). In innate way monocytes/macrophages are recruited to the injured site by some molecules, like P-selectin expressed endothelial cells. Macrophages can also take up lipid antigens and form foam cells. Therefore, high lipid level is a marked risk factor for developing atherosclerosis. Apolipoprotein E -/- (ApoE-/-) mouse model is deficient of ApoE, which is important for transport and metabolism of lipids. In ApoE-/- mouse model plasma cholesterol level is markedly elevated and an early and severe atherosclerotic lesions can be observed.

Antigen presentation occurs in atherosclerotic lesions and trigger T cells responses. In atherosclerotic plaques, macrophages, dendritic cells and T cells can all be detected. Pevious studies have been focused on antigens that drive in this process. Low-density lipoproteins (LDL) can be modified into oxidized low density lipoprotein (OxLDL). OxLDL is an important self-antigen as phospholipids released from LDL can activate endothelial cells to express adhesion molecule (1). OxLDL –specific T cells have been detected in atherosclerotic plaque (2) and the transfer of

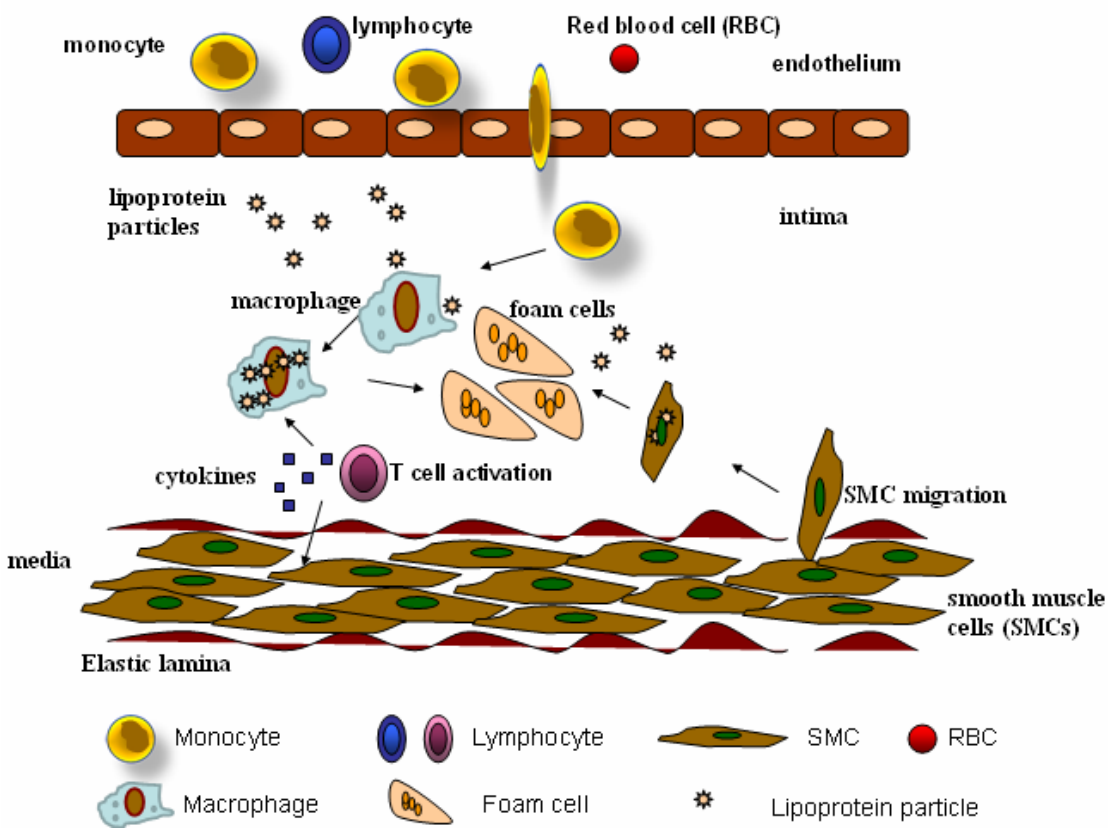

Figure 1. Schematic representation of oxidized lipid-activated T lymphocyte immune responses in atherosclerosis. Monocytes adhere to endothelial cell expressing adhesion molecules when stimulated by OxLDL. Then monocytes migrate into the intima and differentiate into macrophages, which take up lipoproteins and form foam cells. Activated T cells secrete cytokines, which promote uptaking of lipids by macrophages, also cause smooth muscle cells in the media to migrate to the atherosclerotic lesion and proliferate.

this group of T cells exacerbates atherosclerosis (3). It has been also found that antibody titers to OxLDL and oxidized phospholipid (OxPL) are increased in atherosclerosis patients (4). It further proved the importance of oxPL in the development of atherosclerosis. Another antigen is heat shock protein (HSP) 65 that can activate auto-reactive T cells and aggravate fatty streak formation (5). Autoantibodies against beta2-glycoprotein I are also detected in atherosclerosis patients (6).

As the responder to antigens presented by APCs, T cells regulate the magnitude of atherosclerosis. In atherosclerotic plaques cluster differentiation 4 (CD4)+ cells are more abundant than cluster differentiation 8 (CD8)+ cells and these T cells are mainly found in shoulder area. CD4+ T cells are considered as proatherogenic and displayed activated/memory phenotype (7). ApoE-/- mice reconstituted with CD4+ T cells develop accelerated atherogenesis (8). Although less abundant than CD4+ cells, CD8+ cells also accelerate atherosclerosis development. Recent data also showed natural kill T (NKT) cells can recognize lipids presented by cluster differentiation 1(CD1) molecules and may contribute to the development of atherosclerosis. Cytokines secreted by activated T cells influence the progression of atherosclerosis. Interferon-γ (IFN-γ) is a major proatherogenic Th1 cytokines by activating monocytes/macrophages and dendritic cells (DCs). IFN-γ can also inhibit vascular smooth muscle cells (SMCs) and cause thinning and destabilization of fibrous cap of atherosclerotic plaque. Not only Th1 cells produce IFN-γ, CD8+ T cells and NKT cells are also sources of IFN-γ. Presently, the role of Th2 cytokines is poorly

understood.

2. CD1 family

2.1 Architecture and groups of CD1 proteins

About a decade ago，it was recognized that lipid antigens can be presented by CD1 and can function as T cell antigens, which nourished the traditional concept of antigen presentation by major histocompatibility complex (MHC). Because of its recent discovery, CD1 remains unknown by immunologists and taken for granted to compare to MHC based on their similar structures.

In contrast to MHC, which presents diverse peptides, CD1 is a family of nonpolymorphic cell-surface receptors that presents a growing number of identified lipids. However, they share a very similar structure consisting of heavy α chain and a non-covalently, stably linked β2-microglobulin (β2M) (Figure 2). The heavy chain is organized into three parts, α1, α2, α3, in which α1 and α2 mainly shapes the hydrophobic lipid binding pocket. It results in lipid buried and exposing other parts like antigen peptides as T cell binding and activating sites. Furthermore, α3 domain is associated with β2M and is highly conservative in CD1 family. Whole α chain is anchored in the cell membrane by transmembrane domain. Depending on the lipids presented by CD1 to T cells, the responder T cells can initiate adaptive immunity in microbe defense, or various immune reactions in tumor and autoimmune diseases.

There are three classified groups in CD1 antigen-presenting molecules based on their structures and functions: CD1a-c represents group 1, CD1d represents group

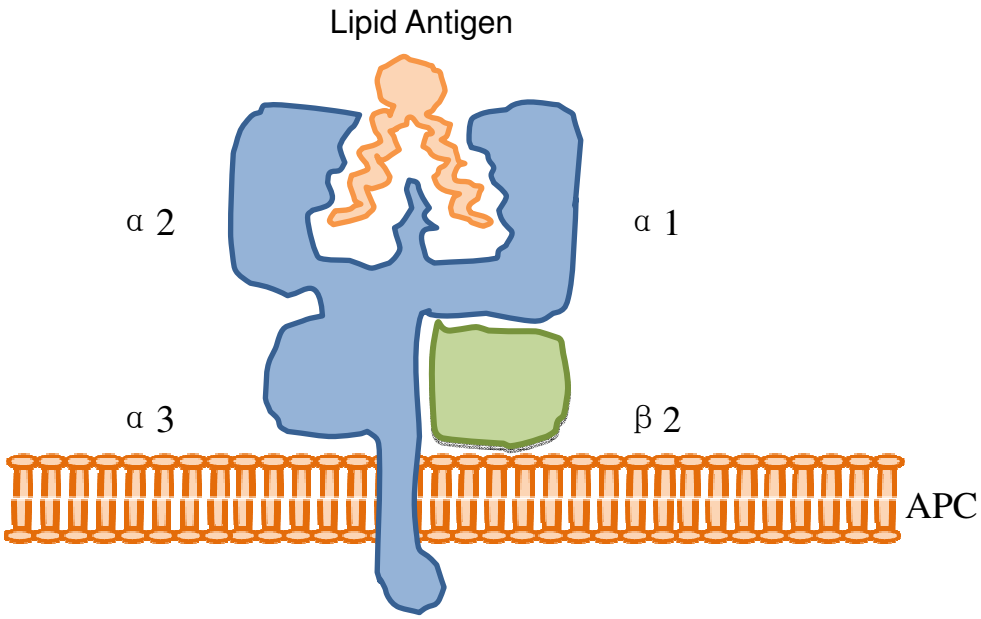

Figure 2. Diagram of CD1d-lipid complex on APC. Lipid antigen binds to the hydrophobic binding pocket shaped by α 1 and α 2 and other exposed parts like peptides are T cell binding and activating parts. α 3 domain is associated with β 2-microglobulin and is highly conservative. These three parts: α 1, α 2, α 3 are organized into a heavy α chain. The whole α chain is anchored in the APC cell membrane by transmembrane domain.

2 (9), while CD1e constitutes the third group (10). CD1e has been found participating in lipid precession and loading instead of lipid presentation. To date, group 1 is found in all mammalian animals including human, rabbit (11-13).Whereas, only CD1d is expressed in mice and rat (Figure 3).

2.2 Characteristics of CD1 binding groove and CD1 family ligands

Due to a closer and elevated sitting of α1 and α2, the central binding groove of CD1 is deeper and narrower compared to MHC peptide binding groove (14). Two anti-parallel α-helices, α1 and α2 sit on the top of a six-stranded β–sheet platform, while different amino acids located in α1-α2 domain form specific CD1 isotype individual binding grooves. In the CD1 family, CD1a has the smallest binding groove, and CD1b has the largest and strikingly different one. No crystal structures of CD1c and CD1e have been described to date. However, more progress has been achieved in the CD1d field.

As for CD1a, there are two groups of ligands identified. One is sulfatide demonstrated by the carbohydrate headgroup being the major epitope in activating T cell receptor (TCR) of CD1a-restricted T cells (15). The other group is didehydroxymycobactin lipopeptides (16). The ligands are considered to maneuver into CD1a binding grooves based on the little changes of CD1a structures in CD1a-ligand complex. With the largest binding groove in the CD1 family，CD1b is supposed to bind larger antigens. It has been proved that mycolate derived from mycobacteria and phosphatidylinositol and GM_2 ganlioside (17) can be complexed with CD1b. Few ligands have been identified with CD1c and CD1e due to the lack of

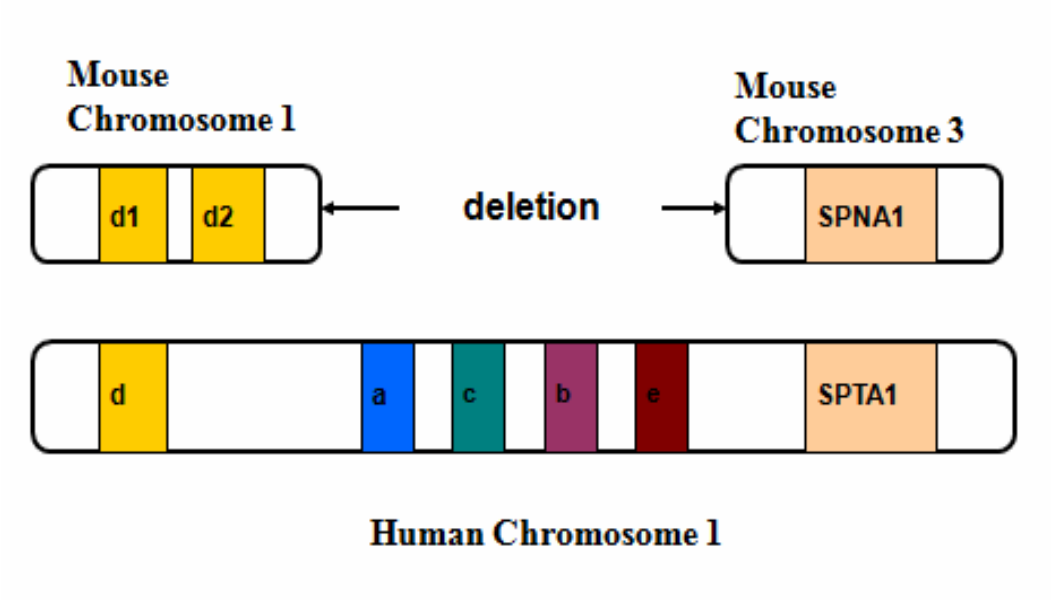

Figure 3. Localization of CD1 genes in human and mouse chromosome. CD1a-e is fully expressed on human chromosome 1. In mouse, only CD1d is expressed and located on chromosome1. There are two isoforms of mCD1d: CD1d1 and CD1d2. SPNA1, spectrin alpha 1; spherocytosis. SPTA1, spectrin alpha erythrocytic 1

determinations of crystal structures.

When it comes to CD1d, the classical ligand α-galactosylceramide (α-GC) has been proved to bind with both mouse and human CD1d (18). However, α-GC is derived from marine sponge and is not a natural ligand for CD1d. In a recent study phosphatidylcholine (PC) was identified as an endogenous ligand for CD1d (19). Following this finding, an increasing number of ligands have been identified: α-GC (20), sulfatide (21). In contrast to group 1 CD1 molecules, where extensive hydrophobic and van der Waals interactions are the main forces between ligands and CD1 molecules, the hydrogen bond network is the dominate force in CD1d. By studying the difference between human CD1d and mouse CD1d in ligand binding, it has been found that the structures and their binding with α-GC are very similar. The only difference is that tryptophan at position 153 in human isoform tilts galactose headgroup slightly which is replaced by glycine 155 and has no effect on binding capability.

2.3 Tissue distribution of CD1 and expression in disease

For a complete understanding of CD1 function, the expression of CD1d has been detected in both normal tissue and alteration in disease. Group 1 molecules are exclusively found on APCs and thymocytes. The peripheral expression of CD1a and CD1b is restricted to DCs, while CD1c is expressed on both DCs and B cells (22, 23). When it comes to disease, CD1a, CD1b and CD1c have been shown to be induced on DCs in dermal granuloma in Mycobacterium leprae (24). Melian et al has detected CD1a, CD1b, CD1c and CD1d expression in lipid-laden foam cells in atherosclerotic

lesions (25). Also CD1b and CD1c have been found to be increased in mycosis fungoides (26), and CD1-positive DCs have been presented in human breast cancer (27, 28). CD1c has been found to be decreased in B chronic lymphatic leukemia (29).

In human peripheral blood, CD1d is mainly found in B cells, monocytes and activated T cells. Outside of the hematopoietic compartment, CD1d is found in hepatocytes, pancreas, kidney, breast, skin, testis, epididymis, small bowel, and colon (30, 31). For mouse hematopoietic cells, CD1d has been detected on B cells, T cells, macrophages and $CD11c^{+}$DCs (32). The tissue distribution of CD1d in mouse is quite similar to human. In terms of disease, CD1d has been found to be overexpressed in inflammatory bowel disease, primary biliary cirrhosis, sarcoidosis and psoriatic lesions (30, 33). Moreover, human CD1d has been shown as upregulated in hepatocytes infected with hepatitis C virus (34). It is also noticed that CD1d is expressed in many tumors, like leukemia, brain tumor and myeloma (35, 36). According to these studies, CD1d expressed tumors can be lysed by α-GC expanded invariant natural killer T (iNKT) cells.

3. CD1-restricted T cells

3.1 Group 1 versus Group 2 CD1-restricted T cells

T cells are the downstream cells that react with the antigens presented by CD1, so called CD1-restricted T cells. Accordingly, group 1 CD1 including CD1a, b, c activated T cells are classified as group1 CD1-restricted T cells. CD1d-restricted T cells are group 2 CD1-restricted T cells, which have apparently different expression

and function. CD1e is designated as group 3 CD1-restricted T cell and little is known about this group. The limited expression of group 1 CD1 in few cell types restricted the function of group 1 CD1-restricted T cells. Group 1 CD1-restricted T cells have been demonstrated to be linked to antigen-specific adaptive immunity. Meanwhile, they can provide immunity memory in a manner similar to MHC-restricted T cells. However, CD1d-restricted T cells are associated with innate immune system based on the activating antigens.

3.2 Subgroups of CD1d-restricted T cells

There are two distinct subgroups of CD1d-restricted T cells differentiated by TCR arrangement: type I, iNKT cells have highly conserved TCR repertoire consisting of Vα14-Jα281 (in mice) or Vα24-Jα18 (in human); type 2, noninvariant NKT cells have more diverse TCRs. Type I CD1d-resticted T cells are CD4-CD8- though a small subset expresses CD8. Previous studies have shown that Vα14 exclusively uses Jα281 for junction (37). Later it was found that $V\alpha14^{+}$-$NK1.1^{+}$ cells were CD1d-specific (38). Ligand α-GC is specifically presented by CD1d and has been applied for CD1d-restricted T cells identification. Due to high conservation of CD1d and NKT cell receptor，human CD1d can present α-GC to mouse NKT cells and vice versa (39, 40). Type 2 noninvariant NKT cells are mainly detected in murine bone marrow and human liver and bone marrow (41). And little specific antigen has been identified except some group of self-derived glycolipid antigen, which is different from the one recognized by iNKT cells (40).

3.3 Activation of CD1d-restricted T cells by microbial or self lipid antigens

It has been well established that CD1d-restricted T cells participate in the infection defense by recognizing microbial lipid antigens. CD1d-restricted T cells are activated by CD1d, antigen and TCR complex analogous to the way of MHC-restricted T cells activated by specific antigens. Foreign lipid antigens can either bind and presented directly by CD1d to activate CD1d-restricted T cells, or activate APCs to provide a co-stimulating signal to stimulate weakly autoreactive CD1d-restricted NKT cells (Figure 4). To date, very limited microbial antigens have been identified to activate CD1d-restricted T cells including mycobacterial lipids (42), monoglycosylceramides from sphingomonas species (43, 44), and lipophosphoglycan from Leishmania donovani (45, 46).

Another characteristic of both invariant and diverse CD1d-restricted T cells is self-reactive nature, which means responding to self-lipid antigens. Similar to binding and recognition of microbial lipid antigens, CD1d can present self-lipids to TCR and CD1d-lipid complex is the key stimuli for CD1d-restricted T cells (47). Some self-lipids identified for CD1d-resticted T cells activation require accessory co-stimulatory signals. For example, only with cytokines such as interleukin-2 (IL-2) supplemented, primary self-lipid-APCs complex can recognize NKT cells in vitro (Figure 4) (48). The activation CD1d-restricted T cells results in IFN-γ, interleukin-4 (IL-4) and interleukin-10 (IL-10) production. IFN-γ can either induce CD1d expression on APCs and further enhances the activation of CD1d-restricted T cells, or modulates other inflammatory cells such as macrophages, DCs and Th1/Th2 balance. The production of IL-4 and IL-10 can lead to stronger Th2 response, which may

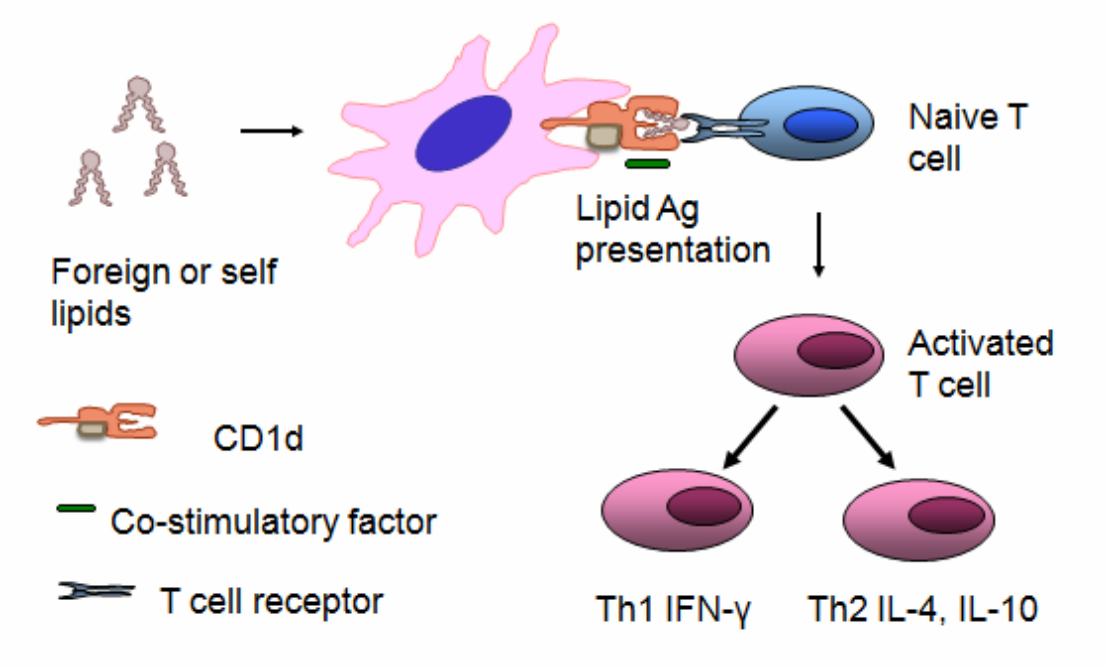

Figure 4. Activation of CD1d-restricted T cells by foreign or self lipid antigens.

Foreign or self lipid antigens can either bind and presented directly by CD1d to activate CD1d-restricted T cells, or activate APCs and provide co-stimulating signal to stimulate weakly autoreactive CD1d-restricted NKT cells. The activation CD1d-restricted T cells results in Th1 cytokines like IFN-γ, and Th2 cytokines like IL-4 and IL-10 production.

explain some auto reactivity in autoimmune diseases.

4. Oxidized Phospholipids

4.1 Origin and structure of oxidized phospholipids

OxPLs are self antigens mainly derived from cellular membrane phospholipids and phospholipids contained in circulating lipoprotein as low-density lipoproteins (LDLs) when undergoing oxidative modification. There is an increased level of OxPLs as decreased antioxidant defense or enhanced reactive oxygen species occurred in atherosclerosis (49) and cell apoptosis (50). One major phospholipid present in cell membrane and LDL is 1-palmitoyl-2-arachidonoyl-sn-glycero-3-phosphrylcholine (PAPC). The chromatographic separation of PAPC oxidation products identified 1-palmitoyl-2-(5-oxovaleroyl)-sn-glycero-3-phosphatidylcholine (POVPC), 1-palmitoyl-2-glutaroyl-sn-glycero-3-phosphatidylcholine (PGPC), 1-palmitoyl-2-(5,6-epoxyisoprostane E2)-sn-glycero-3-phosphatidylcholine (PEIPC) and oxidation products binding to CD36 called $oxPC_{CD36}$. (Figure 5) (51).

4.2 Receptors for OxPLs

Based on structure diversity of OxPLs, it has been postulated that there are multiple receptors for OxPLs.

Scavenger receptors. Cluster of differentiation 36 (CD36), a member of the scavenger receptor class B family has been indicated as a putative receptor for oxidized low-density lipoproteins (OxLDL). The acyl chains of OxPLs protruding from cell membrane are the key recognition sites for CD36 on macrophages (51).

Recent studies have shown that OxPLs derived from PAPC are ligands for CD36 (52). The interaction between platelet CD36 and OxPLs is associated with dyslipidemia and prothrombosis (53).

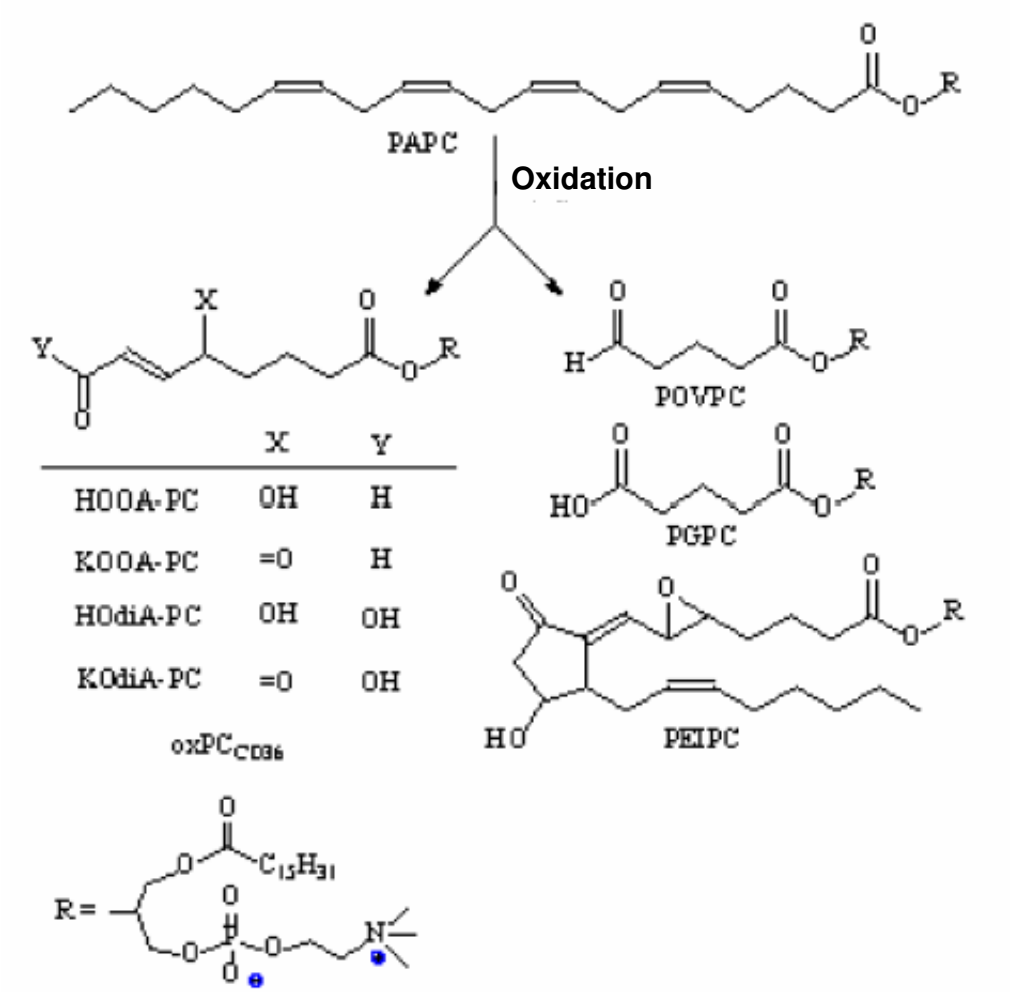

Figure 5. Chemical structures of oxidized phospholipids formed during oxidation of PAPC. PAPC oxidation products include 1-palmitoyl-2-(5-oxovaleroyl)-sn-glycero-3-phosphatidylcholine (POVPC), 1-palmitoyl-2-glutaroyl-sn-glycero-3-phosphatidylcholine (PGPC) 1-palmitoyl-2-(5,6-epoxyisoprostane E2)-sn-glycero-3-phosphatidylcholine (PEIPC) and oxidation products binding to CD36 called oxPC$_{CD36}$.

G-protein-coupled receptors (GPCRs). Parhami et al. has demonstrated that GPCR can be bound by OxPLs (54). Lipoprotein-associated phospholipase A2 catalyzes the conversion of OxPLs into lysophospholipids, which are potent ligands for GPCR (55). Moreover, free oxidized fatty acids released from oxidized phosphocholine are ligands of GPCR (56). It was also shown that PEITPC can activate GPCRs prostaglandin E2 and prostaglandin D2 receptor (57).

Toll-like-receptors (TLRs). TLRs consist of extracellular leucine-rich and intracellular Toll/IL-1 domains and are highly conservative during evolution. Twelve different TLRs have been identified, in which TLR1, 2 and 4 have been found expressed in both human and mouse atherosclerotic lesions, which are also induced by interleukin-1 (IL-l) (58). Leitinger et al has found that OxPLs induced inflammation was TLRs related. (59). Oxidized PAPC (OxPAPC) has been shown inducing interleukin-8 (IL-8) synthesis via TLR-4 and causing inflammatory effect (60).

Peroxisome proliferator-activated receptors (PPARs). PPARγ and PPARα, nuclear receptor proteins regulating gene expression have been found to activate OxLDL. For instance, OxLDL can activate PPAPα dose-dependently on endothelial cells without affecting PPAPα protein expression level (61).

4.3 OxPLs and atherosclerosis

Various studies have proved that OxPLs play an important role in atherogenesis, including monocytes activation; extravasations and adhesion; inflammatory cytokines production and thrombogenesis induction (53, 62). Abundant

accumulation of OxPLs has been demonstrated from early fatty streaks to advanced atherosclerotic lesions.

Monocytes activation. Previous studies have shown that OxPLs can activate monocytes binding to vascular endothelial cells by synthesizing adhesion proteins like connecting segment1 and monocyte chemotactic protein 1 (63) (Figure 6）. An alternative pathway suggested the involvement of lipoxgenase, which was demonstrated by a lipoxgenase inhibitor. The inhibitor decreased minimally modified low density lipoprotein (MM-LDL) and POVPC-induced binding of monocytes to endothelial cells (ECs) (64).

Inflammatory cytokines production. Cytokines play important roles in the development of atherosclerosis. It has been found that the treatment of OxPLs induced the production of IL-8, interleukin-6 (IL-6), macrophage inflammatory protein-1 alpha (MIP-1α) and macrophage inflammatory protein-1 beta (MIP-1β) (65). IL-8 can be produced by macrophages and endothelial cells. and functions as chemoattractant for neutrophils, which causes migration and phagocytosis. IL-6 can be secreted by macrophages and T cells in response to specific microbial molecules, usually working as a proinflammatory cytokine and increase inflammatory cytokine production. MIP-1 including MIP-1α and MIP-1β is produced by macrophages stimulated with bacterial endotoxins, which act as chemoattractant to a variety of cells including monocytes, T cells, B cells and eosinophils. The complicate network between cytokines induced by OxPLs and immune cells initiates and promotes inflammatory process during atherosclerosis.

Thrombogenesis induction. The atherosclerotic plaque may rupture and cause thrombosis to form. OxPLs can enhance tissue factor expression in endothelial cells, which is the cell-surface receptor for factor VIIα, an important factor in thrombosis formation. Furthermore, OxPLs can activate platelet and cause proatherogenic effect on the vascular wall.

Chapter 2 Hypothesis and Specific Aims

1. Autoantigens and atherosclerosis:

Currently, atherosclerosis is considered a chronic inflammatory disease involving both adaptive and innate immunity (66). Given abundant accumulation in the atherosclerotic plaque, lipids are suggested as the main target in this complex network. These lipids induce the infiltration of specific APCs and T cells in the atherosclerotic lesions, which boosts the inflammation and leads to the development of atherosclerosis.

Initially, with a fat-rich diet, the large or medium sized arteries deposited the LDL in the wall, which is assembled from the fat-derived components like cholesterol, phospholipids. More and more LDL is accumulated in the artery wall and further modified into Ox-LDL under oxidative stress. Meanwhile, the mechanical changes, infection or immunological injuries prompt the release of chemokines from the vascular cells as the “bait”, which attracts peripheral monocytes to the injury site. Then these monocytes can extravagate the endothelial layer aided by endothelium adhesion molecules (67). The latter is up-regulated on endothelial cells in response to inflammation. After extravagation monocytes differentiate into macrophages or DCs, which can uptake lipids and come into being foam cells. Furthermore, these lipid-laden foam cells serve as the main APCs and recruit effective lymphocytes to the site, which amplifies the immunological response. In pathology from the earliest visible stage fatty streak to the advanced atheroma the lipid deposition, foam cells and

T cells can all be detected with different proportionally composition (68).

As mentioned above there are three main lipid components involved in the atherosclerotic plaque: phospholipids, fatty acids and cholesterol. All of them are derived from oxidation of LDL which occurs predominantly in the intima of artery. Examination of foam cells isolated from both human and rabbit atherosclerotic aorta showed high levels of oxysterols. Among lipid components 7-keto-cholesterol is the major one followed with 7 beta-hydroxycholesterol and 7-alpha hydroxycholesterol (69). On the other hand, more and more evidence suggested the OxPLs play an important role in atherogenesis. Phospholipids are main components of cell membranes and susceptible to the oxidation stress presented in the atherosclerosis. OxPLs are more biologically active than unoxidized form. They can be recognized by CD36 scavenger receptor on macrophages or SMCs to promote foam cells formation (52). During atheroma progression OxPLs can regulate smooth muscle proliferation and ultimately lead to apotosis. The apoptotic cells attract more monocytes and lymphocytes: “inflammation bursts”. Meanwhile the retained OxPLs can activate platelet and cause thrombosis, which is a key step in the progress of atherosclerosis. When it comes to the fatty acid Waddington et al also demonstrated that fatty acid oxidation products are dispersed in the human plaques by using high-performance liquid chromatography (70). The precise mechanism of how fatty acid affects atherosclerosis development is currently unclear.

The auto-lipid antigens recognized by CD1d in atherosclerosis are unclear. Several studies have indicated that three groups of oxidized lipids are involved in the

proatherogenic process: phospholipids, fatty acids, and cholesterol (71). Due to the harsh environment in artherosclerotic plaque, the oxidative lipids serve as the main antigens. Whether these molecules bind to CD1d leading to atherosclerosis is currently unknown. Following the antigens identified, the downstream of antigen stimulated T cells responses is a very interesting field to explore.

Above all, the process of lipid oxidation products interacting with other immunology molecules in the atherosclerosis is intriguing and remains to be further addressed.

2. CD1 and atherosclerosis:

CD1 is a family of cell surface receptors consisting of four distinct members, CD1a-d. They are classified into two groups based on their structure and function: CD1a-c is group1 while CD1d is group 2 (9). CD1e gene was identified recently, but little is known about it (10). The genes of CD1 family are located at chromosome 1, 1q22-23 together with MHC related gene and other inflammation associated genes. To date, group 1 is found in all mammalian animals including human, rabbit (11-13). In mice and rat, only CD1d is expressed. As for tissue distribution group, 1 CD1 is mainly found on APCs and thymocytes (72). CD1d is expressed more extensively including monocytes, DCs, B cells and activated T cells. Outside the hemopoietic part, CD1d is also detected in liver, kidney, spleen, breast, skin. This broad expression of CD1d implicates its pivotal role in the body defense.

In contrast to MHC which presents peptide antigen, CD1 is a specific lipid

antigen present molecule. A growing number of lipid ligands from mycobacterial glycolipid to self phospholipids are revealed. In atherosclerosis, the CD1 family is found in lipid-laden foam cells while non-detected in normal arterial tissue (25). The lipids presented in atherosclerotic plaques contain oxidized cholesterol, fatty acid and phospholipids. The question is which lipids antigens are presented by CD1 and progressing into atherosclerosis.

3. CD1-restricted T cells related inflammation in atherosclerosis

T cells are the downstream cells that react with the antigen presented by CD1d, so called CD1-restricted T cells. To date, there are two characterized populations. One has invariant TCR alpha (Vα14/Jα18 in murine and Vα24/Jα18 in human) paired with TCR beta. Consistent with the marker of NKT cells: NKT lineage receptors specifically NK1.1, this population is a subset of NKT. Recently, another population of CD1 recognized T cells are revealed, which have diverse of TCR α and β (14). These T cells have shown Th1/Th2 cytokine secretion in response to diverse antigens. It is clear that NKT cells play important role in adaptive immunity. CD1 have been found in mycobacterial tuberculosis defense. The first CD1-restricted T cells were identified in culturing monocyte-derived DC with crude extract of M.tuberclosis. Double negative (CD4-CD8-) TCR αβ+ T cells were isolated and cytokine production observed (73, 74). The ligands identified in mycobacterial extract include mycolic acids, phosphatidylinositol mannosides and they are presented by CD1b, CD1c. Other studies also found sulfide and gangliosides can be presented by CD1a. For CD1d, one

sponge-derived α-Galcer is proved to be a specific ligand of CD1d. Accumulating evidence shows that CD1-restricted T cells, related to these CD1 molecules, can initiate immune response and modulate the development of the disease like autoimmune disease, tumor and allergy (75). Prosperous cytokines are induced in the CD1 stimulated T cell reactions. It is believed that Th1 cytokines like IFN-γ are proatherogenic while Th2 like IL-10 are antiatherogenic. The possible role of CD1 gene family in atherosclerosis has been investigated in the mouse model (76, 77). In CD1d knockout mice, less aggravation of early atherosclerosis was observed and a large panel of cytokines was detected. Further investigation reported CD1 deficiency as protective, as noted by attenuation in the advancement of atherosclerosis (78).

4. Inflammation in atherosclerosis with obesity and hyperlipidemia

Coronary heart disease (CHD) due to atherosclerosis is becoming a leading cause of morbidity and mortality in type 2 diabetic patients (79). Type 2 diabetes is characterized by elevated LDL and triglyceride, lowered high density lipoprotein (HDL) (80, 81). Type 2 diabetes accounts for 95% diabetes mellitus and is caused by insulin resistance rather than insulin deficiency (82, 83). In diabetes high glucose level in the blood promotes the accumulation of plaques. The high blood glucose level can also cause production of free radicals, which attack intact cells and cause cell damage. Therefore, diabetes accelerates atherosclerosis-related inflammation and diabetic patients are twice likely to have a heart attack.

Nuclear factor-kappa B (NF-κB) is a family of transcription factors that

mediate inflammatory, immune responses and cell growth. It can be activated by various stimuli including proinflammatory cytokines, lipopolysaccharide, and reactive oxygen species. The process of activation of NF-κB included phosphorylation and subsequent proteolytic degradation of the inhibitory protein inhibitor of kappa B (IκB) by specific IκB kinases. Then the heterodimer of p50 and p65, free NF-κB could bind to κB sites located in nucthe leus (Figure 6). NF-κB pathway is activated in different stages of atherosclerotic plaques and contributed to initiation and progression of atherosclerosis. The activation of NF-κB has been detected in atherosclerotic plaques (84). In ECs NF-κB activity is elevated in arterial vessel exposed to disturbed blood flow and susceptible to atherosclerosis (85). In NF-κB signal pathway ECs inflammatory cells are recruited to the vessels by expressing Inter-Cellular Adhesion Molecule 1(ICAM-1), vascular cell adhesion molecule 1(VCAM-1), P- and E-selectins on ECs.

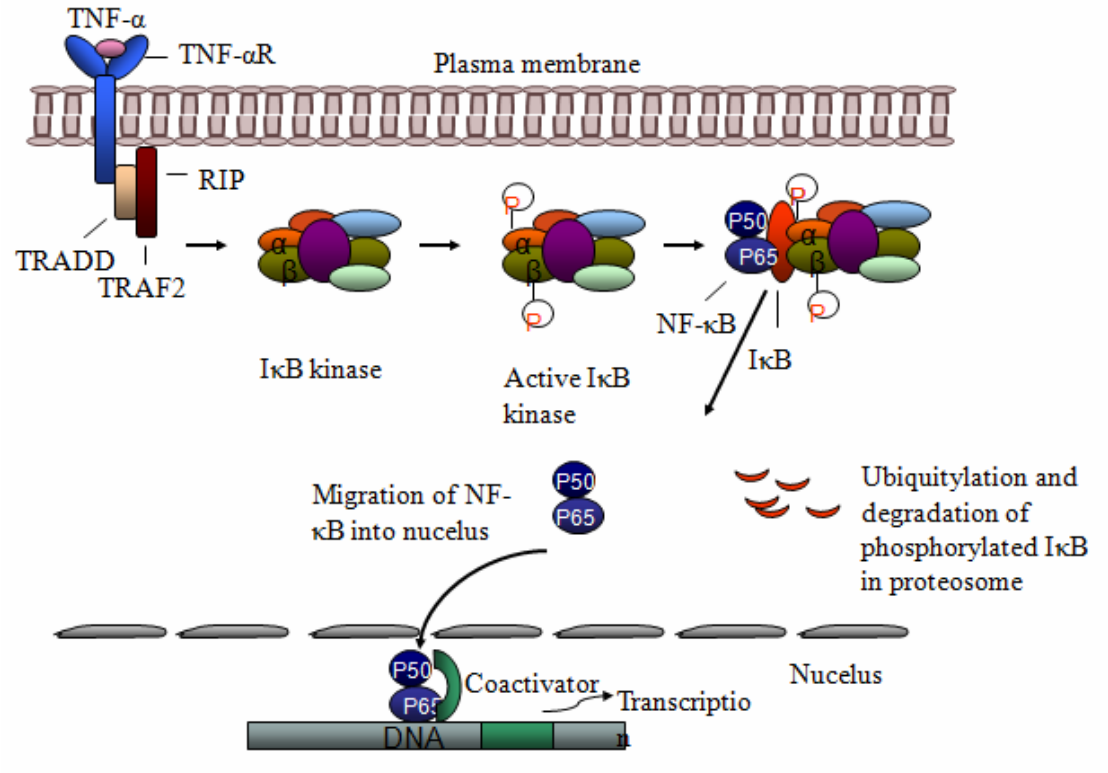

Figure 6. Activation of NF-κB by the TNF-α pathway.

(1) Binding of TNF-α to its receptor recruits TRADD (TNF receptor-associated death domain protein), RIP (receptor-interacting protein) and TRAF2 (TNF receptor-associated factor 2).

(2) TRAF2 activates IκB kinase (IKK).

(3) The active IKK activates NF-κB by degrading the inhibitor protein IκB.

(4) After NF-κB is activated, it may serve as a transcription factor or inhibit apoptosis.

It has been found that the recognition of peptide bound with MHC to TCR of

T lymphocytes or the cross-linking of TCR by anti-TCR antibody orchestrate intracellular protein tyrosine phosphorylation events. This process further produces NF-κB. Whether the recognition of lipid bound to CD1d leads to NF-κB release and causes inflammation is still unknown. The stimulation of CD1d-restricted T cells by lipids can also cause release of tumor necrosis factor alpha (TNF-α). TNF-α can activate NF-κB by phosphorylation dependent ubiquitination and degradation of inhibitor of IκB proteins, which is carried out by a multiprotein kinase inhibitor of kappa B kinase (IKK) complex (Figure 6). Therefore, the release of TNF-α by stimulated CD1d-restricted T cells may have role to the direct effect of CD1d.

Hypothesis: In summary CD1 plays an important role in hyperlipidemia related to obesity and atherosclerosis. The identification of antigens presented by CD1 in atherosclerotic plaques remains to be elucidated. The central hypothesis is that oxidative lipids generated in hyperlipidemia associated with arthrosclerosis serve as autoantigens that activate NK-T cell and trigger proinflammatory signaling, leading to the enhancement of autoimmune or pro-inflammatory responses during the development of atherosclerosis lesion. CD1d-mediated pro-inflammatory signaling may occur in atherosclerosis-prone, obese animals and contributes to the cardiovascular dysfunctions triggered by hyperlipidemia.

Specific Aims:

Aim 1: To identify and characterize the lipid antigens recognized and

presented by CD1d to activate CD1d-restricted T cells in atherosclerosis.

a). Conduct GC-MS analysis and biochemical characterization of atherosclerosis-prone lipids that function potentially as the ligands for CD1d.

b). Determine whether the oxidized phospholipid PGPC acts as an autoantigen for CD1d stimulating CD1d-restricted T cells.

Aim 2: To define whether CD1d mediates pro-inflammatory signaling and cardiovascular dysfunction in mice with atherosclerosis and obesity.

a). Analyze whether CD1d deficiency alters cytokine production in atherosclerosis-prone or obese mice.

b). Determine whether CD1d regulates pro-inflammatory signaling in mice with hyperlipidemia.

Chapter 3 Methods and Materials

1. Hypothetic prediction of lipid-CD1d interaction by computer stimulation

The structures of the all candidates of lipid ligands were obtained from NIH Pubchem library. The 3D crystal structures of human and mouse CD1d were obtained from Protein Data Bank (PDB, Figure 7). The binding capacities of the lipid molecules with the CD1d were analyzed by docking procedure SYBYL program, which was designed for determination of the interaction forces between the ligand and the target modeling. This part of experiment was assisted by Center for Experimental Therapeutics and Pharmacoinformatics, Department of Pharmacological and Pharmaceutical Sciences, College of Pharmacy, University of Houston.

2. Gas-chromatography (GC) /mass-spectrometry (MS) of lipids

Mice were sacrificed by 100% carbon dioxide, skin was disinfected with 70% ethanol. The thoracic cavity were open and heart was completely exposed. Blood was drawn from the heart, preferably from the ventricle by using a 26 gauge needle. The blood was drawn slowly to prevent heart collapsing. Approximately 1ml blood was collected into a tube containing 10 μl heparin sodium (APP Pharmaceuticals, LLC, Schaumburg, IL Cat # 27602). Then the same volume of PBS was added and centrifuged at a speed of 2000 rpm for 15 minutes. The supernatant was transferred to a new tube and immediately delivered for GC/MS analysis (Center for Experimental Therapeutics and Pharmacoinformatics, Department of Pharmacological and

Pharmaceutical Sciences, College of Pharmacy, University of Houston.)

3. Cell lines and culture

3.1 Culture of mouse CD1 transfected HEK293 (mCD1-HEK293) cells and HeLa cells

mCD1-HEK293 cell line was made by Corina Rosales (previous Ph.D graduate student) and stored in liquid nitrogen tank. HeLa cells were purchased from American Type Culture Collection (ATCC) (Manassa, VA, Cat # CCL-2). For the use of culture, cells were quickly thawed in 37°C and grown in complete culture medium-Dulbecco's Modified Eagle's Medium (DMEM, Sigma-aldrich, St Louis, MO, Cat#D5796) supplemented with 20% fetal bovine serum (FBS, Atlanta biologicals, Lawrenceville, Ga, Cat#S11050), 1:100 (v/v) diluted antibotic antimyotic solution (Sigma-aldrich, St Louis, MO, Cat#A5955). For sub-culture, cells seeded in 75cm^2 flasks were treated with EDTA/Trypsi (Sigma-aldrich, St Louis, MO, Cat# T4049) for 5 minutes at 37°C

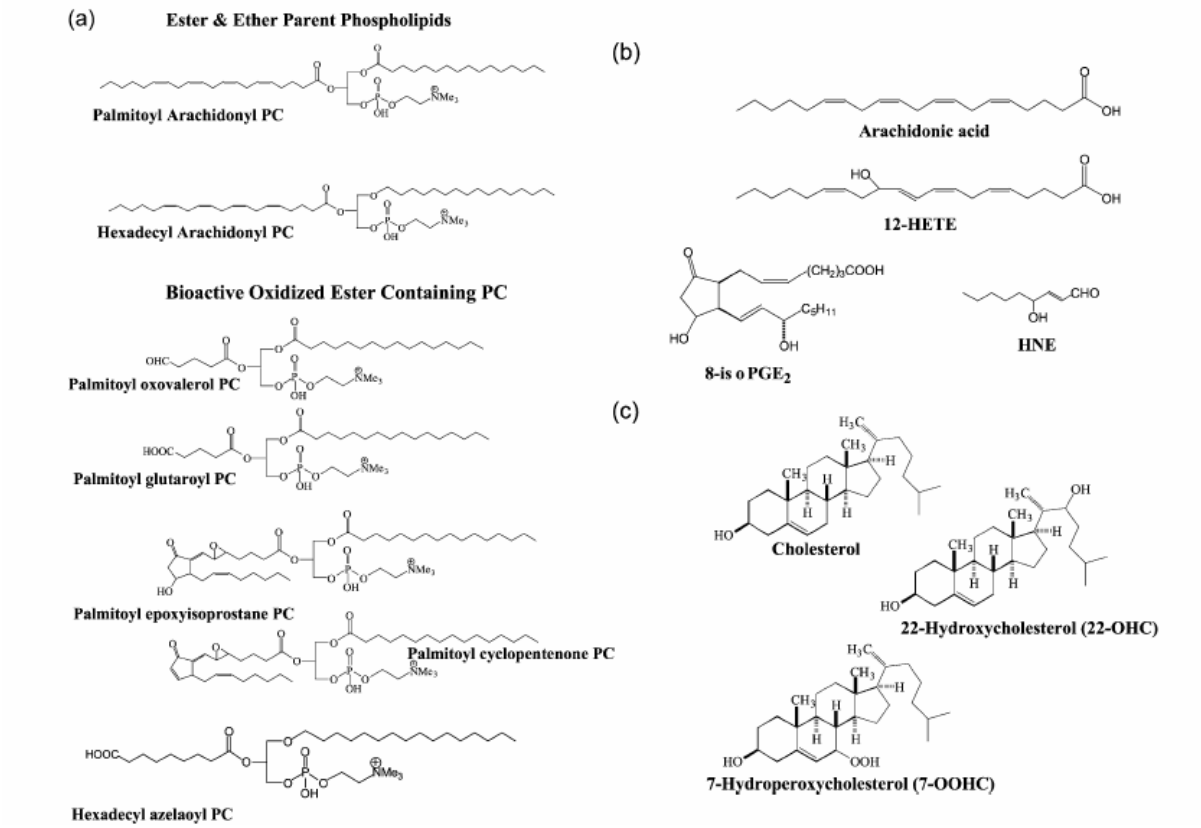

Figure 7. Chemical structures of lipids commonly found in atherosclerotic lesions.

There are three main lipid components involved in the atherosclerotic plaque: phospholipids, fatty acids and cholesterol. Oxidation products of these lipids predominantly exist in atherotic plaque.

incubator. Then 10^4 suspended cells were seeded into 10 ml pre-warmed complete culture medium. Only cells less than ten passages were used in the following experiments. For preservation, cells were suspended in 90% FBS mixed with 10% sterile DMSO then kept into 2 ml cryo-vial (Phenix research products, Candler, NC, Cat # C40F) and stored in liquid nitrogen following a slowly frozen procedure (around 1 °C decrease per minute).

3.2 Culture of MOLT-4 cells

MOLT-4 cell line was purchased from ATCC (Cat # CRL-1582). Cells were quickly thawed in 37°C and grown in complete culture medium-RPMI 1640 (Invitrogen, Carlsbad, CA, Cat#72400) supplemented with 20% FBS, 1:100 (v/v) diluted antibotic antimyotic solution. The subculture and freezing methods were the same as described above.

3.3 Culture of DN32.D3

DN32.D3 is a murine NKT hybridoma cell line including Vα14-Jα18 TCR, which was kindly provided by Dr. Steven Porcelli (Albert Einstein College of Medicine, New York, NY). Cells were cultured in complete medium consist of RPMI 1640, 20% FBS, 1:100 (v/v) diluted Antibotic antimyotic solution, 50μM 2-mercaptoethanol (Sigma-aldrich, St Louis, MO, Cat #6250) and 1mM HEPES (4-(2-hydroxyethyl)-1-piperazineethanesulfonic acid) (Sigma-aldrich, St Louis, MO, Cat #0891). The subculture and frozen methods are the same as described above.

3.4 Culture of Peripheral Blood Mononuclear Cells (PBMCs)

PBMCs are mixed cells consisting of lymphocytes, monocytes and

macrophages. The lymphocytes include T cells (CD4 and CD8 ~75%), B cells and NKT cells (~25% combined). The isolation of PBMCs was processed by Ficoll according to density gradient method. Briefly, 5ml buffy coat peripheral blood was diluted with two volumes of PBS. Then 3 ml of Ficoll was layered up on the top. With 800 g centrifuge for 30 minutes at RT, human PBMCs can be visible at PBS/Ficoll interface. PBMCs were carefully harvested and washed with PBS twice. Isolated cells were dispensed in 6-well plates and cultured in RPMI 1640 supplemented with 20% FBS, 1:100 (v/v) diluted antibotic antimyotic solution stabilized. The frozen method is the same as described as above.

3.5 Isolation and culture of mouse spleen cells

Spleen cells are consisted of lymphocytes, granulocytes and other immune cells. The procedure to isolate spleen cells is described as below:

Mice were sacrificed by 100% carbon dioxide. Skin was disinfected with 70% ethanol, the abdominal cavity open and spleen removed. Spleen was placed into cold PBS and mashed by using the plunger of the syringe and passed through 70 μM cell strainer (BD science, Franklin Lakes, NJ, Cat # 352350). Red cell lysis buffer (Biolegend, San Diego, CA, Cat # 420301) was applied to remove red blood cells. After washing with PBS by centrifuging at 400g twice, cells were cultured in RPMI 1640 supplemented with 20% FBS, 1:100 (v/v) diluted antibotic antimyotic solution stabilized. The frozen method is the same as described as above.

4. **cDNA cloning and transfection**

4.1 Generation of hCD1d cDNA:

MOLT-4 is derived from human lymphoblast and has rich CD1d expression. RNA isolation from MOLT-4 was processed by using RNeasy Mini Kit (Qiagen, Valencia, CA, Cat #74104). First 10^7 cells were centrifuged at 300g for 5 minutes and cell pellet was loosened by buffer RLT. Then cell lysate was pipetted into QIAshredder column and centrifuged for 2 minutes. 70% ethanol was added into homogenized lysate for precipitation and buffer RW1 was used for wash. Buffer RPE was used for final RNA elution. Isolated RNA was stored in -80°C for future use. Complimentary DNA (cDNA) was synthesized by using superscript III Platinum Two-step quantitative real time polymerase chain reaction amplification (qRT-PCR) Kit (Invitrogen, Carlsbad, CA, Cat #11734-050) under the instructions of the manual. The RNA reaction system was consisted of 2 x RT reaction mix 10μl; RT enzyme mixes 2μl; RNA 8μl. All components were mixed and incubated at 25°C for 10 minutes then 42°C for 50 minutes. The reaction was terminated at 85°C for 5 minutes, and then chilled on ice. And 2U of E.coli RNase H was added and incubated at 37°C for 20 minutes. The synthesized cDNA was stored in -20°C until use. Then cDNA was used for PCR by using Platinum Pfx DNA polymerase (Invitrogen, Cat # 11708-013). The RT-PCR reaction system consisted of Plantinum Pfx buffer 5μl, 10mM dNTP 1.5μl, 50mM MgSO4 1μl, primers 1.5μl each, template DNA 100ng, 10%DMSO 2.5μl, Pfx DNA polymerase 0.4μl, and distilled water(ddH_2O) to 50μl. The primers were used for amplifying hCD1d: Forward,

5'-3' GCGATATGGGGTGCCTGCTG, Reverse, 5'-3' AACAGGACGCCCTGATAGGAAGTTTGC. The PCR amplification was as following: denaturing at 94°C for 15 seconds, annealing at 55°C for 30 seconds, extending at 68°C for 1 minute. Total 30 cycles were performed.

4.2 cDNA subcloning and plasmid construction:

The cloned gene hCD1d was ligated into Zero Blunt PCR cloning plasmid (Invitrogen, Cat # K270020)). The ligation reaction system included 5μl T4 DNA ligase buffer, 2μl DNA, 1μl vector, 1μl T4 DNA ligase (Invitrogen, Cat # 15224-041) and 1μl ddH2O. The reaction was incubated in room temperature for 5 minutes. The ligated product was separated with unligated reaction components by running on 0.8% agrose gel (Invitrogen, Cat # 15510-027). Predicted size band was excised under the observation of UV-light. The cut gel band was isolated by using QIAquick Gel Extraction Kit (Invitrogen, Cat # 28704). First, three volumes buffer QG was added to 1 volume gel and incubated at 50°C for 10 minutes until the gel is dissolved. Then one volume of isopropanol was added and sample was transferred to a QIAquick column for spinning. Buffer PE was used for washing the sample collected in the spin tube then buffer EB was used for eluting DNA. Isolated DNA was further digested with restriction endoneuclease enzymes XhoI (New England Biolabs NEB, Ipswich, MA, Cat # R0146S), KpnI (New England Biolabs NEB, Ipswich, MA, Cat # R0142S). The endonuclease digestion reaction system is as following: 3μl DNA, 1μl enzyme, 0.2μl BSA, 2μl enzyme buffer. The reaction was incubated at 37°C for one hour. Digested products were separated by running on 0.8% agrose and excised for isolation

by QIAquick Gel Extraction Kit as described above. Using sticky ends produced by digestion hCD1d was cloned into pEGFP-N3 plasmid with CMV promoter (Clontech, Mountain View, CA, Cat # 6080-1) (Figure 8). The cloned plasmid was first verified by restriction endonuclease digestion (Figure 9a). All plasmids were finally verified by sequencing (Seqwright, Houston, TX) (Figure 9b). The sequencing primers applied are: GFPN3primer, 5'-3'GCTAGCGCTACCGGACTCAGATCTCGA, GFPprimer, 5'-3'GTACCAGGACGACCCTAAGCA.

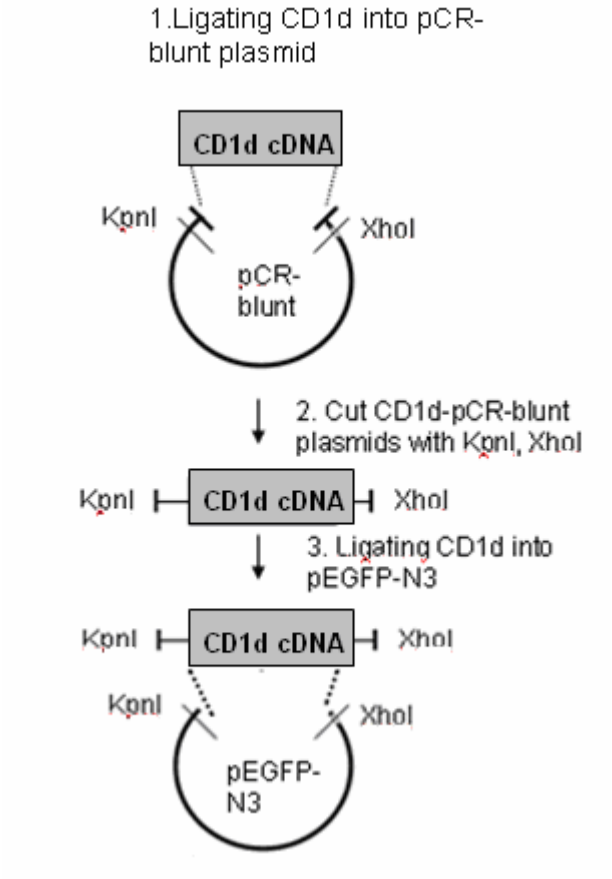

Figure 8. Construction of CD1d-pEGFP-N3 plasmid. The cloned gene hCD1d was ligated into Zero Blunt PCR cloning plasmid. The ligated plasmid was further digested with restriction endonuclease enzymes XhoI and KpnI. Using sticky ends produced by digestion hCD1d was cloned into pEGFP-N3 plasmid with CMV promoter.

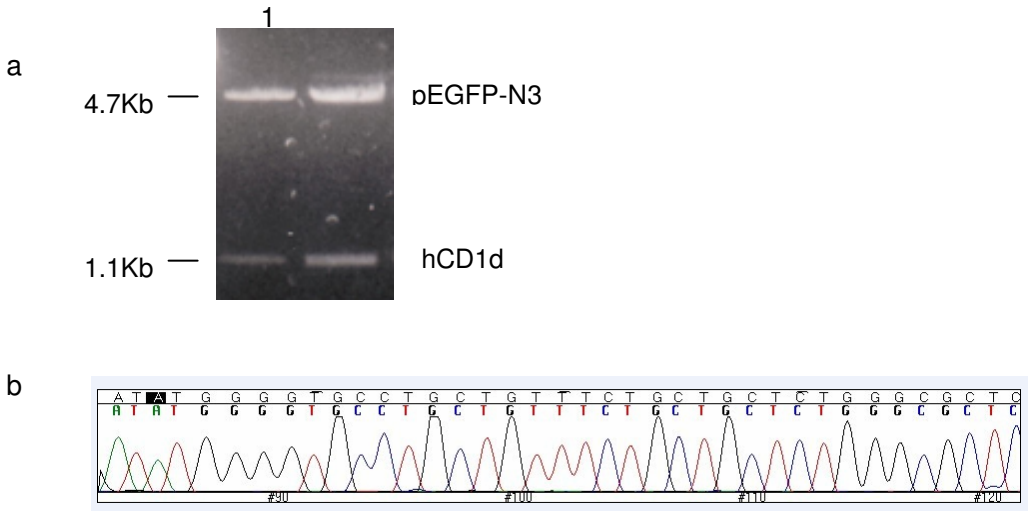

Figure 9. Verification of CD1d cDNA sequence in hCD1d-pEGFP- N3 plasmid.

a. hCD1d-pEGFP-N3 was cut by KpnI, XhoI. There are 4.7kb and 1.1kb bands observed after endonuclease digestion and separated on 0.8% agrose. Lanes 1, 2 stand for different colonies. b. Demonstration of sequencing results of hCD1d-pEGFP-N3 by GFPN3primer, 5'-3'GCTAGCGCTACCGGACTCAGATCTCGA. “ATG” indicated in the picture represents the start code.

4.3 Plasmid transfection and stable cell line set up:

To ensure high efficiency of transfection, Attractene Transfection Reagent (Qiagen, Cat # 301105) was used and HEK293 (ATCC, Cat # CRL1573) was selected as host cells. The transfection was carried out according to the manufacturer's instructions. Briefly, $4x10^5$ HEK293 cells were seeded in 6-well plate in complete culture medium the day before transfection. For transfection, 1.2 μg DNA was diluted in 100μl culture medium without serum. Then 4.5 μl Attractene Transfection reagents (Qiagen, Cat # 301005) were added and mixed by vortex. After 15 minutes incubation, the mixture was added into cells by drop-wise. After 24 hours, the efficiency of the transfection was observed under florescence microscope and the expression of transfected CD1d was detected by Western-blotting assay. Plasmids hCD1d-pEGFP-N3 and pEGFP-N3 only were transfected then selected by HyClone G418 (600μg/ml) (Thermoscientific, Barrington, IL Cat # SV30069.01) after 48 hours. Survived colonies were picked up and cultured as stable cell lines.

5. Analysis of cell proliferation

5.1 Thymidine incorporation into DNA

In order to detect mCD1-restricted T cells responses to lipids, pulsed APCs with lipids were co-cultured with responder T cells and thymidine uptake by T cells was observed. 4×10^5 mouse DCs or 5×10^4 mCD1d stable cells were incubated with 0-15μg/ml lipids in 48-well plate overnight at 37°C. Then, all cells were irradiated in 3000 rad and extensively washed before added into 4×10^4 mouse spleen cells or 5 x

10^4 DN32.D3. Sixteen hours later, 1μM ^{3}H thymidine (GE healthcare Amersham biosciences, Pittsburgh, PA, Cat # TRK296) was added into each well. After 24 hours incubation, DNA was extracted from cells by using ice cold 5% trichloroacetic acid (TCA, EMD chemicals, Raleigh, NC, Cat # TX1045-1). After treated with TCA for 30 minutes at 4°C, precipitated DNA was collected and washed by PBS once, then dissolved in 0.5N NaOH (Sodium hydroxide, Sigma-aldrich, Cat # S8045) /0.5% SDS(Sodium dodecyl sulfate, USB, Cleveland, Ohio, Cat # 21651). The DNA was put in scintillation vial for beta counter (Beckman Coulter, BioSurplus Inc, San Diego, CA, model # LS6500) reading. All assays were done in triplicate.

5.2 Proliferation assay of splenocytes

Since mouse spleen cells contain both APCs (macrophages and monocytes) and reactive T cells, treatment of mouse spleen cells with lipids can be used directly for observing ligand actived CD1d-restricted T cells response. In this experiment, BALB/c and CD-/-BALB/c spleen cells were treated with lipids and thymidine uptake was observed. Briefly, 4 x 10^5 mouse spleen cells were incubated with 0-15μg/ml lipids in 48-well plates overnight at 37°C. Sixteen hours later the proliferation of mouse spleen cells was measured by reading ^{3}H thymidine uptaken as described above.

Spleen cells from both BALB/c and CD1-/-BALB/c were used for measurement of CD1d-restricted T cells response to PGPC and PAPC. Fresh splenic cells 4x10^5 from BALB/c or CD1-/-BALB/c were seeded in 96-well plates and treated with increasing concentrations of PGPC and PAPC (0.3-9.6 μg/ml). After 72 hours,

cells proliferation was measured by Quick Cell Proliferation Assay kit II (Biovision, Moutain View, CA, Cat # K302-500). Briefly, 10µl WST reagent was added to each well and cells were incubated at 37°C for 3 hours. The absorbance of the treated samples at 415 nm was measured and 655 nm was used as reference wavelength.

6. Lipids binding assays

6.1 Lipid preparation and storage

PGPC (Avanti polar lipids Alabaster, Alabama, Cat # 870602), PAPC (Avanti polar lipids, Cat # 850459) were dissolved in 100% ethanol at a stocking concentration of 10mg/ml and stored at 4°C. Cholesterol (Sigma-aldrich, Cat # C3045) was dissolved in chloroform at a stocking concentration of 10 mg/ml and stored at 4°C. ^{3}H-7-K-Cholesterol(^{3}H-7-K-Cho) dissolved in ethanol (American Radiolabeled Chemicals Inc, St. Louis, MO, Cat # ART1174) was stored at 4°C and diluted in PBS for experimental use.

6.2 Lipid binding assay

For assessment of binding capacity of lipids to CD1d, mCD-HEK293 cells are applied for lipid binding assay. Stable cell line mCD1-HEK293 and HEK293 were seeded into 96-well plate (10^{4}/well) for overnight (O/N). The next day, complete culture medium in cells was removed and serum-free medium was replaced. Then cells were shaken on ice for 15 minutes. A series of dilution of labeled ^{3}H-7-K-Cho (0.005, 0.01, 0.5, 2, 3.5, 5 M) was added into cells and incubated for another 15 minutes on ice. Then cells were washed with PBS twice and lysed by scintillation

liquid. The radioactivity was read by a beta-counter. For inhibitor competitive assay, PGPC and cholesterol were tested. After seeded in 96-well plate (10^4/well) for O/N, cells were washed by PBS twice, replaced with serum-free medium and incubated with 4 nmols of lipids for 15 minutes on ice. After washing with PBS twice, cells were incubated with ^{3}H-7-K-Cho (0.005, 0.01, 0.5, 2, 3.5, 5 M) on ice for another 15 minutes. The isotope reading method is described as above. Blank control was set up with the same dose of ^{3}H-7-K-Cho without cells.

7. Fluorescent detection of lipid loaded cells

Mouse spleen cells were seeded $2x10^6$ per well in 1ml full medium in chamber slides. These cells were treated with PGPC 4.8 μg/ml overnight and used for lipid analysis by Nile Red (Sigma, Cat # N3013)staining according to standard protocol (87). In brief, PGPC treated cells were washed in PBC with 2 mg/ml albumin twice, then 1.5% glutaraldehyde was applied for 5 minutes to fix cells. Stocking solution of Nile Red was diluted to 100 ng/ml to stain cells for 5 minutes. 4′,6-Diamidino-2-phenylindole dihydrochloride (Dapi, Sigma Cat # D9564) was diluted to 3μM for cell nuclei staining at 37°C for 10 minutes. HeLa cells $2x10^5$ per well were plated in 1ml full medium in chamber slides. The hCD1d-GFPN3 and GFPN3 plasmids were transfected into HeLa cells by attractene transfection kit. Tansfection efficiency was determined by observing GFP fluorescence. Approximately 80% of the cells were successfully transfected with plasmids. The

transfected cells were treated with PGPC 4.8 μg/ml for 3 hours then used for Nile Red staining as described above.

8. Measurement of cytokine production

In addition to thymidine uptake assay, direct cytokine production is also a strong indication for lipid activation of responder T cells. To assay the cytokine production, a total of 15μg/ml lipids were incubated with APCs (mCD1-HEK293 and hCD1d-HEK 293) 4-5 hours at 37°C. Then stimulator APCs were fixed with 0.05% glutaraldehyde（Sigma Aldrich Cat # G7651）in PBS for 30 seconds and the same volume of 0.4 M glycine (Sigma Aldrich, Cat # 410225) was added to stop the reaction. Fixed cells were washed in DMEM twice and APCs culture medium once before added into the responder T cells. Cytokines were collected from supernatant and analyzed at time points of 6 hours, 24 hours, and 48 hours. BD Cytometric Bead Array (CBA) mouse Th1/Th2 cytokine kit (BD Bioscience, Franklin Lakes, NJ, Cat # 551287) was applied for measuring IL-2, 4, 5, IFN-γ and TNF-α. The principle for this method is as following: The capture bead has been conjugated with specific antibodies, for example, anti-IL-2; the detection reagent is a mixture of phycoerythrin (PE)-conjugated antibodies. When the sandwich complexes capture bead, analyte and detection reagent is formed, the fluorescence is analyzed in proportion to the amount of bound analyte. Flow cytometry was used for measuring the fluorescence and sample was quantified by using standard curve. All assays were done in triplicate.

9. Induction and detection of CD1d expression in PBMCs

Freshly isolated PBMCs 10^8 were seeded in 6-well plates then pulsed with 15 μg lipids for 24 hours. After removing culture medium, cells were washed by PBS twice and lysis buffer were added. The cells were lysed for 10 minutes at room temperature. Cell lysates were transferred into eppendorf tube and centrifuged at 13,000x g for 15 minutes at room temperature. The supernatant was collected and stored in -80°C freezer for future use.

Protein concentration was determined with BCA reagent protein assay kit (Pierce, Rockford, IL, Cat # 23227). The basic procedure is as following: Firstly mix reagent A and B at the ration of 50:1. Next 2.0 ml mixture was introduce into 0.1ml sample (standard and unknown) and mix. The mixture was incubated at 37°C for 30 minutes then read at 562 nm by spectrometer (Biorad, Ultramark).

The CD1d expression was detected by Western-blot analysis. Total 20μg protein samples mixed with 6 x loading buffer (NEB, Cat # B7021) was first boiled at 95°C for 3 minutes, then separated on 4–15% gradient polyacrylamide gel (Biorad, Hercules, CA, Cat # 1611158) and transferred onto PVDF membrane. After transfer, the membrane was blocked with 3% nonfat milk (Santa Cruz Biotechnology Inc, Santa Cruz, CA, Cat # SC2324) for one hour at room temperature. PVDF membrane was then probed with anti human CD1d antibody (Santa Cruz Biotechnology Inc, Cat # SC19632). GAPDH (Abcam, Cambridge, MA, Cat # ab9483) was used as internal standard for control.

10. Flow cytometry

10.1 Intracellular IFN-γ immunostaining

To further identify IFN-γ secreting cells, we treated BALB/c mouse spleen cells with 4.8μg/ml PGPC for 24h and stained these cells with anti-IFN-γ-Alexa647 (BD Bioscience, Cat # 557735) and anti-mouse cluster differentation3 (CD3) - Fluorescein isothiocyanate (FITC) (BioLegend, San Diego, CA, Cat # 100204) antibodies. The cell preparation for flow cytometry is as following: 10^6 cells were collected by centrifugation at 1000 rpm for 5 minutes, and resuspended cells in 0.5 ml PBS. Thereafter, cells were fixed by 2% paraformaldehyde (USB Corporation, Cleveland, OH, Cat # 19943) at 37°C for 10 minutes. Tube was chilled on ice for 1 minute. Cells were permeabilized by ice-cold 100% methanol for 30 minutes on ice. After centrifugation incubation buffer (0.5 g BSA in 100 ml 1xPBS) was add to suspend cells. Then cells were incubated with anti-IFN-γ-Alexa647 0.5 μg for 40 minutes at room temperature. Cells were rinsed with incubation buffer twice. Cells were incubated with anti-mouse CD3-FITC 0.5 μg for 40 minutes at room temperature. Cells were rinsed with incubation buffer twice. Cells were resuspended in 200 μl incubation buffer. The cells were kept in ice and light-avoided before flow cytometry analysis. Data was acquired by BD-LSRII flow cytometer.

10.2 Flow cytometric staining

Mouse spleen cells were washed using buffer (0.1% sodium azide, 0.1% BSA in PBS) twice and 10^6 cells were suspended in 100μl of wash buffer and used for 1.0μg tetramerized mCD1 staining together with anti-mouse CD3-FITC. PBS-57

loaded CD1d tetramer (NIH tetramer core facility, Atlanta, GA) was used as positive control and unloaded CD1d tetramer (NIH tetramer core facility, Atlanta, GA) as negative control. The tetramer mCD1 was prepared from biotinylated mCD1 monomer (NIH tetramer core facility, Atlanta, GA). The principle of the approach is summarized in the Figure 10.

The tetramer staining method is as follows: CD1d tetramer was spinned at 13,000 g for 3 minutes in a chilled microcentrifuge. And 10^6 mouse splenic cells was washed with wash buffer (0.1% sodium azide, 0.1%BSA in PBS) and resuspended in 200 µl residue liquid. 0.5 µg CD1d tetramer was incubated with cells for 60 minutes. Cells were washed with 2 ml wash buffer and resuspended in residual liquid 200 µl. Anti-mouse CD3 antibody was incubated with cells at room temperature for 60 minutes. Cells were washed twice with wash buffer and resuspended in residual liquid 200µl. The flow cytometric data were acquired using BD-LSRII. Samples from ApoE-/-C57BL/6J (The Jackson Lab , Bar Harbor, Maine, Stock # 002052. 12 months old, male only) and WT C57BL/6J (The Jackson Lab, Stock # 000662. 12 months old, male only) were examined.

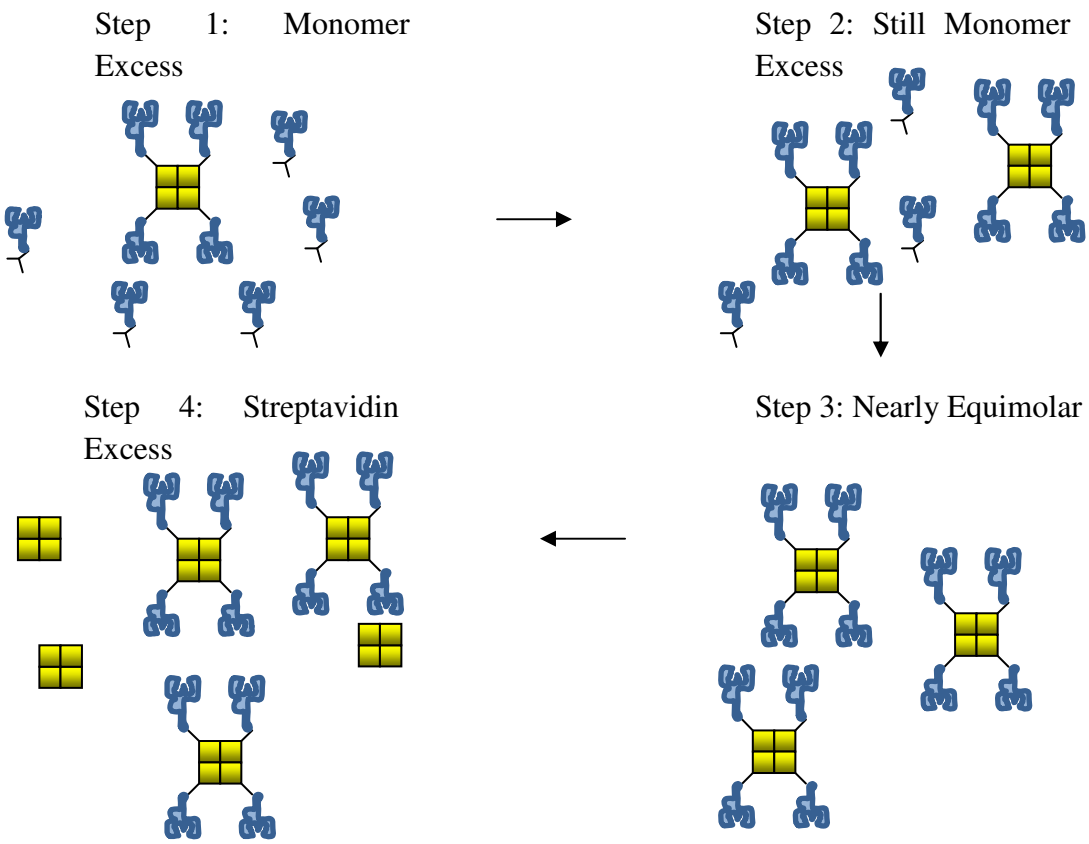

Figure 10. CD1d tetramer preparation. Step 1: The biotin binding sites on the added streptavidin are bound with biotinylated CD1d monomer to form tetramer. Excess biotinylated monomer is present. Step 2: More biotinylated CD1d monomers were bound to streptavidin, still monomer is in excess. Step 3: Almost equimolar of CD1d biotinylated monomer and strepavidin is present. Step 4: Strepavidin is in excess.

10.3 CD1d expression detection by flow cytometry

Spleen cells from db/db C57BL/6J (The Jackson lab, Stock # 000642) and WT C57BL/6J were isolated as descried above. Freshly isolated spleen cells 10^6 were suspended in 100μl of wash buffer and used for PE-anti-mCD1d (BD Science, Cat # 553846) staining. Before staining with PE-anti-mCD1d, anti-mouse CD16/32 mAb (BD Science, Cat # 553141) was applied for saturating unspecific binding. FACS data were acquired using BD-LSRII. Samples from db/dbC57BL6 (two 2months old and two12 months old mice, male only) and WT C57BL/6J (two 2months old and two 12 months old mice, male only) were examined.

11. Reverse-transcription polymerase chain reaction (RT-PCR) for detection of T-cell receptor (TCR) mRNA

11.1 T-cell repertoire analysis

RNA was isolated from sorted cells with PGPC loaded CD1d tetramer and CD3 staining double positive by using RNeasy mini kit as described above. First-strand cDNA synthesis was performed using superscript III Platinum Two-step qRT-PCR Kit as described above.

11.2 RT-PCR for detection of TCR mRNA

PCR amplification was performed as described elsewhere (86). In brief, the murine TCR repertoire was analyzed using a panel of primers specific for TCR Vα14 (5'-AGACCCAAGTGGAGCAGAGTCC-3 , 3'-ACCAGGTATGACAATCAGCTGAGTCC-5') and Vα14 paired with

Jα281(5'-GGGAGATACTCAGCAACTCTGG-3' ，
3'-TCCCAGCTCCAAAATGCAGC-5') for mouse TCR repertoire analysis. Also the single reaction GAPDH specific primer pair (5'-TGATGACATCAAGAAGGTGGTGAAG-3', 3'-TCCTTGGAGGCCATGTGGGCCAT-5') was used as an internal PCR control for verification of cDNA integrity and the fidelity of the single PCR reactions. The first PCR cycle started with 4 minutes in a hot block at 95°C and then at 95°C (15 seconds), 58°C (30 seconds) and 72°C (90 seconds) for 35 cycles. PCR products were analyzed on a high-resolving polyacrylamide gel electrophoresis system.

12. Murine models for atherosclerosis and obesity

BALB/c, CD1-/-BALB/c, C57BL/6J, ApoE-/-C57BL/6J， db/dbC57BL/6J were housed and bred under specific pathogen-free conditions in the Animal Care Facility at The University of Texas Health Science Center and all mice study protocols were approved by the Animal Welfare Committee of The University of Texas Health Science Center.

12.1 ApoE -/- Mice

ApoE is 299 amino acids long lipoprotein mainly synthesized in the liver, also found in spleen, brain and kidneys. Lipoprotein is the molecule formed when protein binds lipid. ApoE is a major lipoprotein consisting very low-density lipoproteins (VLDLs). VLDLs remove extra cholesterol from blood stream by transporting cholesterol to the liver. There are three slightly different alleles of ApoE called e2, e3

and e4 in which e3 is the most common form. ApoE-/- mouse model has hyperlipidemia and develop atherosclerosis in the early age when fed western-type diet due to lipoprotein metabolism dysfunction. The atherosclerotic plaque lesion components are similar between ApoE-/- and human. This mouse model has been used for several years to study the impact of risk factors causing atherosclerosis, and pathological mechanism during atherosclerosis. Wild type (WT) mouse strain C57BL/6JJ has a very low genetic variation between siblings. Therefore, ApoE-/- was built on this wild type mouse model.

12.2 db/db mice

Leptin can regulate fullness and energy use by binding to leptin receptor expressed in the hypothalamus. Db/db mouse has a mutation on leptin receptor causing loss of function. There is significant obesity, fasting hyperglycemia, and hyperinsulinemia in db/db mouse model. It provides an ideal diabetic atherosclerosis mouse model for studying the mechanism of diabetes-accelerated atherosclerosis and exploring the therapeutic approaches.

12.3 Blood lipid and glucose analysis

Mice were sacrificed by 100% carbon dioxide, skin was disinfected with 70% ethanol. The thoracic cavity was open and heart was completely exposed. Blood was drawn from the heart, preferably from the ventricle by using a 26 gauge needle. The blood was drawn slowly to prevent heart collapsing. Approximately 1ml blood was collected into a tube containing 10 µl heparin sodium (APP Pharmaceuticals, LLC, Schaumburg, IL Cat # 27602). Then the same volume of PBS was added and

centrifuged at a speed of 2000 rpm for 15 minutes. The supernatant was transferred to a new tube and immediately delivered for lipid and glucose level analysis (Equiche Laboratories Inc, Houston, TX).

12.4 Tissue preparation and histochemistry

Wild-type C57BL/6J and db/db/C57BL/6J mice were sacrificed following anaesthesia with intraperitoneal injection of a cocktail containing 65 mg/Kg ketamine and 13 mg/mL xylazine in sterile normal saline. The thoracic cavity was open and heart was removed. Then, the abdominal cavity was open and spleen was removed. Both harvested heart and spleen tissue were put in RNAlater RNA Stabilization Reagent (Qiagen, Cat # 76104) for further mRNA isolation. For immunohistochemistry, mice hearts were perfusion-fixed with 4% paraformaldehyde and 5% sucrose in PBS for 10 min, then embedded in optimal-cutting-temperature (OCT) compound, frozen on dry ice and stored at -70°C until sectioning. Serial 7-µm-thick sections were obtained using a sliding criotome. For immunofluorescence staining, these sections were permeabilized, blocked for 30 min in phosphate-buffered saline (PBS) containing 1% BSA, and incubated for 1 h at 4°C with primary antibody against rabbit sarcomeric α-actinin cross-reacting with mouse. After washing with PBS, heart sections were incubated with FITC-conjugated antirabbit secondary antibody. The slides were washed, mounted and viewed through a fluorescence microscope.

Heart sections were also prepared with H&E stain for structural analysis by light microscopy, with Sirius red stain to assess the presence and extent of fibrosis,

and with Oil Red O (ORO) to identify intramyocardial lipid deposition. The images of heart sections were obtained by digital camera and analyzed using the Metamorph Image System (Molecular Devices Corp., Downingtown, PA).

12.5 RNA isolation and RT-PCR analysis

RNA was isolated from mouse heart and spleen by using RNeasy mini kit as described above. First-strand cDNA synthesis was performed using iScript™ cDNA Synthesis Kit (Biorad, Cat # 1708890). The reaction system includes: 5 x iScript reaction mix 4 μl, iScript reverse transcriptase 1μl, RNA template 0.5 μg and Nuclease-free water to total volume 20 μl. Experiment was done following the reaction protocol: 5 minutes at 25°C, 30 minutes at 42°C, 5 minutes at 85°C. The specific aimed genes was analyzed using a panel of primers specific for mCD1(5'-AAGCTGGTCCCGCACAGA-3' , 3'-GCTGATGGTGGCTGAGTCATT-5'), TNFα (5'-TCGTAGCAAACCACCAAGTG-3', 3'-AGATAGCAAATCGGCTGACG-5'), TNFα receptor1(5'-CCATCTTCGGTCCTAGTAACTG-3', 3'-CAGGTTCATCTTGGAAAGCAC-5'), TNFα receptor2 (5'-GATGCCAAGGTGCCTCATG-3', 3'-GAGCTGCTACAGACGTTCACG-5'). IQSYBR Green Supermmix (Biorad, Cat # 170-8880) was applied for semi-quantitative RT- PCR. And GAPDH was used for internal PCR control. The RT-PCR reaction system consists of 25 μl reaction buffer, 200nM final concentration of forward primer and reverse primer, 50ng cDNA and ddH_2O to final volume 50 μl. Before semi-quantitation, the product annealing and melting curve were optimized.

Then Ct value is optimized by running with 3 minutes in a hot block at 95°C and then at 95°C (10 seconds), Tm°C (30 seconds) and 72°C (90 seconds) for 35 cycles. A series of sample dilutions were tested. Ideally the Ct value is linear between dilutions. With optimal Ct value and sample dilution the qRT-PCR reaction was done.

12.6 Electrophoretic Mobility Shift Assays (EMSA)

Nuclear proteins from wild-type C57BL/6J and db/db/C57BL/6J mice were extracted from snap-frozen hearts. Double-stranded NF-kB oligonucleotides (5'-AGT TGA GGG GAC TTT CCC AGG C-3' and 5'-CCT GGG AAA GTC CCC TCA ACT-3') (Promega, Madison, WI) were labeled with [γ-^{32}P]ATP. Binding reactions containing 10 μg of crude nuclear extract were performed by using an EMSA core system (Promega, Cat # E3050) according to the manufacturer's protocol. For supershift assays, goat monoclonal anti- p65 antibody (Santa Cruz, Cat # sc109) was used.

12.7 Immunoblotting of p65 NF-κB subunits

An aliquot of the nuclear extracts used for EMSA and cytosolic or total extracts were loaded on 5-10% SDS-polyacrylamide gel electrophoresis under reducing conditions and was detected by Western-blotting method as described above. The following primary antibodies were applied: 1) polyclonal anti-rabbit p65 (Santa Cruz， Cat # sc101748); 2) anti-β-actin (Sigma Aldrich, Cat # A2547); 3) anti-lamin B (Santa Cruz, Cat # sc6217).

13. Statistical Analysis

All results are presented as means ± SD. Two-group comparisons were performed

with the use of a Student t-test for unpaired values. Multiple-group comparisons were made with analysis of variance (ANOVA).A p-value less than 0.05 was considered significant. Statistical analyses were carried out with the SPSS 15.0 version software Chicago IL.

Chapter 4 Results

1. Prediction of lipid ligands for CD1d by computer stimulation

The lipid profile in atherosclerotic plaque is complex and usually classified into three derivations: cholesterol, phospholipids and fatty acid. Under oxidative stress in the local environment they undergo oxidation modification and produce more pro-atherogenic compounds. To identify possible ligands among these pro-atherogenic compounds to CD1d, a molecular modeling program SYBYL was applied to screen the three groups of compounds. Their structures are input SYBYL program and binding capacity was displayed by score: higher binding capacity corresponds to higher score (Figure 11). The result showed that phospholipids and its oxidation derivatives have the highest binding affinity. Both fatty acid and cholesterol groups were weaker than the phospholipid group (Table 1). Based on these results, I selected PGPC, PAPC as my main target ligands in my experiments, 7-K-Cho, and cholesterol were used as control ligands.

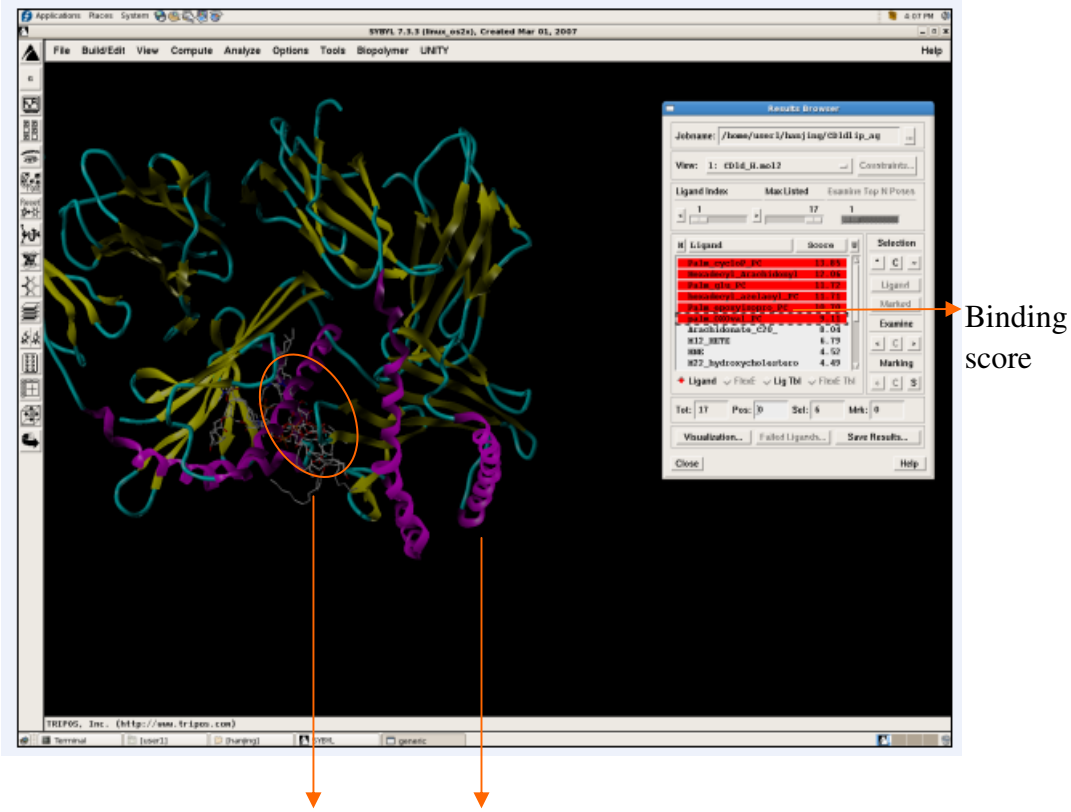

Figure 11. Predicted CD1d capacity binding to three groups of lipids by running SYBYL program. A molecular modeling program SYBYL was applied to screen all these three groups of compounds. The structures of three groups of lipids and crystal structure of CD1 is input SYBYL program. The binding capacity was displayed by score: higher binding capacity corresponds to higher score.

Group	Lipid type	Name	Binding Score	
			mCD1d	hCD1d
Group I	Phospholipid	PAPC*	9.39	8.04
	Oxidized	C16-20:4 PC	12.43	12.06
	Oxidized	POVPC	9.79	9.11
	Oxidized	PGPC*	11.02	11.72
	Oxidized	PEIPC	11.10	10.7
	Oxidized	16:0 cyclo PC	10.02	13.85
	Oxidized	Hex PC*	9.89	11.71
Group II	Arachidonic acid	AA	7.90	8.04
	Oxidized	12-HETE	7.74	6.79
	Oxidized	8-isPGE2	6.19	4.01
	Oxidized	HNE	7.30	4.52
Group III	Cholesterol	Cho*	2.56	2.62
	Oxidized	22-OHC	1.42	4.49
	Oxidized	7-k-cho*	3.49	3.52
	Oxidized	25-OHC	3.41	3.06

Star marked lipids chosen in the following experiments

Table 1. Assessment of CD1d binding to three groups of lipids by computer molecular stimulation . By using SYBYL program the binding capacity of three groups of lipids with CD1d was displayed by score: higher binding capacity corresponds to higher score. Among these groups of lipids, phospholipids and their oxidation derivatives have the highest binding capacity. Both fatty acid and cholesterol groups were weaker than the phospholipid group.

The binding capacity is mostly decided by crucial residues in CD1d since the hydrogen network is mainly accounted for the interaction between ligands binding to CD1d (Figure 12). The summary of these crucial residues in CD1d is displayed in table 2. Mouse and human CD1d are very similar in terms of structure and crucial binding sites. The only difference is tryptophan in human CD1d at position 153 and glycine at corresponding site in mouse. This difference does not influence ligand binding.

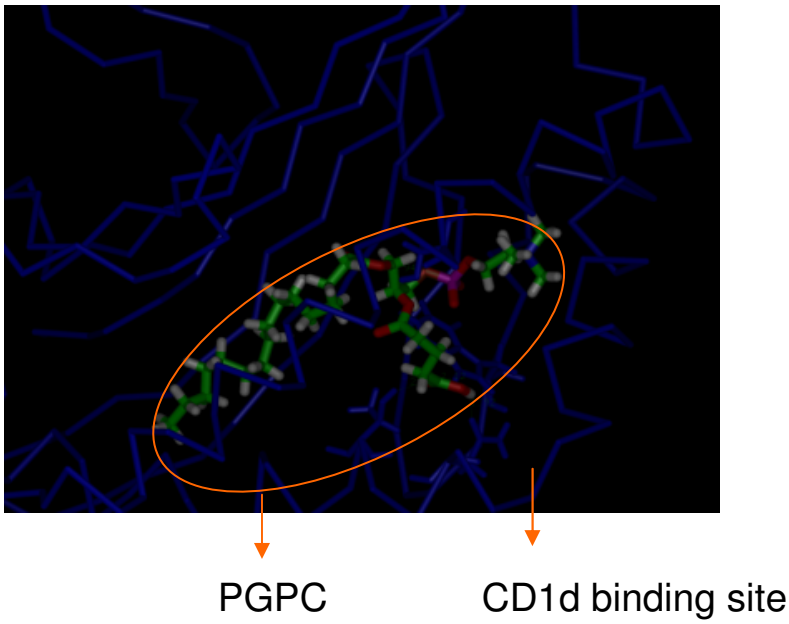

Figure 12. Prediction of interaction between CD1d and lipid. The binding capacity is mostly decided by crucial residues in CD1d since the hydrogen network is mainly accounted for the interaction between ligands binding to CD1d.

Lipid name	Key binding sites	
	mCD1d	hCD1d
PAPC	Thr177 , Thr 173	Thr177 , Thr 180
PGPC	Thr177 , Thr 173	Thr177 , Thr 180, Ser 99, Asn134
7-K-cho	Glu156	Glu150
Chol	None	None

Table 2. Key binding sites between CD1d and lipids. Mouse and human CD1d share similar crucial binding sites in PGPC, PAPC and Chol.

2. Detection of lipids by GC/MS in murine plasma.

Based on the computer prediction results, GC/MS was applied for detecting the lipid levels in plasma of BALB/c mice. My results showed PAPC, PGPC, 7K and Chol can all be detected in the plasma of wild type (WT) BALB/c mice (Figure 13). The presence of these lipids in mice plasma indicated the potential biological effect of these lipids in mice.

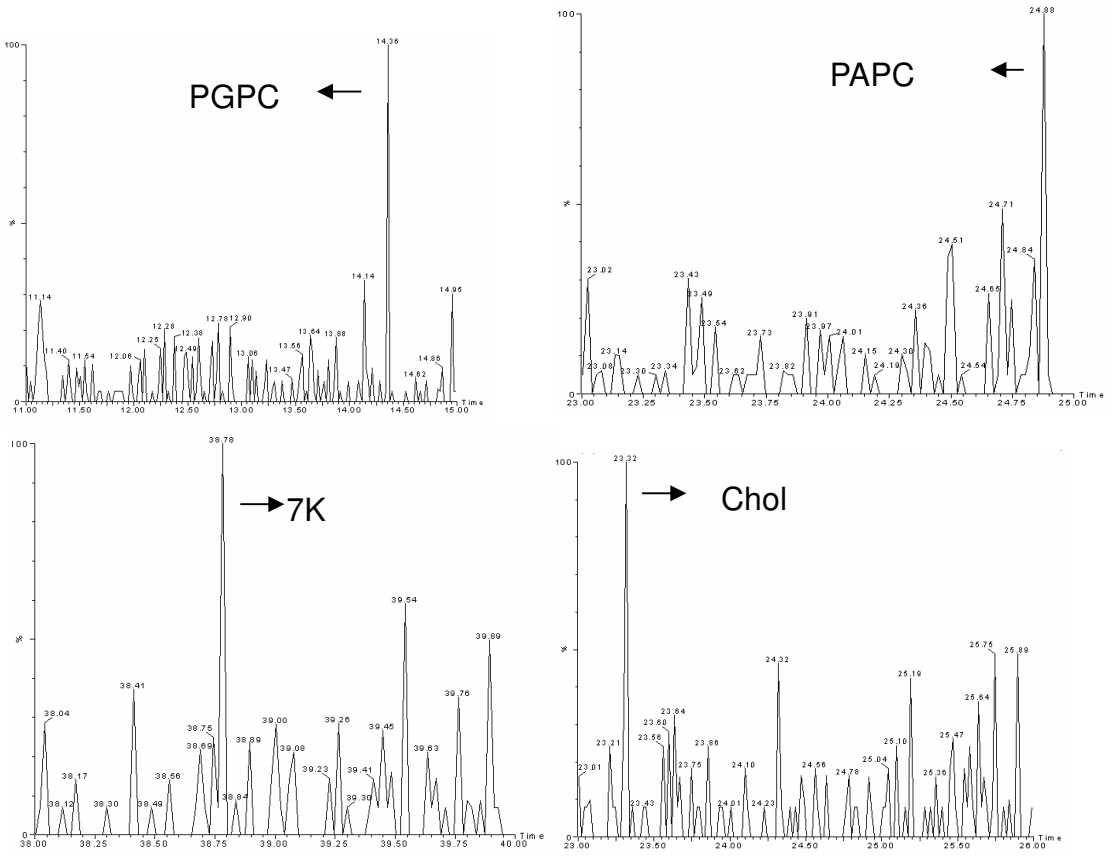

Figure 13. GC/MS analysis of presence of PGPC, PAPC, 7-K and Chol in the plasma of BALB/C mice

By applying GC/MS the BALB/c mice plasma was analyzed, certain levels of PGPC, PAPC, 7K and Chol were all detected.

3. Biology analysis of potential lipid ligands to CD1d by lipid binding assay

Based on computer prediction results, biology analysis of these lipid ligands is further applied. As mentioned above, little difference exists between human and mouse CD1d in term of ligand binding theoretically. Our computer prediction results is in accordance. Therefore, in first part of the experiment, mouse CD1d was tested. Results showed that mCD1-HEK293 cells have higher ^{3}H-7-K-Cho binding than untransfected HEK293 cells (Figure 14). Addition of excess PGPC but not cholesterol can inhibit ^{3}H-7K-Cho binding in mCD1-HEK293 cells. These results are in liner with computer prediction results. Therefore, in further experiments I continued testing PGPC, PAPC as my main target ligands, 7-K-Cho and cholesterol were used as control ligands.

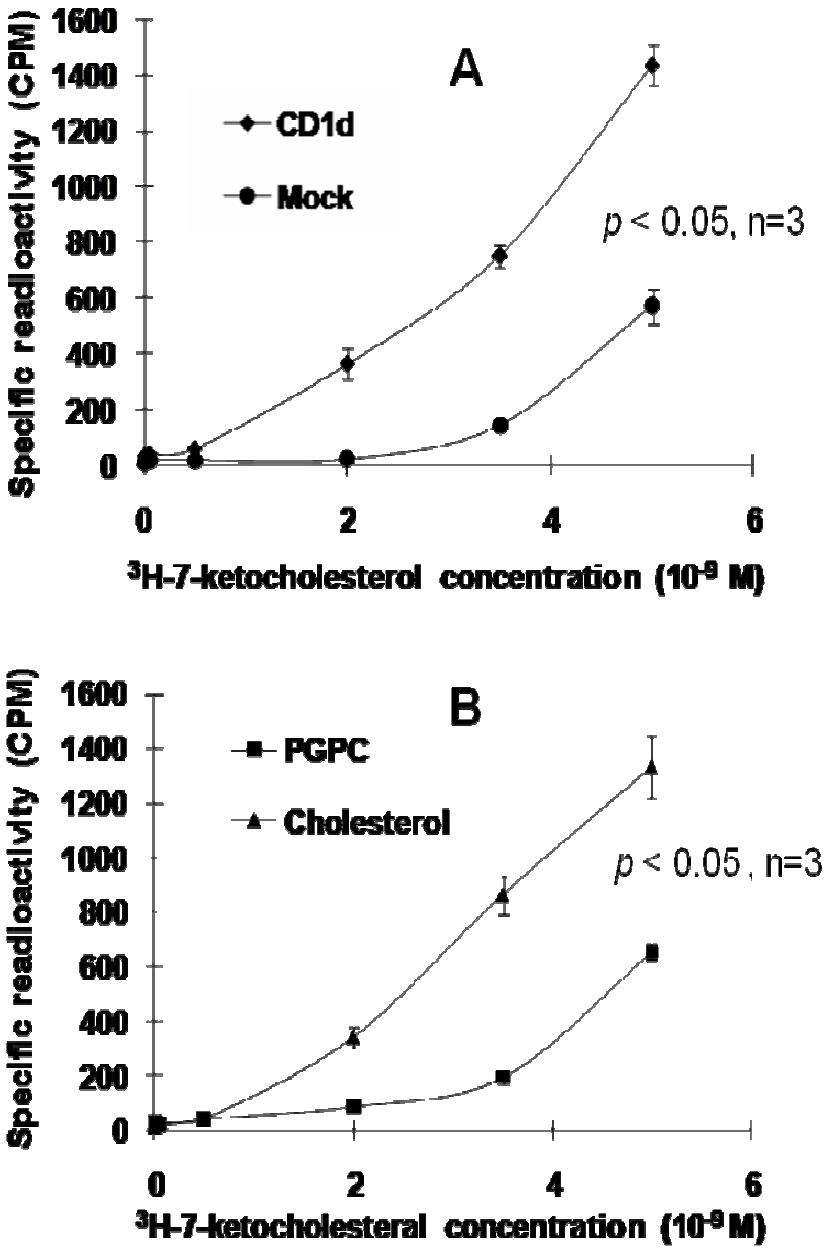

Figure 14. ^{3}H-7-K-Cho binding to CD1d in the presence or absence of PGPC and free cholesterol. Results showed that CD1d transfected HEK293 cells have higher ^{3}H-7-K-Cho binding than untransfected HEK293 cells. Addition of excess PGPC but not cholesterol could inhibit ^{3}H-7K-Cho binding in mCD1d stable cell lines.

4. CD1d-mediated lipid accumulation in spleen derived macrophages and CD1d transfect Hela cells (hCD1d-Hela) incubated with PGPC

Lipid uptake and accumulation in mouse splenocytes were analyzed by fluorescence scanning confocal microscopy after staining with Nile Red, a lipid-binding fluorochome. The presence of hCD1d in hCD1d-Hela was proved by fluorescence observation and Western-blotting analysis (Figure 15). GFP was observed in both hCD1d-GFPN3 and GFPN3 plasmid transfected Hela cells. It indicates the successful transfection of plasmids into cells. By applying Anti-GFP antibody there was 72 KD protein detected in hCD1d-GFPN3 transfected Hela cells, while 34 KD protein was detected in GFPN3 transfected Hela cells. It indicated the presence of GFP in both transfected Hela cells. By applying anti-CD1d antibody there was still 72 KD protein detected in hCD1d-GFPN3 transfected Hela cells, while no protein was detected in GFPN3 transfected Hela cells. Therefore, hCD1d fused with GFP was successfully expressed in Hela cells.

Under baseline conditions, without PGPC treatment, there was a weak signal for Nile Red staining in the cytoplasm of splenocytes (Figure 16a). However, when the cells were incubated with 4.8 μg/ml PGPC for 24 hours there was a substantial increase of Nile Red related fluorescence as visualized by fluorescence scanning confocal microscopy. The increased cellular Nile Red lipid stains existed not only in the cytoplasm of splenocytes incubated with PGPC, but also was patched on the cellular membrane (Figure 16b). Interestingly, the PGPC-associated lipid uptake and accumulation was diminished in the splenocytes of CD1-/- mice (Figure 16c). In Hela

cells transfected with hCD1d an increased level of cellular Nile Red lipid stains was observed when treated with 4.8 μg/ml PGPC. In Mock-Hela cells fewer stains was detected under confocal microscopy. The stains existed in both cytoplasm and the cellular membrane of PGPC treated hCDd-Hela cells, similarly to the distribution in splenocytes (Figures. 16d-f). The analysis of Nile Red intensity also showed higher level in PGPC treated CD1+/+ mouse splenocytes compared to untreated CD1+/+ mouse splenocytes, or treated CD1-/- mouse splenocytes (Figure. 16f). Thus, CD1 expression contributes to the uptake and accumulation of PGPC.

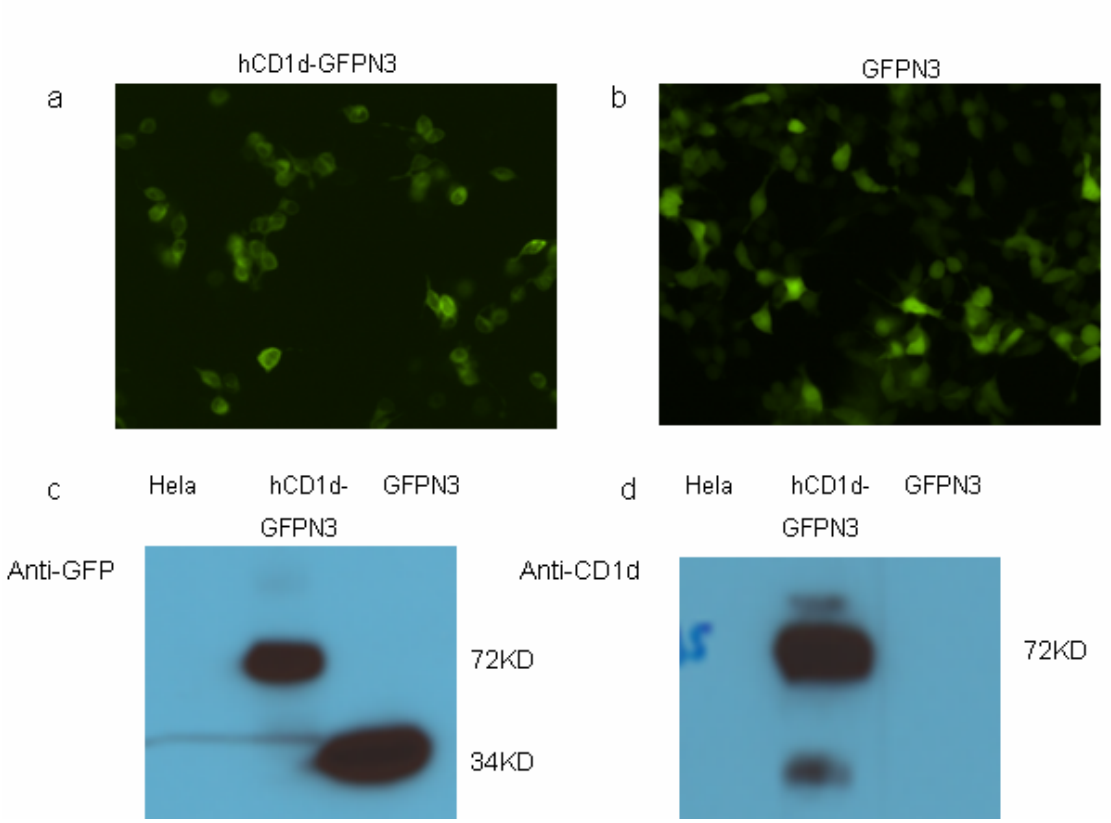

Figure 15. Expression of hCD1d-GFP fusion protein in Hela cells transfected with hCD1d-GFPN3. a, b GFP was observed in both hCD1d-GFPN3 and GFPN3 plasmid tranfected Hela cells. It indicates the successful transfection of plasmids into cells. c, d. By applying Anti-GFP antibody there was 72 KD protein detected in hCD1d-GFPN3 transfected Hela cells, while 34 KD protein was detected in GFPN3 transfected Hela cells. It indicated the presence of GFP in both transfected Hela cells. By applying anti-CD1d antibody there was still 72 KD protein detected in hCD1d-GFPN3 transfected Hela cells, while no protein was detected in GFPN3 transfected Hela cells. Therefore, hCD1d fused with GFP was successfully expressed

in Hela cells.

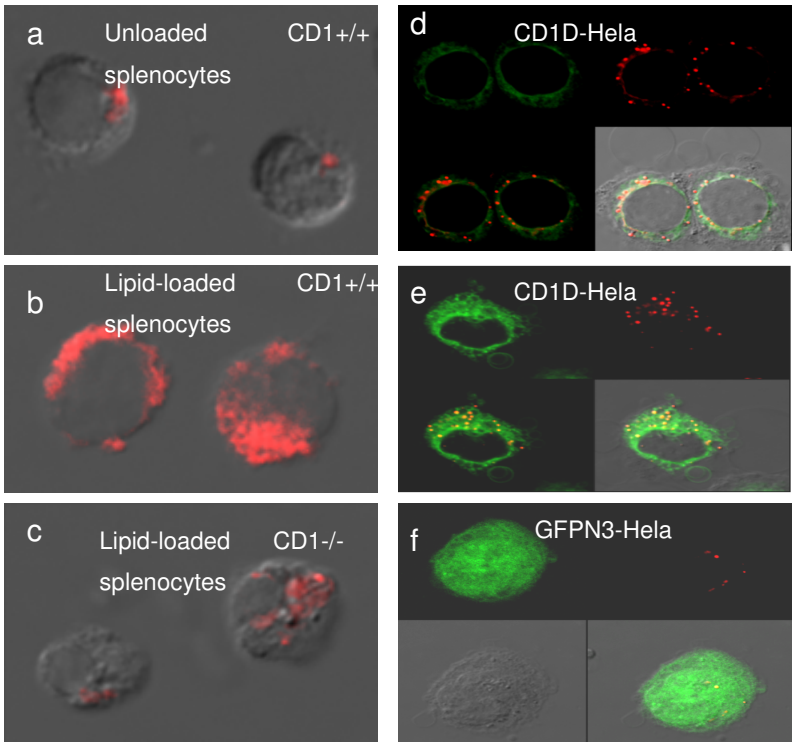

Figure 16. Nile Red fluorescence in CD1+/+ mouse splenocytes and hCD1d-Hela cells incubated with or without PGPC. A weak signal for Nile Red staining in the cytoplasm of splenocytes was detected (a). A substantial increase of Nile Red related fluorescence as visualized by fluorescence scanning confocal microscopy when cells were incubated with 4.8 μg/ml PGPC for 24 hours. The increased cellular Nile Red lipid stains existed not only in the cytoplasm of splenocytes incubated with PGPC, but also was patched on the cellular membrane (b). Interestingly, the PGPC-associated lipid uptake and accumulation was diminished in the splenocytes of CD1-/- mice (c). In Hela

cells transfected with hCD1d an increased level of cellular Nile Red lipid stains was observed when treated with 4.8 μg/ml PGPC. In Mock-Hela cells fewer stains was detected under confocal microscopy. The stains existed in both cytoplasm and the cellular membrane of PGPC treated hCDd-Hela cells, similarly to the distribution in splenocytes (d-f). The analysis of Nile Red intensity also showed higher level in PGPC treated CD1+/+ mouse splenocytes compared to untreated CD1+/+ mouse splenocytes, or treated CD1-/- mouse splenocytes (a-c).

5. PGPC as a potential ligand for CD1d stimulating CD1d-restricted T cells

5.1 Stimulation of mCD1d-restricted T cells by PGPC

T0 specifically test PGPC as a ligand for CD1d, mCD1d transfected HEK293 stable cells were used as APCs. The mCD1d stable cells were incubated with 0-15μg/ml PGPC O/N then added to NKT hybridoma DN32.D3 cells. mCD1-HEK293 cells were loaded with lipid particals and "touching reaction" was observed between mCD1-HEK293 and DN32.D3 in both PGPC and 7-K-Cho treated groups. ^{3}H thymidine was used for measuring the proliferation of NKT cells. In mCD1-HEK293 cells high thymidine uptake occured in PGPC, PAPC and positive control α-GC stimulated groups (Figure 17a). Moreover, 15μg/ml PGPC and 15μg/ml PAPC groups showed higher stimulation compared to untransfected 293 cells ($P<0.05$, $n=3$) (Figure 17a).

Cytokines secreted in the above assay were also detected. Both Th1/Th2 cytokines (IL-4, IL-5, TNF-α, IFN-γ) were detected in all lipids treated cells after 24 hours. PGPC, PAPC treated mCD1-HEK293 had higher cytokine secretion tendency compared with 7-K-Cho, Chol. My data show that the level of TNF-α was the highest, following by IFN-γ during all cytokines detected.

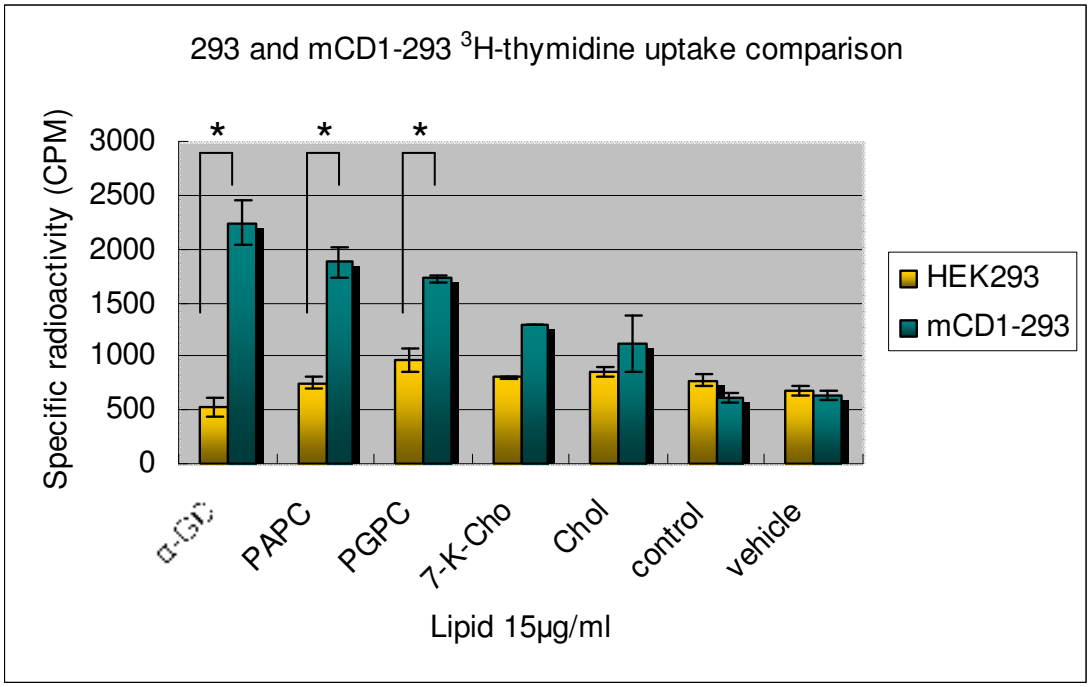

Figure 17. Comparison in thymidine incorporation between NKT hybridoma cells co-cultured with lipid treated 293 and mCD1-293. a. Measurement of proliferation of NKT cells stimulated by lipid treatment. In mCD1-HEK293 cells high thymidine uptake occured in PGPC, PAPC and positive control α-GC stimulated groups. Moreover, 15 μg/ml PGPC and 15 μg/ml PAPC showed higher stimulation compared to untransfected 293 cells (* $P<0.05$, n=3). Control group: Mock-293 cells; Vehicle: ethanol treated mCD1-293 cells.

5.2 Induction of CD1d expression in natural CD1d+ antigen presenting cells

CD1d+ APCs in PBMCs include monocytes and macrophages. These cells have been proved certain CD1d expression. As a specific receptor for lipids, CD1d expression is assumed to be enhanced after treated with lipids. There is higher induction of CD1d in PAPC and PGPC treated PBMCs compared with 7-K-Cho and Chol groups (Figure 18). Positive control α-GC treated PBMCs showed induction of CD1d compared to control. Similar to PGPC, Hexadecyl Arachidonyl PC (HexPC) is one kind of oxidized PAPC, while HexPC group was not as high as the PGPC/PAPC group (Figure 18).

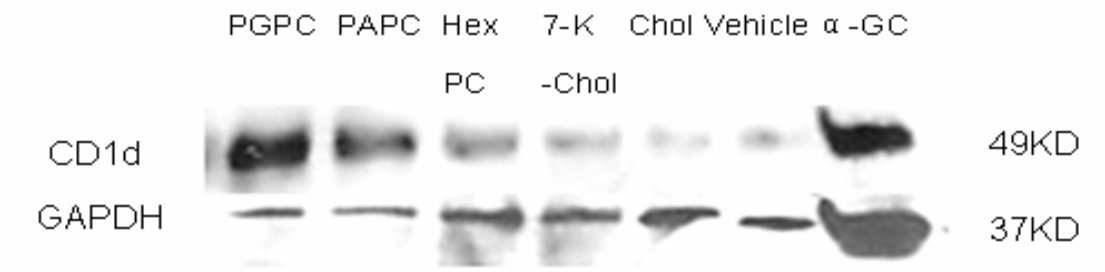

Figure 18. Western- Blotting assay for CD1d and GAPDH in lipid treated PBMCs. Higher induction of CD1d in PAPC and PGPC treated PBMCs compared with 7-K-Cho and Chol groups. Positive control α-GC treated PBMCs showed induction of CD1d compared to control. Similar to PGPC, HexPCgroup was not as high as the PGPC/PAPC group.

6. CD1d-mediated splenocytes responses to oxidized phospholipids

For identifying the role of CD1d in PGPC stimulated T cells reaction, WT BALB/c and CD1-/-BALB/c mice were used for this experiment. In BALB/c spleen cells the highest ^{3}H thymidine uptake occured in PGPC, PAPC and positive control α-GC stimulated groups (Figure 19a). BALB/c spleen cells had the highest thymidine uptake when stimulated with 7.5μg/ml PGPC, 3.75μg/ml PAPC, while in the CD1-/-BALB/c group this effect was not observed (Figure 19b).

a

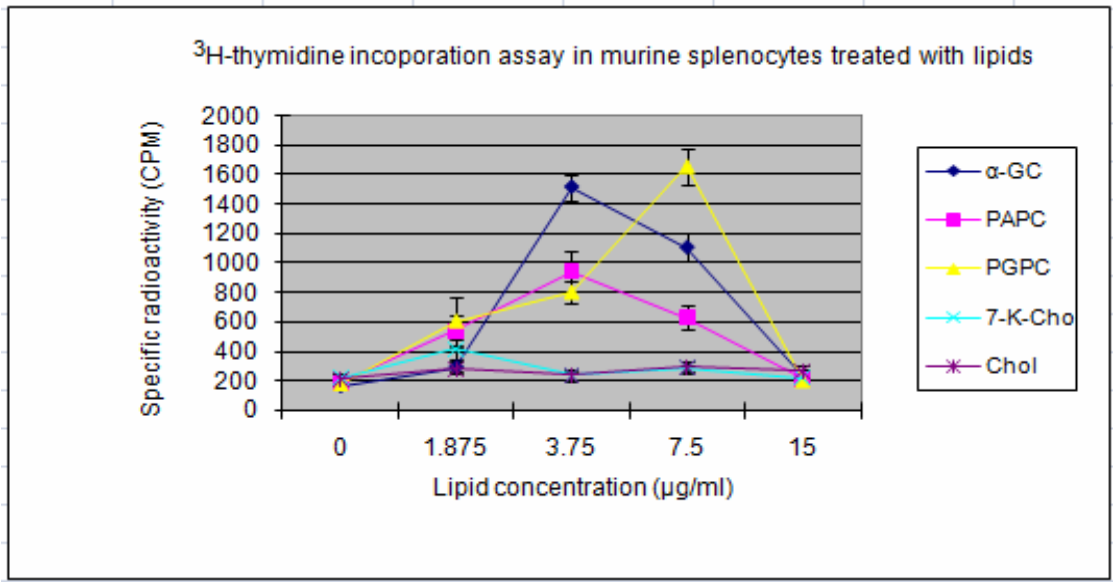
3H-thymidine incoporation assay in murine splenocytes treated with lipids
Specific radioactivity (CPM)
2000
1800
1600
1400
1200
1000
800
600
400
200
0
0
1.875
3.75
7.5
15
Lipid concentration (µg/ml)
α-GC
PAPC
PGPC
7-K-Cho
Chol

b

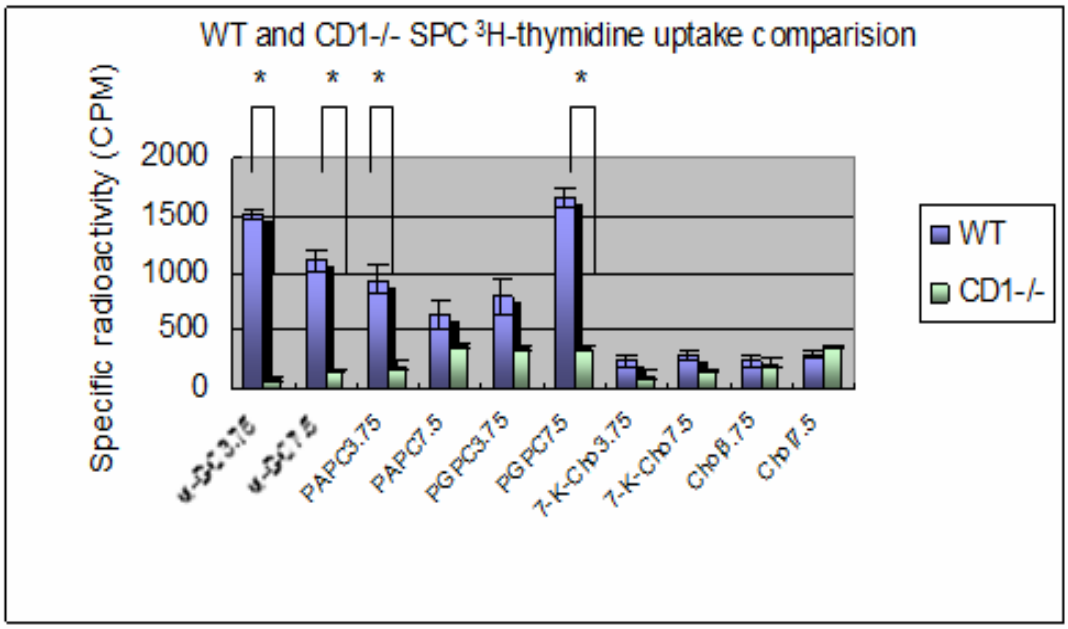
WT and CD1-/- SPC 3H-thymidine uptake comparision
Specific radioactivity (CPM)
2000
1500
1000
500
0
*
*
*
*
PAPC3.75
PAPC7.5
PGPC3.75
PGPC7.5
7-K-Chb3.75
7-K-Chb7.5
Chob.75
Chb7.5
WT
CD1-/-

Figure 19. Comparison in thymidine incorporation between CD1-/- BALB/C and BALB/C splenocytes. a. Measurement of proliferation of splenic cells stimulated by lipid treatment. In BALB/c spleen cells the highest ^{3}H thymidine uptake occured in PGPC, PAPC and positive control α-GC stimulated groups. b. BALB/c spleen cells had the highest thymidine uptake when stimulated with 7.5 μg/ml PGPC, 3.75 μg/ml PAPC, while in CD1-/- BALB/c group this effect was not observed. (n=3, * $p<0.05$)

In order to observe the immune response of PGPC *in vitro*, spleen cells from BALB/c mice, as well as CD1-/- mice were stimulated with different concentrations of PGPC. Proliferation of spleen cells was dose-dependent, in corresponding to range from 0 μg/ml to 9.6 μg/ml. The optimal stimulation dose was 4.8 μg/ml. However, there was no significant proliferation index observed in CD1-/- spleen cells group (Figure 20a). The production of IFN-γ showed the same tendency (Figure 20b). For PAPC there were no significant difference of proliferation and IFN-γ production observed between CD1+/+ and CD1-/- spleen cells (Figure 20a, b).

a

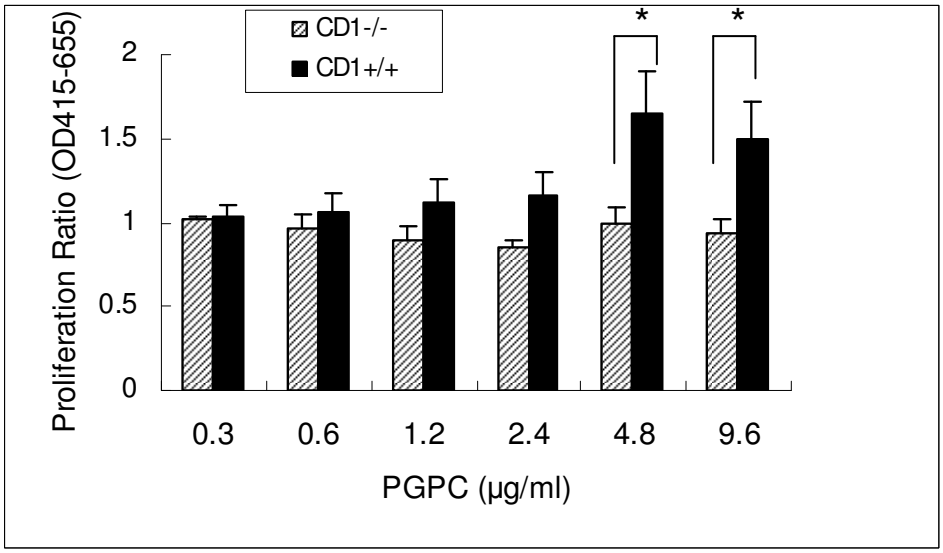
CD1-/-
CD1+/+
Proliferation Ratio (OD415-655)
2
1.5
1
0.5
0
*
*
0.3
0.6
1.2
2.4
4.8
9.6
PGPC (μg/ml)

b

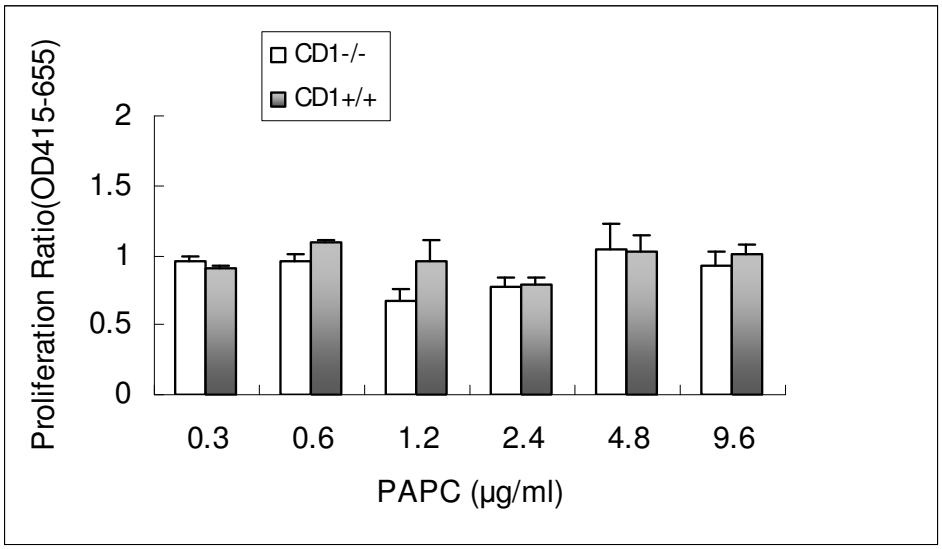
CD1-/-
CD1+/+
Proliferation Ratio(OD415-655)
2
1.5
1
0.5
0
0.3
0.6
1.2
2.4
4.8
9.6
PAPC (μg/ml)

c

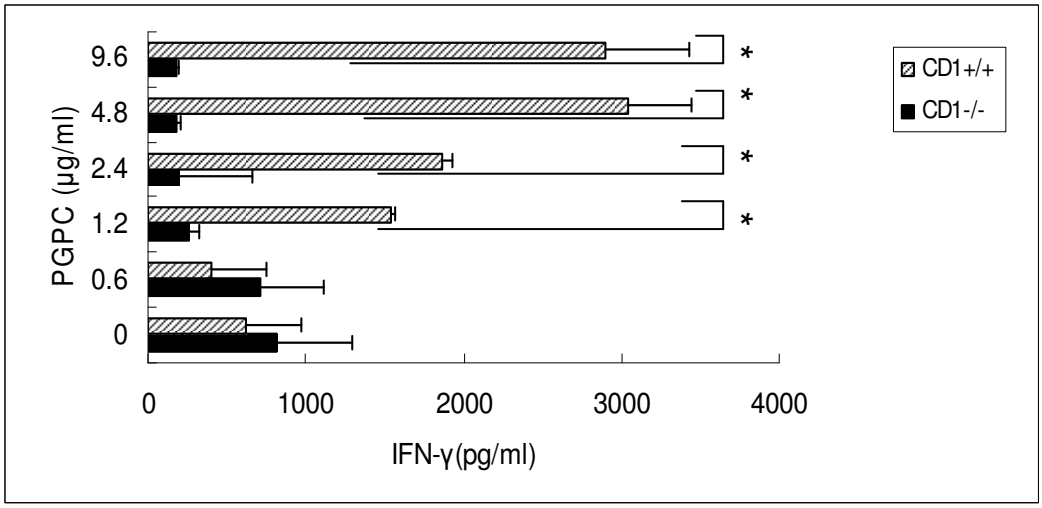

d

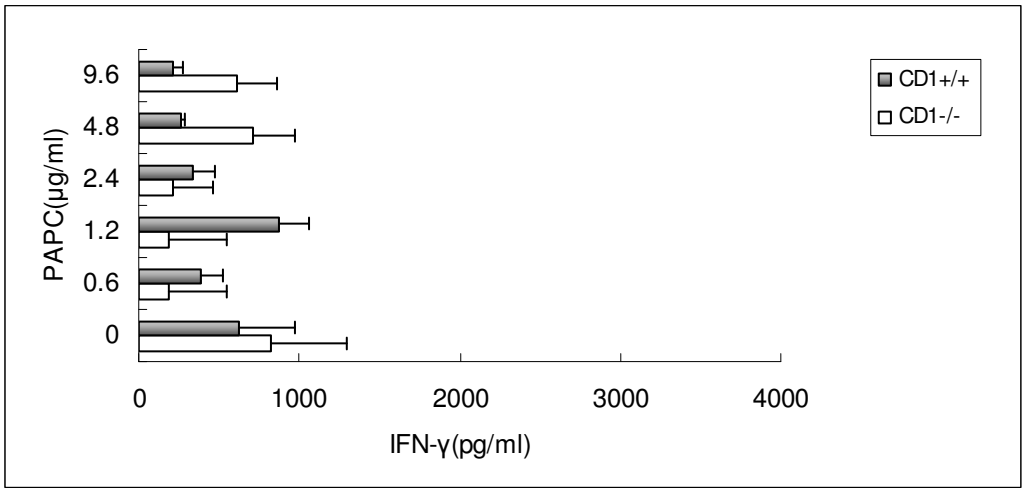

Figure 20. The response of PGPC was CD1d mediated. PGPC and PAPC were used to stimulate spleen cells from BALB/c and mCD1d-deficient mice *in vitro*. Fresh

splenic cells from BALB/c or CD1-/-BALB/c $4x10^5$ were plated in 96-well plate and pulsed with 0.3-9.6 μg/ml PGPC/PAPC. a, b. After 72 hours of culture, spleen cell proliferation was measured (n=4). c, d. After 48 hours of culture, supernatants were collected and IFN-γ production was measured (n=2). (* $p<0.05$）

7. Detection of cell type producing IFN-γ stimulated with PGPC

To further identify IFN-γ secreting cells, we treated BALB/c spleen cells with 4.8μg/ml PGPC for 24 hours and stained these cells with anti-IFN-γ-Alexa647 and anti-CD3-FITC antibodies. The IFN-γ secreting cell group was mostly detected in CD3+ positive cells in both α–GC and PGPC treated cells (Figure 21 a). Approximately 1.43 ± 0.17% (n=3) of the CD3 positive cells were secreting IFN-γ after PGPC treatment. In contrast, only 0.24 ± 0.06% (n=3) of the cells secreting IFN-γ were detected in the vehicle group (Figure 21 b). Only 0.38 ± 0.31 % (n=3) of CD3 negative cells produced IFN-γ after PGPC treatment. When CD3 negative cells was treated with α–GC, only 0.33 ± 0.13% (n=3) of IFN-γ secreting cells were detected.

a

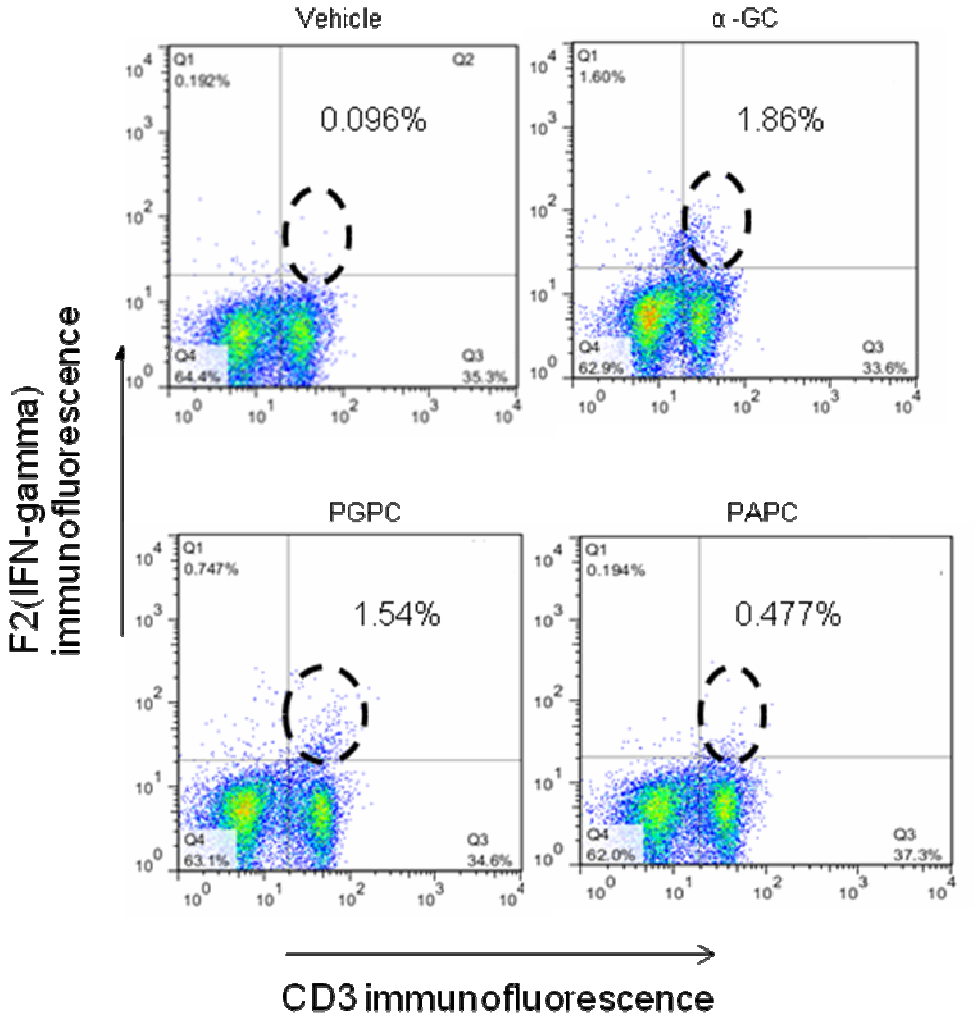
Vehicle
α -GC
PGPC
PAPC
0.096%
1.86%
1.54%
0.477%
F2(IFN-gamma) immunofluorescence
CD3 immunofluorescence

b

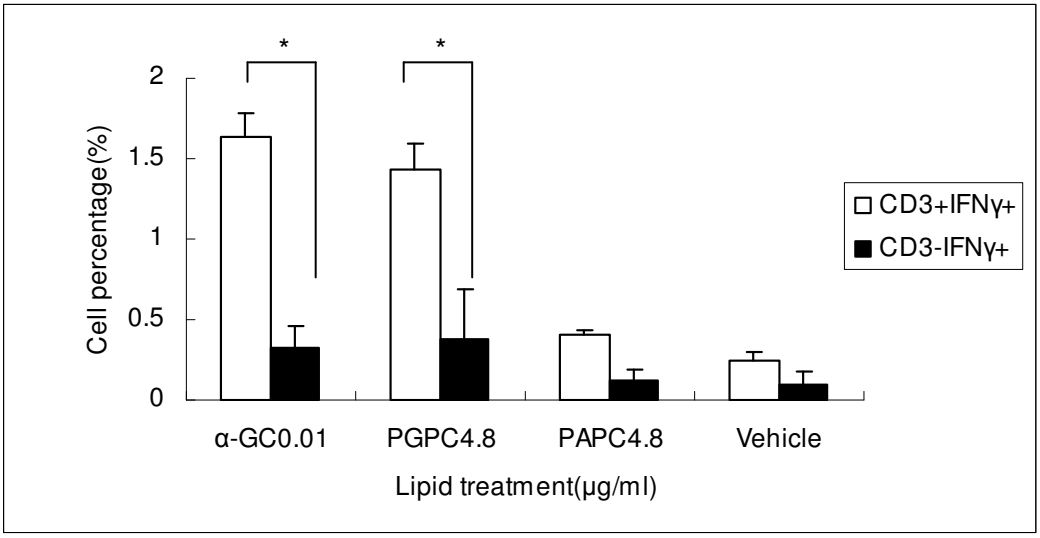

Figure 21. Responder T cells in lipid treated BALB/c spleen cells. 10^7 BALB/c spleen cells were treated with 4.8 μg/ml PGPC and collected for FACS analysis after 24 hours. Anti-IFN-γ-Alexa647 and anti-CD3-FITC antibodies were applied for double staining after cells were fixed by 4% formaldehyde and permeabilized with 90% methanol. a. Q2 percentage stands for the percentage of IFN-γ secreting cells in CD3+ cells. b. The positive IFN-γ secreting cells were analyzed and compared between CD3+ and CD3- cells.

8. Presence of PGPC reacting CD1-restricted T cells in ApoE-/- mice and WT mice

To examine the population of reactive NKT cells in mouse, we stained spleen cells from ApoE-/- C57BL/6J and WTC57BL/6J with PGPC-loaded mCD1d-tetramers. There was clear staining of CD3+ cells stained by PGPC-loaded mCD1d-tetramers. In spleen cells from WT mice only 0.9 ± 0.3% (n=3) (Figure 22, Q2) of the T cells were stained with PGPC-loaded mCD1d tetramers, and 0.9 ± 0.23% of T cells stained with PGPC-loaded mCD1d tetramers was found in ApoE-/- mice spleen cells (n=3)

.

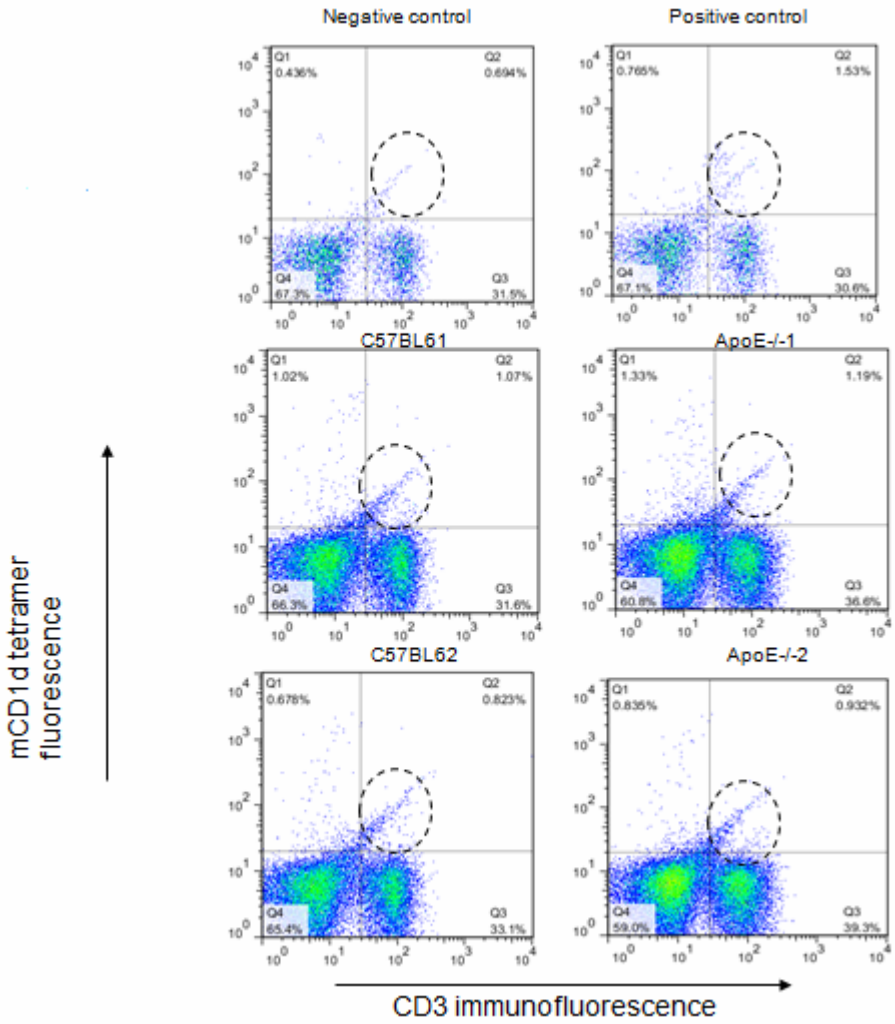

Figure 22. Flow cytometry of CD1d-tetramers loaded with PGPC stained CD3+T cells. CD1d-tetramers loaded with PBS-57 (+), unloaded CD1d-tetramer (-) were also used as controls to stain ApoE-/- and C57BL/6J spleen cells. Numbers in the quadrant correspond to percent cells out of total CD3+ cells and data shown are gated live cells (n=3).

9. **Analysis of TCR repertoire**

To further characterize the responder T cells to PGPC, we sorted CD3 and CD1d tetramer double positive cells from ApoE-/- CD57BL/6 and WT CD57BL/6 mouse spleen cells and applied RT-PCR to analyze T cell receptor repertoire. Our results revealed these sorted cells are Vα14, Jα281 positive for mouse T receptor (Figure 23). These data showed that PGPC reacted T cells are TCR Vα14, Jα281 NKT subgroup in mouse.

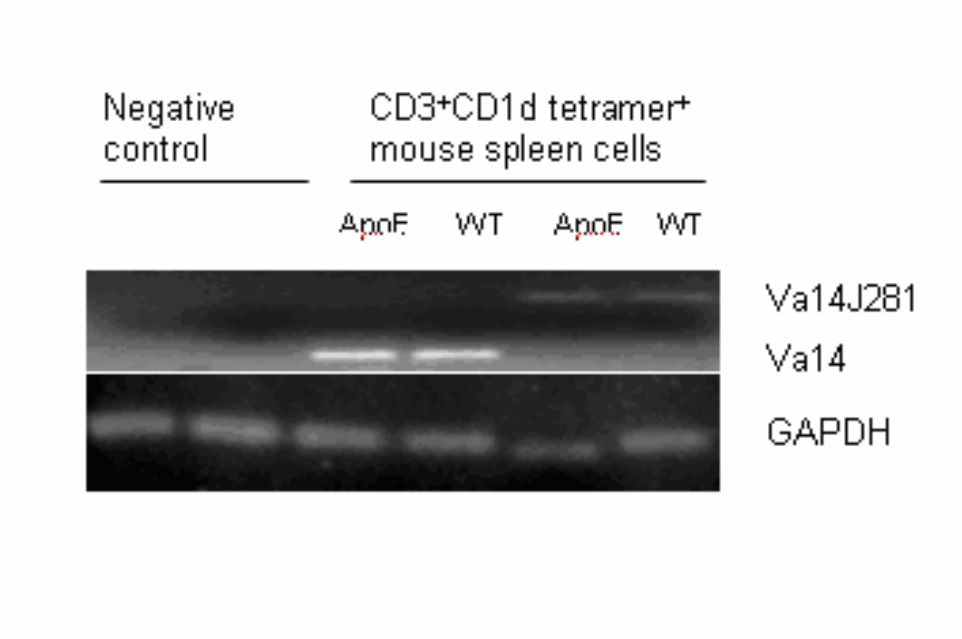

Figure 23. RT-PCR analysis of TCR repertoire in ApoE-/- and WT C57BL/6J mice. ApoE-/- C57BL/6J and WT C57BL/6J mouse spleen cells were stained with PGPC loaded mouse CD1d-tetramer and mCD3. Double positive cells were collected by flow cytometry sorting and total RNA was extracted and analyzed by RT-PCR by using V α 14.2, J α 281 primer pairs. GAPDH was used as a control. Negative control: murine embroynic stem cells.

10. Development of hyperlipidemia and hyperglycemia in db/db mice

To testify the lipid level in the db/db mouse model, fresh blood was used for analysis of lipid profile and glucose level. Results are shown in Table 3. There was significant body weight (BW) ($P<0.01$, n=3) and heart weight (HW) ($P<0.05$, n=3) increase in db/db compared to WT. All lipid levels increased in db/db compared to WT, among triglyceride at very high level 769 ± 206 (n=3). LDL, cholesterol and VLDL in db/db mice also increased significantly compared to WT ($P<0.01$, n=3). Therefore, hyperlipidemia exists in db/db mouse model.

Table 3. Physiological and biochemical parameters in db/db and C57BL/6 mice

	db/db	*C57BL/6*
Body weight (g)	76 ± 5**	22 ± 4
Heart weight (g)	0.4 ± 0.05*	0.1 ± 0.03
HW-BW ratio	0.005 ± 0.05*	0.004 ± 0.00
Glucose (mmol/L)	120 ± 8**	19 ± 2
Total cholesterol (mmol/L)	251 ± 53**	45 ± 7
Triglycerides (mg/dL)	769 ± 206**	61 ± 5
LDL cholesterol (mg/dL)	154 ± 41**	21 ± 2
VLDL cholesterol (mg/dL)	62 ± 7*	24 ± 3

Data are means ± SD. *P < 0.05, **P < 0.01 n=3 db/db vs C57BL/6 mice.

Legend: HW, heart weight; BW, body weight; LDL low density lipoprotein;

VLDL, very low density lipoprotein.

Table 3. Lipid profiles and glucose levels in serum of db/db C57BL/6J and C57BL/6JJ mice. There was significant body weight (BW) (P<0.01, n=3) and heart weight (HW) (P<0.05, n=3) increase in db/db compared to WT. All lipid levels were increased in db/db compared to WT among triglyceride at very high level 769±206 (n=3). LDL, cholesterol and VLDL in db/db mice also increased significantly compared to WT (P<0.01, n=3).

11. Different expression of CD1d between db/db and C57BL6 spleen cells

CD1 expression on db/db C57BL6 and WT C57BL6 spleen was detected by anti-mCD1 mAb conjugated with PE as shown in Figure 24a, b. The analysis revealed higher level of CD1 expression in spleen of 2 months old db/db mice (56.9± 2.3%, n=3) compared to WT mice (42.8± 5.8%, n=3), not observed in spleen of 12 months old mice. Interestingly, the CD1 expression was found decreased in 12 months old db/db mice spleen (45.8± 6.6%, n=3) compared to 2 months old db/db mice. In addition, we observed CD1 mRNA level on db/db and WT mice spleen. As shown in Figure 24c, there is 1.34 fold increased CD1 mRNA expression in db/db mice spleen after normalization with GAPDH.

a

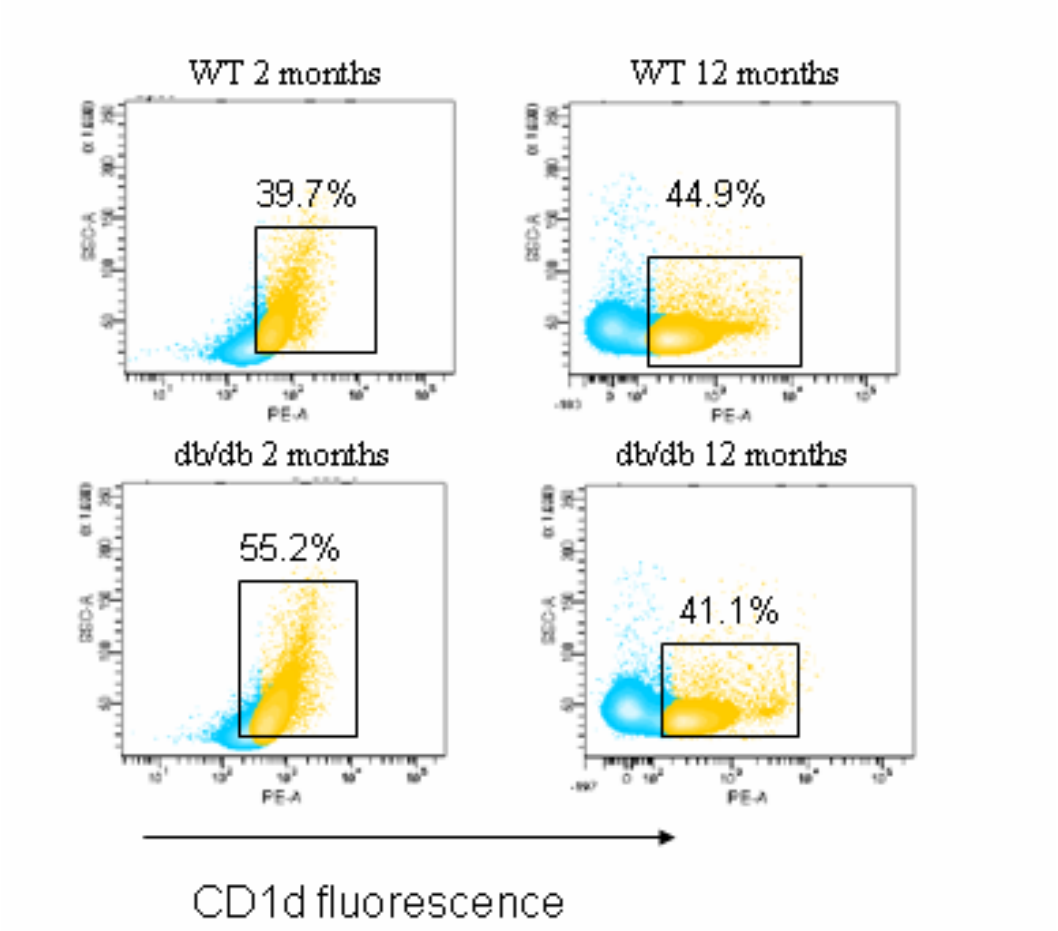
WT 2 months
39.7%
WT 12 months
44.9%
db/db 2 months
55.2%
db/db 12 months
41.1%
SSC-A
PE-A
CD1d fluorescence

b


CD1 expression on db/db and WT mouse spleen cells
CD1 expression (%)
70
60
50
40
30
20
10
0
*
2 months
12 months
WT
db/db

c

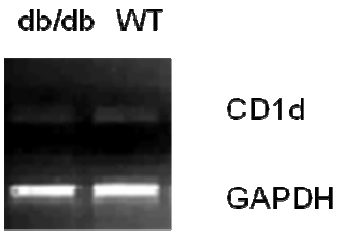
db/db WT
CD1d
GAPDH

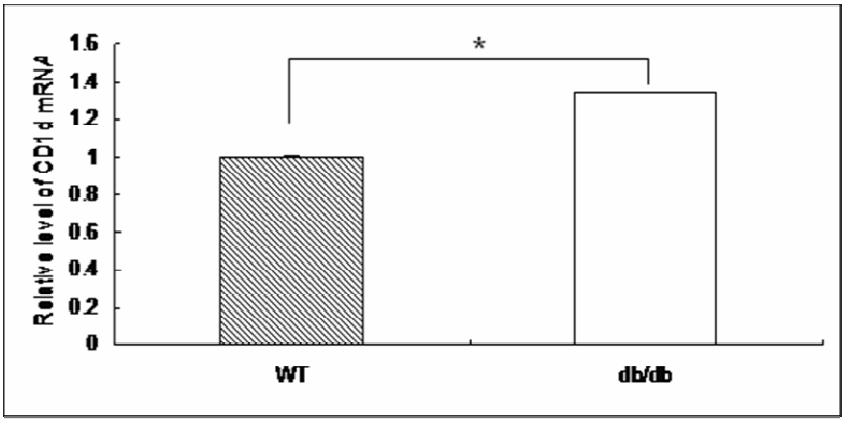
Relative level of CD1d mRNA
1.6
1.4
1.2
1
0.8
0.6
0.4
0.2
0
*
WT
db/db

Figure 24. Comparsion of CD1 expression in spleens of db/db and WT mice. The analysis revealed higher level of CD1 expression in spleen cells of 2 months old db/db mice (56.9± 2.3%, n=3) compared to WT mice (42.8± 5.8%, n=3), which is not observed in spleen cells of 12 months old mice. Interestingly the CD1 expression was found decreased in 12 months old db/db spleen cells (45.8± 6.6%, n=3) compared to 2 months old db/db mice. In addition, we observed CD1 mRNA level on db/db and WT spleen cells. As shown in figure 23 (c), there is 1.34 fold increased CD1 mRNA expression in db/db spleen cells after normalization with GAPDH. * $p<0.05$, n=3.

12. Increased TNFα expression in db/db spleen cells and TNFα receptor1 in cardiac cells

The TNFα mRNA expression in db/db spleen cells was detected by quantitative RT-PCR and showed 6 folds increase of TNFα expression in db/db spleen cells compared to WT spleen cells (Figure 25a). We further detected TNFα receptor1 and TNFα receptor2 mRNA expression in cardiac cells of db/db and WT mice. Only TNFα receptor1 mRNA had 4.89 folds increase in db/db cardiac cells compared to WT (Figure 25b), no significant TNFα receptor2 mRNA expression difference was found between db/db and WT cardiac cells.

a

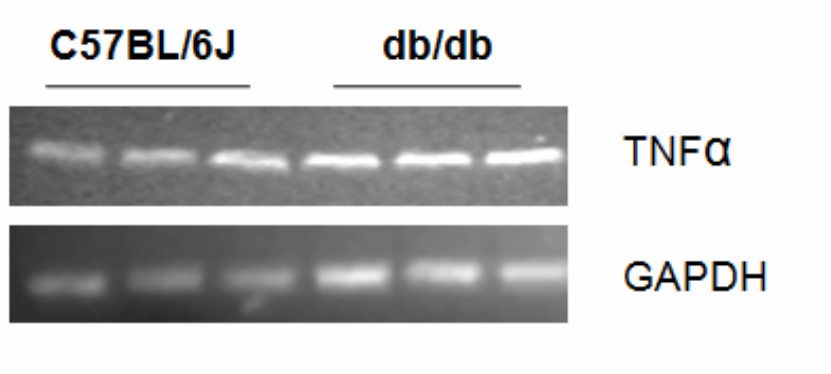
C57BL/6J
db/db
TNFα
GAPDH

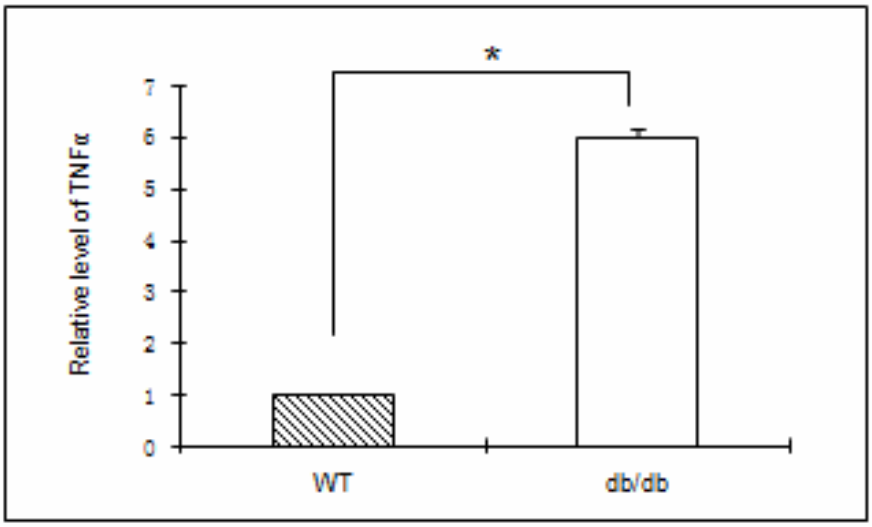
*
Relative level of TNFα
0
1
2
3
4
5
6
7
WT
db/db

b.

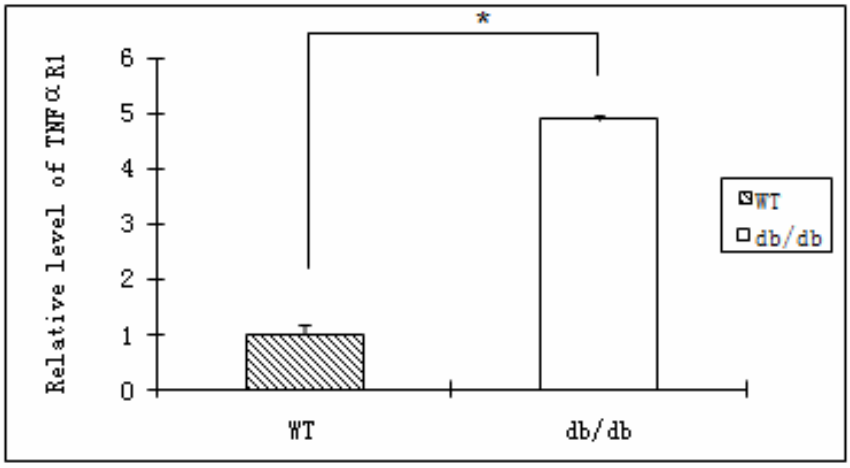

Fig 25. Expression of TNF α in db/db and WT spleen and TNF α R1 in db/db and WT heart. The TNFα mRNA expression in db/db spleen cells was detected by quantitative RT-PCR and showed 6 folds of increased TNFα expression in db/db spleen cells compared to WT spleen cells (a). We further detected TNFα receptor1 and TNFα receptor2 mRNA expression in cardiac cells of db/db and WT mice. Only TNFα receptor1 mRNA had 4.89 folds increase in db/db cardiac heart tissue compared to WT (b). No significant TNFα receptor2 mRNA expression difference was found between db/db and WT cardiac cells.

13. Lipid accumulation and NF-kB activity in hearts of db/db mice.

Insulin resistance is frequently associated with lipid deposition in nonadipose tissue. Db/db mice showed significantly larger fatty liver and lipid accumulation in hearts (Figure. 26a) compared with C57BL/6J mice (Figure. 26e). In the db/db mice there was no apparent cardiac hypertrophy (Figure 26b) or fibrosis (Figure. 26d) compared with C57BL/6J mice (Figure. 26f and h). Immunofluorescence staining for sarcomeric markers such as α-sarcomeric actinin (a crucial Z-disc protein that cross-links sarcomeric actin) revealed sarcomeric integrity with the absence of cardiac anomalies including loss of muscle striation or pathological myofibre disarray in the diabetic hearts (Figure. 26c) as well as C57BL/6J mice (Figure. 26g).

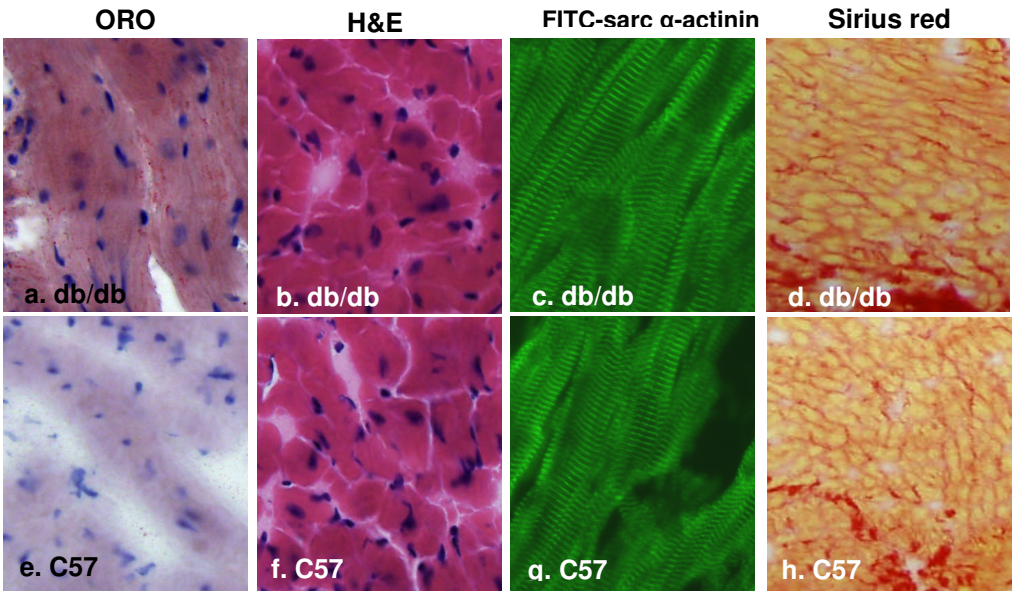

Figure 26. **Histochemistry of heart sections from db/db and WT mice.** db/db mice showed significantly larger fatty liver and lipid accumulation in hearts (a) compared with C57BL/6J mice (e). In the db/db mice there was no apparent cardiac hypertrophy (b) or fibrosis observed (d) compared with C57BL/6J mice (f and h). Immunofluorescence staining for sarcomeric markers such as α-sarcomeric actinin (a crucial Z-disc protein that cross-links sarcomeric actin) revealed sarcomeric integrity with the absence of cardiac anomalies including loss of muscle striation or pathological myofibre disarray in the diabetic hearts (c) as well as C57BL/6J mice (g).

The nuclear transcription factor NF-κB binds to the promoter critical for the transcription of many proinflammatory genes. We examined the expression and activation of NF-κB in the hearts of adipose diabetic (db/db) and nondiabetic control mice, by using the gel shift assay with a with a ^{32}P end-labeled NF-κB oligonucleotide. The nuclear proteins were isolated from nitrogen snap-frozen hearts and subjected to EMSA for NF-kB activity. As shown in Figure. 28 a, NF-kB binding activity is low in age-matched normal hearts but significantly increased in db/db hearts (Figure 27a, lanes 1-4 vs. 5-8). The specificity of the NF-κB DNA protein complex formation was verified by cold oligonucleotides and by the addition of anti-p65 NF-κB antibody which super-shifted the bands of NF-κB/DNA complexes (lanes 1, 3, 5, 7). Antibody to p65/RelA was capable of supershifting a portion of the protein binding to the DNA, indicating the involvement of, but not limited to p65 subunit in the activation of NF-kB transcriptional in the db/db hearts. There was no significant binding with the oligonucleotide probe alone or by omitting protein substrate. Levels of p65 subunit were determined by Western blot in db/db in comparison with their respective background wild-type C57BL/6J. Nuclear levels of p65 in db/db mice and nondiabetic C57BL/6J control mice reflected the NF-kB binding activity data (Figure 27b). The total protein content of NF-κB p65 (Figure 27b) subunit was similar in hearts from db/db mice and nondiabetic C57BL/6J controls. Interestingly, immunoblotting demonstrated decreased nuclear accumulation of NF-κB p65 subunit in the hearts of CD1d-knockout compared with control mice (Figure 27c). The presence of NF-κB p65 subunit was highly detectable in cytosolic extracts from CD1d-knockout mice

(Figure 27c), indicating the lack of cytosolic-nuclear redistribution of p65 and therefore no activation of canonical NF-κB in the absence of CD1d.

a

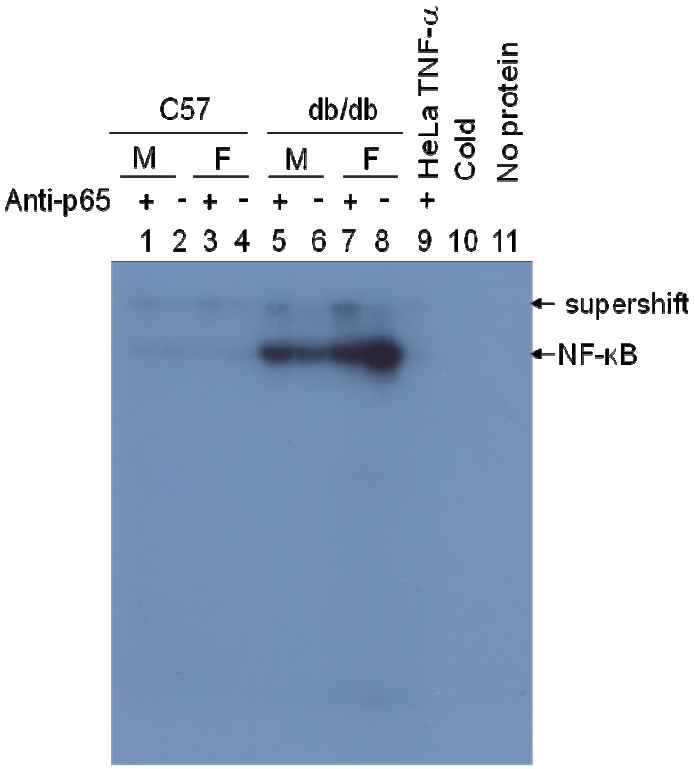
C57
db/db
M
F
M
F
HeLa TNF-α
Cold
No protein
Anti-p65 + - + - + - + - + + +
1 2 3 4 5 6 7 8 9 10 11
supershift
NF-κB

b

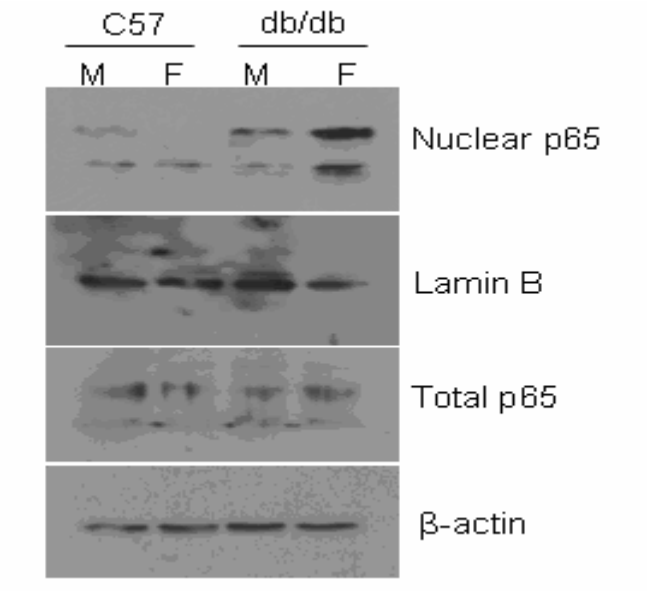
C57
db/db
M
F
M
F
Nuclear p65
Lamin B
Total p65
β-actin

.

c.

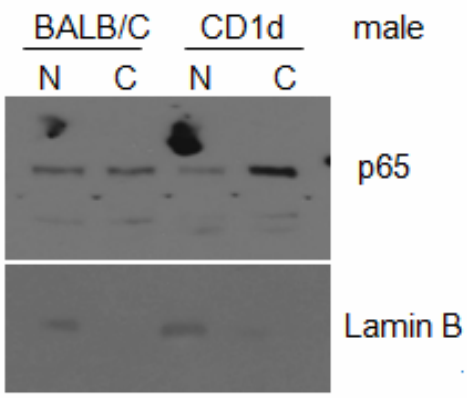

Figure 27. NF-κB activity in hearts of db/db mice. As shown in Figure. 28 a, NF-kB binding activity is low in age-matched normal hearts but significantly increased in db/db hearts (lanes 1-4 vs. 5-8). The specificity of the NF-κB DNA protein complex formation was verified by cold oligonucleotides and by the addition of anti-p65 NF-κB antibody which super-shifted the bands of NF-κB/DNA complexes (lanes 1, 3, 5, 7). There was no significant binding with the oligonucleotide probe alone or by omitting protein substrate. Levels of p65 subunit were determined by Western blot in db/db in comparison with their respective background wild-type C57BL/6J. Nuclear levels of p65 in db/db mice and nondiabetic C57BL/6J control mice reflected the NF-kB binding activity data (b). The total protein content of NF-κB p65 (b) subunit was similar in hearts from db/db mice and nondiabetic C57BL/6J controls. The immunoblotting demonstrated decreased nuclear accumulation of NF-κB p65 subunit in the hearts of CD1d-knockout compared with control mice and NF-κB p65 subunit was highly detectable in cytosolic extracts from CD1d-knockout

mice (Figure 27c).

Chapter 5: Discussion

1. Identification of ligands for CD1d related in atherosclerosis

My study has identified PGPC as a novel lipid autoantigen recognized by CD1-restricted T cells. As atherosclerosis is considered as inflammation, my finding revealed that atherosclerosis is an autoimmune disease. The lipid components in atherosclerotic plaque are complexe. SYBYL program filters the lipid component as possible ligands for CD1d. In recent years, increasing numbers of ligands of CD1d have been studied. Most studies were based on individual analysis and testing. The screening method by applying SYBYL is novel in terms of exploring CD1d ligands. This method is repeatable, low cost and in line with biological results, which was proved through biological experiment results. Although this software analysis is theoretical, the needs for biological tests are requested. For CD1d, hydrogen bond is the main force between ligand and CD1d binding site. Therefore, my analysis is mainly based on hydrogen bond analysis, which neglects other interaction forces. To some extent, this method is not appropriate for comparing the capacity of similar ligands. In my study, PAPC and its oxidative product PGPC showed very close binding score. They were both tested in later biological experiments.

Among the three groups of lipids phospholipids, fatty acid and cholesterol and their oxidation products, phospholipids and its oxidative phospholipids has shown highest binding capability to CD1d followed by arachidonic acid group and the cholesterol group. Phospholipids are the main component of cell membrane and circulating LDL. In atherosclerosis, phospholipids are prone to be oxidized under the

oxidative stress. My findings revealed high possibility of phospholids and oxidative phospholipids as ligands for CD1d. In atheroma there is high level of detected oxysterols. High cholesterol in the blood stream is the main risk for developing atherosclerosis. When cholesterol is deposited and modified by oxidative stress, it becomes the target of local APCs like DCs and SMC. The expression of CD1d on these APCs indicates that oxysterols could be ligands for CD1d in athersoclerosis. Nonetheless, my results showed very low binding capacity of CD1d to this group of lipids. Past studies have found that cluster of differentiation 36 (CD36) could be the main receptor for oxysterols.

Fatty acid and its oxidation products also exist in atherosclerotic plaque. In contrast to OxPLs and oxysterols, oxidized fatty acids play less important role in atherosclerosis development due to their low amount and weaker atherogenic role. The binding score showed comparatively lower binding strength between CD1d and this group of lipids. Hence, OxPLs are strong candidates as ligands for CD1d in atherosclerosis according to SYBYL program predicted results.

In terms of the receptors related to phospholipids, several ligands have been found to be involved in binding to OxPLs. The scavenger receptor CD36 has been identified as a receptor for OxPAPC. CD36 is mainly expressed on monocytes, platelets and erythrocytes in vessels. Oxidized lipids mainly locate in atherosclerotic plaque, where main CD36 positive cells are SMCs. SMCs turns into foam cells after uptaking oxidized lipids. OxPLs could be the potential ligand for CD36 expressed on SMCs in late stage of atherosclerosis. Another potential receptor TLR can be detected

on monocytes/macrophages and DCs. In atherosclerotic plaques TLR1, 2, 4 have been detected in both human and mice samples, and induced by IL-1 (58). Hence, there is possibility that OxPLs are presented by TLR and contribute to the development of atherosclerosis.

My results also showed a close binding score between hCD1d and mCD1 in most lipids. The structures of human CD1d and mouse CD1 are very similar. The only difference is that tryptophan at position 153 in human isoform is replaced by glycine 155, which does not affect binding capability. Previous studies showed that mouse CD1 can activate human CD1d-restricted T cells and vise versa. Therefore, my results are consistent with previous studies.

The phospholipid PAPC oxidation products are the main components activating endothelial-monocyte interaction in MM-LDL (49, 88). When human aortic endothelial cells (HAECs) were treated with OxPAPC an IL-8 synthesis was observed. This cytokine is one of the main signals for monocyte transmission into vessels (60). In atherosclerotic plaques, accumulated PAPC oxidation derivatives can be detected. Pidkovka and co-workers found that OxPAPC can cause phenotypic switching of SMCs and contribute to the progression of atherosclerosis (89, 90). Earlier reports have indicated that apoptotic cells contain higher level of PAPC oxidation derivatives (91). The apoptotic cells attract more monocytes and lymphocytes leading to an "inflammation burst". Furthermore, the retained OxPLs can activate platelets and cause thrombosis, which is a crucial step in the progression of atherosclerosis (62). The PAPC oxidation product, PGPC is an effective component of OxLDL causing

atherosclerotic plaque. During atherosclerosis progression, apoptotic cells become another origin for PGPC. Previous studies have suggested that CD1d-restricted T cells aggravate atherosclerosis in the mouse model. The natural antigens presented by CD1d to T cells are critical in atherosclerosis progression and new therapeutic targets can be explored based on identified natural antigens.

As mentioned above there are several lipid transporters responsible for the translocation through the lipid bilayer. My data shows that there is an increased level of PGPC uptaken by CD1+/+ mouse spleen cells compared to CD1-/- (Figure 3). Also, CD1d transfected Hela cells showed an increased uptake of PGPC compared to mock Hela cells. These data suggested that CD1d functions as an important transporter for PGPC into the cells.

Based on computer prediction and GC/MS analysis of lipids in BALB/c mice plasma, PAPC and PGPC were further tested on HEK293 stably expressing mCD1. There is higher ^{3}H-7-K-Cho binding in mCD1d stably expressed HEK293 compared to HEK293. The CD1d expression is very low in untransfectted HEK293. The high binding of ^{3}H-7-K-Cho that occurred in mCD1d-HEK293 indicates an important role of CD1d in lipid binding. Since the binding assay was carried out in cold temperature, lipid uptake effect is mostly blocked due to “low mutability” of the cell membrane. The binding effect was observed in the greatest extent. Therefore, even low score has been predicted by molecular modeling analysis，the binding between CD1d and ^{3}H-7-K-Cho was observed in my experiments. When PGPC was added into mCD1d-HEK293 before ^{3}H-7-K-Cho, there was very low binding of ^{3}H-7-K-Cho

detected. I presumed that PGPC has stronger binding capacity with CD1d than 7-K-Cho. In contrast, the addition of Chol before ^{3}H-7-K-Cho can not block the binding of ^{3}H-7-K-Cho to CD1d. As predicted by SYBYL, the binding score of Chol with CD1d was very low. Over all, the lipid binding assay further proved that PGPC is a possible ligand for CD1d.

When lipid is presented by CD1d to CD1d-restricted T cells, T cells are activated and release cytokines. The activation of T cells can be measured by thymidine uptake. The incorporation of thymidine mainly reflects the proliferation of T cells as thymidine is the material for synthesizing DNA. We used mCD1-HEK293 as APCs and treated with lipids for O/N. Then DN32.D3 was used as effector T cells and co-cultured with lipid treated mCD1-HEK293.

Thymidine uptake assay results demonstrated that high thymidine uptake occurred in PGPC, PAPC and positive control α-GC treated mCD1-HEK293 cells. When comparing to untransfected HEK293, 15μg/ml PGPC and 15μg/ml PAPC treated mCD1-HEK293 groups showed higher stimulation. This further proved the important role of CD1d in stimulating CD1d-restricted T cells. Compared to 7-K-Cho and cholesterol, PGPC and PAPC are stronger in stimulating T cells, consistent with lipid binding results. Only 100 ng/ml α-GC is enough to stimulate CD1d-restricetd T cells, while 15μg/ml PGPC or 15μg/ml PAPC is needed for the highest stimulation of T cells. The ligand α-GC is derived from marine sponge and does not exist in human body. It is mostly synthesized and has a very specific binding effect to CD1d. PGPC is found mainly in atherosclerotic plaques; therefore most likely contribute to activate T

cells, leading to atherosclerosis.

Besides the thymidine uptake assay, the measurement of cytokine secretion provides proof of activation of T cells. My results showed very low secretion of cytokines including IL-4, IL-5, IFN-γ and TNF-α in all lipids treated HEK293. In lipids treated mCD1-HEK293, PGPC, PAPC and 7-K-Cho all above four cytokines have been detected with TNF-α as the highest, followed by IFN-γ, IL-5 and IL-4. PGPC and PAPC treated groups had higher cytokines secretion than 7-K-Cho. This result further proved the strong effect of PGPC and PAPC in activating CD1d-restricted T cells. The higher secretion of IFN-γ and TNF-α means the inflammatory effect is the main consequence of T cell activation.

Since PAPC and PGPC have been found as strong ligands for CD1d, the induction of CD1d by this group of lipids further proved a possible amplification effect. Western blot results showed stronger induction of CD1d protein in PGPC, PAPC and HexPC treated PBMCs compared to 7-K-Cho and Chol treated PBMCs. The induction of CD1d may exemplify the ligand-CD1d presentation effect and activate more CD1d-restricte T cells. Due to mixed cell components in PBMCs, no exact cell types were identified as induced cell origin. It is postulated that CD1d positive APCs are the main cell sources for the enhanced CD1d.

2. CD1d mediated immune reactions in atherosclerosis

NKT hydrioman DN32.D3 can be activated by phospholipids treated mCD1d-HEK293 as proved by cell proliferation and cytokine secretion. As CD1d is

transfected into HEK293, the role of CD1d observed is magnified and PGPC as a ligand of CD1d may be amplified. In order to further prove the PGPC ligand effect and test that PGPC caused T cell activation is CD1d medicated, CD1-/- was applied in a series of experiments.

In the measurement of proliferation of WT and CD1-/- splenic cells in response to lipid treatments by thymidine uptake assay, only α-GC, PGPC and PAPC groups had strong proliferation at both concentrations of 3.75 μg/ml and 7.5 μg/ml (Figure18). In α-GC group, 3.75μg/ml is enough to get highest stimulation of splenic cells, while in PGPC group, 7.5μg/ml had higher stimulation than 3.75μg/ml. This result is consistent with previous mCD1-HEK293 thymidine uptake results. PAPC group was not observed as strong stimulation as PGPC, which is consistent with previous results.

In addition to measuring the proliferation by thymidine uptake assay, cell proliferation was also measured using Quick cell proliferation assay. This assay is based on the cleavage of the tetrazolium salt to formazan by cellular mitochondrial dehydrogenase. Therefore, the dye generated by this cleavage is directly proportional to the number of live cells. The result also showed robust response of BALB/c mouse spleen cells to PGPC, which indicated that PGPC acts as an important antigen for T cells. The absence of response in CD1-/- mouse spleen cells treated with PGPC further implies that the effect is CD1d dependent. Currently, two families of self antigens have been known to stimulate T cells: sphingolipids and phospholipids (92). Gumperz et al found that murine CD1d-restricted T cells recognize cellular lipids (47).

Our results are consistent with these results. Moreover, we identified the lipid autoantigen presented by CD1d related to atherosclerosis. In my experiment, the WTBALB/c splenic cells responded to PGPC dose dependently (0.3-9.6μg/ml), among which the highest splenic cell proliferation occurred at 4.8μg/ml. The optimal PGPC stimulation concentration is lower in WT splenic cells (4.8μg/ml) than mCD1-HEK293 (7.5μg/ml). This can be partially explained by highly expressed CD1d in mCD1-HEK293 than WT splenic cells, since the former is mCD1d fully expressed and the latter is mixed cells with only percentage cells expressing mCD1d. We observed only a minor effect of PAPC in causing murine T cells proliferation similar to above results.

I demonstrated that PGPC not only can induce proliferation of mouse spleen cells, but it also stimulated cytokine secretion. In PAPC treated splenic cells, there was low level of IFN-γ production, suggesting that OxPLs may mediate inflammatory effects occurred in atherosclerotic plaques. It is consistent with a previous study in which Melian et al found the increased expression of CD1d in human atherosclerotic plaques (25). Moreover, Yeh et al has indicated that PAPC has no effect in the induction of IL-8 in both human aortic endothelial cells and Hela cells. Other reports indicate that iNKT can cause plaque neovascularization and destabilization in human atherosclerosis by releasing IL-8 (93, 94). We did not measure IL-8, a potential cytokine associated with atherosclerosis, but we will consider measuring it in a future study. Chiappori et al found that a phospholipid [phosphatidylethanolamine (PTY)] is a ligand for endothelial protein C receptor (EPCR), a CD1-like transmembrane

glycoprotein regulating protein C (PC) pathway and produces anticoagulant, anti-inflammatory, and anti-apoptotic effects (95). These reports, together with our data, suggest that PGPC may act as a ligand for EPCR and induce inflammatory effect similar to CD1d.

There are several lipid transporters responsible for the translocation through the lipid bilayer. We show that there is an increased level of PGPC that is taken in by CD1+/+ mouse spleens cells compared to CD1-/-. Also, CD1d transfected Hela cells showed an increased uptake of PGPC compared to mock Hela cells. These data suggest that CD1d functions as an important transporter for PGPC into the cells. Furthermore, we detected that the IFN-γ secreting cells consisted mainly of T cells. Effector T cells secret inflammatory molecules and directly contribute to the progression of atherosclerosis. IFN-γ secreted by T cells after stimulated with PGPC revealed the pathological significance of PGPC related to atherosclerosis. It is also interesting that a robust IFN-γ secretion was observed when cells were treated with 1.2 μg/ml of PGPC. The earlier detection of IFN-γ compared to proliferation may be due to method sensitivity, or that IFN-γ signaling precedes the response of PGPC stimulation.

T cells are usually considered as effector cells for antigens presented by CD1d. CD3 is part of TCR on mature T cells. Therefore, anti CD3 antibody was applied in order to identify if T cells are IFN-γ secreting cells. The result showed higher double staining of CD3 and IFN-γ in both α-GC and PGPC groups than PAPC (Figure 20 a, b). This result further proved T cells produced IFN-γ in response to α-GC and PGPC.

The analysis of IFN-γ secreting cells found that T cells are the main group of cells in secreting IFN-γ (Figure 20 c) in both α-GC and PGPC groups.

To prove the existence of PGPC reacting T cells *in vivo*, we investigated the PGPC-loaded mCD1d tetramer stained with both ApoE-/- and WT mice spleen cells. Previous studies have demonstrated that the specific ligands recognized by CD1d can be analyzed by applying ligand-loaded CD1d tetramer staining (96, 97). Our results showed that the PGPC-loaded mCD1d tetramer binds CD3+ cells. Also, our data suggest that PGPC reacted T cells exist in murine spleen cells. Since there is no significant difference in the percentage of PGPC reacted T cells between ApoE-/- and WT spleen cells, I therefore postulate that endogenous PGPC-loaded T cells may exist in ApoE-/- spleen cells, but they were not detected by our exogenous PGPC loaded method.

Furthermore, we characterized the receptor of this group of T cells. It is consistent with previous murine studies in which the universal recognition of lipids occurs through Vα14, Jα281 NKT cells (98). It has been found that phospholipids can stimulate the regulatory function of human Vα24β11 NKT cells (99), a group of autoreactive T cells homologous to mouse Vα14, Jα281 NKT cells.

We investigated the activation of T cells by PGPC in a murine system. We also demonstrated the presence of PGPC-reacting T cells in blood samples from atherosclerotic patients in which further studies will be conducted. However, our investigation did not study the process of PGPC in cells and exact presentation of PGPC by CD1d. Barral's study showed that CD169(+) macrophages can internalize

and present lipid antigens to NKT cells in CD1d-dependent manner (100). However, little information is available describing how this process occurs in CD1d-positive antigen presented to PGPC in cells. We found the PGPC responder T cells were Vα14, Jα281 NKT cells. Nonetheless, we cannot rule out that other populations of T cells may be involved in PGPC activation.

3. CD1d expression and impact on heart injured by hyperlipdemia

3.1 CD1d-mediated NF-κB signaling

In the db/db mouse model, there is noticeably different lipid profile measured in the blood compared to WTC57BL/6J. The lipid components are consisting of LDL, VLDL, triglyceride, cholesterol and HDL. As anticipated there were increased LDL, VLDL, triglyceride, and cholesterol in db/db peripheral blood in contrast to WT peripheral blood. Triglyceride was the highest increased group among above four lipid groups. The increased lipid level is critical factor causing atherosclerosis. Although no atherosclerosis plaques were noticed in observed db/db samples, the high triglyceride level implicated the high risk of atherogenesis in this mouse model. Since no obvious atherosclerotic plaque was observed, no oxLDL was able to be detected locally like in aorta.

The induction of CD1d by lipids was detected, which is similar to inducing CD1d in lipids treated PBMCs. In mouse spleen is the main organ holding many types of immune cells including CD1d expression cells and CD1d responder cells. Considering high levels of LDL in db/db peripheral blood, the speculation that CD1d

can be induced in spleen in this type of mouse was tested. In 2-months-old, higher expression (56.9± 2.3%, n=2) was detected compared to WT mice (42.8± 5.8%, n=2) by FACS. There was a 1.34 fold increase in CD1 mRNA expression in db/db spleen cells after being normalized with GAPDH. The FACS result is similar to RT-PCR result and both indicated the possible induction of CD1d by high LDL as detected in db/db peripheral blood. FACS only detected the CD1d protein expressed on cell surface, which may partially explain the less detected CD1d compared to total CD1d mRNA. In 12-month-old mice this tendency was not observed. The reduced expression of CD1d in older mice may implicate that CD1d expression can be reduced after long exposure to hyperlipidmia, a characteristic of db/db mice. Type 2 diabetes is considered as a chronic inflammatory disease with circulating proinflammatory factors like TNFα and interleukin-1 (IL-1). It has been reported that the population of NKT cells was reduced in high fat fed mice (Miyazaki et al). Therefore, the exposure to the high fat environment may lead to suppressed CD1d and further NKT cells consequently. This reduces CD1d and suppressed NKT cell expression, likely results in chronic inflammation, which can re-affect the inflammation development.

3.2 CD1d induced inflammation in atherosclerosis and NF-κB activation

Db/db mice showed significant larger fatty liver and lipid accumulation in hearts compared with C57BL/6J mice. In the db/db mice, there was no apparent cardiac hypertrophy or fibrosis observed compared with C57BL/6J mice. Immunofluorescence staining for sarcomeric markers such as α-sarcomeric actinin (a

crucial Z-disc protein that cross-links sarcomeric actin) revealed sarcomeric integrity with the absence of cardiac anomalies including loss of muscle striation or pathological myofibre disarray in the diabetic hearts (Madonna Rosalinda, Hanjing Wu, Yong-jiang Geng. Cardiac expression and activation of NF-kB in association with enhanced spleen inflammation in mice with obesity and diabetes, in preparation). With previous findings that TNFα can be secreted by activated CD1d-restricted T cells originating from the spleen, further inflammatory effects from the spleen was detected. There was 6 folds of increased TNFα expression in db/db spleen cells compared to WT spleen cells. Moreover, in correspondence to the increased TNFα expression in spleen, there was a 4.89 folds of increased TNFα receptor1 mRNA in db/db heart compared to WT. TNFα receptor1 is the main TNFα receptor in the murine heart. Accordingly, elevated TNFα receptor1 is most likely the consequence of increased TNFα in spleen. Hence the heart changes that occurred in db/db mice are more likely from the Para-endocrine factors from the spleen.

As nuclear NF-κB was found activated and increased in the heart of db/db mice compared to WT (Madonna Rosalinda, Hanjing Wu, Yong-jiang Geng. Cardiac expression and activation of NF-κB in association with enhanced spleen inflammation in mice with obesity and diabetes, in preparation), TNFα is considered as a factor contributing to an upstream signal. There are several pathways that can activate NF-κB. My observation indicated possible activation from spleen. Due to limited inflammation observed in the heart, the outer inflammatory stimulator is highly possible. The inflammatory effect from the spleen can not exclude other factors

contributing to the production of NF-κB in the heart. More studies including human studies are needed to examine this inflammatory effect.

In summary, we identified a new self-antigen that can activate murine spleen T cells. Our current data support the idea that PGPC acts as an antigen in the activation of CD1d-restricted T cells. Considering the existence of an elevated PGPC level in atherosclerotic plaques, we suggest that PGPC mainly acts as an autoantigen, capable of activating the CD1d-restricted T cells involved in atherosclerosis. It indicates the autoimmune responses in atherosclerosis. On the other hand, in a high lipid environment the CD1d-restricted T cells produces inflammation in the spleen and can further affect heart function by activation of the NF-kB pathway. Hence, CD1d-restricted T cell responses to autolipid antigen and mediated inflammatory signal may represent a new molecular pathway that triggers cardiovascular tissue injury in atherosclerosis and hyperlipidemia.

Reference

1. Shih, P. T., M. J. Elices, Z. T. Fang, T. P. Ugarova, D. Strahl, M. C. Territo, J. S. Frank, N. L. Kovach, C. Cabanas, J. A. Berliner, and D. K. Vora. 1999. Minimally modified low-density lipoprotein induces monocyte adhesion to endothelial connecting segment-1 by activating beta1 integrin. J Clin Invest 103:613-625.

2. Stemme, S., B. Faber, J. Holm, O. Wiklund, J. L. Witztum, and G. K. Hansson. 1995. T lymphocytes from human atherosclerotic plaques recognize oxidized low density lipoprotein. Proc Natl Acad Sci U S A 92:3893-3897.

3. Zhou, X., A. K. Robertson, C. Hjerpe, and G. K. Hansson. 2006. Adoptive transfer of CD4+ T cells reactive to modified low-density lipoprotein aggravates atherosclerosis. Arterioscler Thromb Vasc Biol 26:864-870.

4. Binder, C. J., S. Horkko, A. Dewan, M. K. Chang, E. P. Kieu, C. S. Goodyear, P. X. Shaw, W. Palinski, J. L. Witztum, and G. J. Silverman. 2003. Pneumococcal vaccination decreases atherosclerotic lesion formation: molecular mimicry between Streptococcus pneumoniae and oxidized LDL. Nat Med 9:736-743.

5. George, J., Y. Shoenfeld, A. Afek, B. Gilburd, P. Keren, A. Shaish, J. Kopolovic, G. Wick, and D. Harats. 1999. Enhanced fatty streak formation in C57BL/6JJ mice by immunization with heat shock protein-65. Arterioscler Thromb Vasc Biol 19:505-510.

6. Wu, R., S. Nityanand, L. Berglund, H. Lithell, G. Holm, and A. K. Lefvert.

1997. Antibodies against cardiolipin and oxidatively modified LDL in 50-year-old men predict myocardial infarction. Arterioscler Thromb Vasc Biol 17:3159-3163.

7. Robertson, A. K., and G. K. Hansson. 2006. T cells in atherogenesis: for better or for worse? Arterioscler Thromb Vasc Biol 26:2421-2432.

8. Mallat, Z., S. Taleb, H. Ait-Oufella, and A. Tedgui. 2009. The role of adaptive T cell immunity in atherosclerosis. J Lipid Res 50 Suppl:S364-369.

9. Park, S. H., and A. Bendelac. 2000. CD1-restricted T-cell responses and microbial infection. Nature 406:788-792.

10. Angenieux, C., J. Salamero, D. Fricker, J. P. Cazenave, B. Goud, D. Hanau, and H. de La Salle. 2000. Characterization of CD1e, a third type of CD1 molecule expressed in dendritic cells. J Biol Chem 275:37757-37764.

11. Martin, L. H., F. Calabi, and C. Milstein. 1986. Isolation of CD1 genes: a family of major histocompatibility complex-related differentiation antigens. Proc Natl Acad Sci U S A 83:9154-9158.

12. Blumberg, R. S., D. Gerdes, A. Chott, S. A. Porcelli, and S. P. Balk. 1995. Structure and function of the CD1 family of MHC-like cell surface proteins. Immunol Rev 147:5-29.

13. Dascher, C. C., and M. B. Brenner. 2003. Evolutionary constraints on CD1 structure: insights from comparative genomic analysis. Trends Immunol 24:412-418.

14. Moody, D. B., D. M. Zajonc, and I. A. Wilson. 2005. Anatomy of CD1-lipid

antigen complexes. Nat Rev Immunol 5:387-399.

15. Shamshiev, A., H. J. Gober, A. Donda, Z. Mazorra, L. Mori, and G. De Libero. 2002. Presentation of the same glycolipid by different CD1 molecules. J Exp Med 195:1013-1021.

16. Moody, D. B., D. C. Young, T. Y. Cheng, J. P. Rosat, C. Roura-Mir, P. B. O'Connor, D. M. Zajonc, A. Walz, M. J. Miller, S. B. Levery, I. A. Wilson, C. E. Costello, and M. B. Brenner. 2004. T cell activation by lipopeptide antigens. Science 303:527-531.

17. Gadola, S. D., M. Koch, J. Marles-Wright, N. M. Lissin, D. Shepherd, G. Matulis, K. Harlos, P. M. Villiger, D. I. Stuart, B. K. Jakobsen, V. Cerundolo, and E. Y. Jones. 2006. Structure and binding kinetics of three different human CD1d-alpha-galactosylceramide-specific T cell receptors. J Exp Med 203:699-710.

18. Koch, M., V. S. Stronge, D. Shepherd, S. D. Gadola, B. Mathew, G. Ritter, A. R. Fersht, G. S. Besra, R. R. Schmidt, E. Y. Jones, and V. Cerundolo. 2005. The crystal structure of human CD1d with and without alpha-galactosylceramide. Nat Immunol 6:819-826.

19. Giabbai, B., S. Sidobre, M. D. Crispin, Y. Sanchez-Ruiz, A. Bachi, M. Kronenberg, I. A. Wilson, and M. Degano. 2005. Crystal structure of mouse CD1d bound to the self ligand phosphatidylcholine: a molecular basis for NKT cell activation. J Immunol 175:977-984.

20. Wu, D., G. W. Xing, M. A. Poles, A. Horowitz, Y. Kinjo, B. Sullivan, V.

Bodmer-Narkevitch, O. Plettenburg, M. Kronenberg, M. Tsuji, D. D. Ho, and C. H. Wong. 2005. Bacterial glycolipids and analogs as antigens for CD1d-restricted NKT cells. Proc Natl Acad Sci U S A 102:1351-1356.

21. Zajonc, D. M., I. Maricic, D. Wu, R. Halder, K. Roy, C. H. Wong, V. Kumar, and I. A. Wilson. 2005. Structural basis for CD1d presentation of a sulfatide derived from myelin and its implications for autoimmunity. J Exp Med 202:1517-1526.

22. Small, T. N., R. W. Knowles, C. Keever, N. A. Kernan, N. Collins, R. J. O'Reilly, B. Dupont, and N. Flomenberg. 1987. M241 (CD1) expression on B lymphocytes. J Immunol 138:2864-2868.

23. Plebani, A., A. R. Proserpio, D. Guarneri, M. Buscaglia, and G. Cattoretti. 1993. B and T lymphocyte subsets in fetal and cord blood: age-related modulation of CD1c expression. Biol Neonate 63:1-7.

24. Sieling, P. A., D. Jullien, M. Dahlem, T. F. Tedder, T. H. Rea, R. L. Modlin, and S. A. Porcelli. 1999. CD1 expression by dendritic cells in human leprosy lesions: correlation with effective host immunity. J Immunol 162:1851-1858.

25. Melian, A., Y. J. Geng, G. K. Sukhova, P. Libby, and S. A. Porcelli. 1999. CD1 expression in human atherosclerosis. A potential mechanism for T cell activation by foam cells. Am J Pathol 155:775-786.

26. Fivenson, D. P., and B. J. Nickoloff. 1995. Distinctive dendritic cell subsets expressing factor XIIIa, CD1a, CD1b and CD1c in mycosis fungoides and psoriasis. J Cutan Pathol 22:223-228.

27. Bell, D., P. Chomarat, D. Broyles, G. Netto, G. M. Harb, S. Lebecque, J. Valladeau, J. Davoust, K. A. Palucka, and J. Banchereau. 1999. In breast carcinoma tissue, immature dendritic cells reside within the tumor, whereas mature dendritic cells are located in peritumoral areas. J Exp Med 190:1417-1426.

28. Iwamoto, M., H. Shinohara, A. Miyamoto, M. Okuzawa, H. Mabuchi, T. Nohara, G. Gon, M. Toyoda, and N. Tanigawa. 2003. Prognostic value of tumor-infiltrating dendritic cells expressing CD83 in human breast carcinomas. Int J Cancer 104:92-97.

29. Zheng, Z., S. Venkatapathy, G. Rao, and C. A. Harrington. 2002. Expression profiling of B cell chronic lymphocytic leukemia suggests deficient CD1-mediated immunity, polarized cytokine response, altered adhesion and increased intracellular protein transport and processing of leukemic cells. Leukemia 16:2429-2437.

30. Canchis, P. W., A. K. Bhan, S. B. Landau, L. Yang, S. P. Balk, and R. S. Blumberg. 1993. Tissue distribution of the non-polymorphic major histocompatibility complex class I-like molecule, CD1d. Immunology 80:561-565.

31. Blumberg, R. S., C. Terhorst, P. Bleicher, F. V. McDermott, C. H. Allan, S. B. Landau, J. S. Trier, and S. P. Balk. 1991. Expression of a nonpolymorphic MHC class I-like molecule, CD1D, by human intestinal epithelial cells. J Immunol 147:2518-2524.

32. Roark, J. H., S. H. Park, J. Jayawardena, U. Kavita, M. Shannon, and A. Bendelac. 1998. CD1.1 expression by mouse antigen-presenting cells and marginal zone B cells. J Immunol 160:3121-3127.

33. Tsuneyama, K., M. Yasoshima, K. Harada, K. Hiramatsu, M. E. Gershwin, and Y. Nakanuma. 1998. Increased CD1d expression on small bile duct epithelium and epithelioid granuloma in livers in primary biliary cirrhosis. Hepatology 28:620-623.

34. Durante-Mangoni, E., R. Wang, A. Shaulov, Q. He, I. Nasser, N. Afdhal, M. J. Koziel, and M. A. Exley. 2004. Hepatic CD1d expression in hepatitis C virus infection and recognition by resident proinflammatory CD1d-reactive T cells. J Immunol 173:2159-2166.

35. Metelitsa, L. S., K. I. Weinberg, P. D. Emanuel, and R. C. Seeger. 2003. Expression of CD1d by myelomonocytic leukemias provides a target for cytotoxic NKT cells. Leukemia 17:1068-1077.

36. Takahashi, T., K. Haraguchi, S. Chiba, M. Yasukawa, Y. Shibata, and H. Hirai. 2003. Valpha24+ natural killer T-cell responses against T-acute lymphoblastic leukaemia cells: implications for immunotherapy. Br J Haematol 122:231-239.

37. Koseki, H., K. Imai, F. Nakayama, T. Sado, K. Moriwaki, and M. Taniguchi. 1990. Homogenous junctional sequence of the V14+ T-cell antigen receptor alpha chain expanded in unprimed mice. Proc Natl Acad Sci U S A 87:5248-5252.

38. Bendelac, A., O. Lantz, M. E. Quimby, J. W. Yewdell, J. R. Bennink, and R. R.

Brutkiewicz. 1995. CD1 recognition by mouse NK1+ T lymphocytes. Science 268:863-865.

39. Brossay, L., M. Chioda, N. Burdin, Y. Koezuka, G. Casorati, P. Dellabona, and M. Kronenberg. 1998. CD1d-mediated recognition of an alpha-galactosylceramide by natural killer T cells is highly conserved through mammalian evolution. J Exp Med 188:1521-1528.

40. Chiu, Y. H., J. Jayawardena, A. Weiss, D. Lee, S. H. Park, A. Dautry-Varsat, and A. Bendelac. 1999. Distinct subsets of CD1d-restricted T cells recognize self-antigens loaded in different cellular compartments. J Exp Med 189:103-110.

41. Nishikawa, H., T. Kato, I. Tawara, T. Takemitsu, K. Saito, L. Wang, Y. Ikarashi, H. Wakasugi, T. Nakayama, M. Taniguchi, K. Kuribayashi, L. J. Old, and H. Shiku. 2005. Accelerated chemically induced tumor development mediated by CD4+CD25+ regulatory T cells in wild-type hosts. Proc Natl Acad Sci U S A 102:9253-9257.

42. Gumperz, J. E. 2006. The ins and outs of CD1 molecules: bringing lipids under immunological surveillance. Traffic 7:2-13.

43. Kinjo, Y., D. Wu, G. Kim, G. W. Xing, M. A. Poles, D. D. Ho, M. Tsuji, K. Kawahara, C. H. Wong, and M. Kronenberg. 2005. Recognition of bacterial glycosphingolipids by natural killer T cells. Nature 434:520-525.

44. Mattner, J., K. L. Debord, N. Ismail, R. D. Goff, C. Cantu, 3rd, D. Zhou, P. Saint-Mezard, V. Wang, Y. Gao, N. Yin, K. Hoebe, O. Schneewind, D. Walker,

B. Beutler, L. Teyton, P. B. Savage, and A. Bendelac. 2005. Exogenous and endogenous glycolipid antigens activate NKT cells during microbial infections. Nature 434:525-529.

45. Amprey, J. L., J. S. Im, S. J. Turco, H. W. Murray, P. A. Illarionov, G. S. Besra, S. A. Porcelli, and G. F. Spath. 2004. A subset of liver NK T cells is activated during Leishmania donovani infection by CD1d-bound lipophosphoglycan. J Exp Med 200:895-904.

46. Fischer, K., E. Scotet, M. Niemeyer, H. Koebernick, J. Zerrahn, S. Maillet, R. Hurwitz, M. Kursar, M. Bonneville, S. H. Kaufmann, and U. E. Schaible. 2004. Mycobacterial phosphatidylinositol mannoside is a natural antigen for CD1d-restricted T cells. Proc Natl Acad Sci U S A 101:10685-10690.

47. Gumperz, J. E., C. Roy, A. Makowska, D. Lum, M. Sugita, T. Podrebarac, Y. Koezuka, S. A. Porcelli, S. Cardell, M. B. Brenner, and S. M. Behar. 2000. Murine CD1d-restricted T cell recognition of cellular lipids. Immunity 12:211-221.

48. Skold, M., X. Xiong, P. A. Illarionov, G. S. Besra, and S. M. Behar. 2005. Interplay of cytokines and microbial signals in regulation of CD1d expression and NKT cell activation. J Immunol 175:3584-3593.

49. Watson, A. D., N. Leitinger, M. Navab, K. F. Faull, S. Horkko, J. L. Witztum, W. Palinski, D. Schwenke, R. G. Salomon, W. Sha, G. Subbanagounder, A. M. Fogelman, and J. A. Berliner. 1997. Structural identification by mass spectrometry of oxidized phospholipids in minimally oxidized low density

lipoprotein that induce monocyte/endothelial interactions and evidence for their presence in vivo. J Biol Chem 272:13597-13607.

50. Chang, M. K., C. J. Binder, Y. I. Miller, G. Subbanagounder, G. J. Silverman, J. A. Berliner, and J. L. Witztum. 2004. Apoptotic cells with oxidation-specific epitopes are immunogenic and proinflammatory. J Exp Med 200:1359-1370.

51. Kar, N. S., M. Z. Ashraf, M. Valiyaveettil, and E. A. Podrez. 2008. Mapping and characterization of the binding site for specific oxidized phospholipids and oxidized low density lipoprotein of scavenger receptor CD36. J Biol Chem 283:8765-8771.

52. Podrez, E. A., E. Poliakov, Z. Shen, R. Zhang, Y. Deng, M. Sun, P. J. Finton, L. Shan, B. Gugiu, P. L. Fox, H. F. Hoff, R. G. Salomon, and S. L. Hazen. 2002. Identification of a novel family of oxidized phospholipids that serve as ligands for the macrophage scavenger receptor CD36. J Biol Chem 277:38503-38516.

53. Podrez, E. A., T. V. Byzova, M. Febbraio, R. G. Salomon, Y. Ma, M. Valiyaveettil, E. Poliakov, M. Sun, P. J. Finton, B. R. Curtis, J. Chen, R. Zhang, R. L. Silverstein, and S. L. Hazen. 2007. Platelet CD36 links hyperlipidemia, oxidant stress and a prothrombotic phenotype. Nat Med 13:1086-1095.

54. Parhami, F., Z. T. Fang, B. Yang, A. M. Fogelman, and J. A. Berliner. 1995. Stimulation of Gs and inhibition of Gi protein functions by minimally oxidized LDL. Arterioscler Thromb Vasc Biol 15:2019-2024.

55. Kabarowski, J. H., K. Zhu, L. Q. Le, O. N. Witte, and Y. Xu. 2001. Lysophosphatidylcholine as a ligand for the immunoregulatory receptor G2A.

Science 293:702-705.

56. Obinata, H., T. Hattori, S. Nakane, K. Tatei, and T. Izumi. 2005. Identification of 9-hydroxyoctadecadienoic acid and other oxidized free fatty acids as ligands of the G protein-coupled receptor G2A. J Biol Chem 280:40676-40683.

57. Li, R., K. P. Mouillesseaux, D. Montoya, D. Cruz, N. Gharavi, M. Dun, L. Koroniak, and J. A. Berliner. 2006. Identification of prostaglandin E2 receptor subtype 2 as a receptor activated by OxPAPC. Circ Res 98:642-650.

58. Xu, X. H., P. K. Shah, E. Faure, O. Equils, L. Thomas, M. C. Fishbein, D. Luthringer, X. P. Xu, T. B. Rajavashisth, J. Yano, S. Kaul, and M. Arditi. 2001. Toll-like receptor-4 is expressed by macrophages in murine and human lipid-rich atherosclerotic plaques and upregulated by oxidized LDL. Circulation 104:3103-3108.

59. Leitinger, N. 2003. Oxidized phospholipids as modulators of inflammation in atherosclerosis. Curr Opin Lipidol 14:421-430.

60. Walton, K. A., X. Hsieh, N. Gharavi, S. Wang, G. Wang, M. Yeh, A. L. Cole, and J. A. Berliner. 2003. Receptors involved in the oxidized 1-palmitoyl-2-arachidonoyl-sn-glycero-3-phosphorylcholine-mediated synthesis of interleukin-8. A role for Toll-like receptor 4 and a glycosylphosphatidylinositol-anchored protein. J Biol Chem 278:29661-29666.

61. Delerive, P., C. Furman, E. Teissier, J. Fruchart, P. Duriez, and B. Staels. 2000.

Oxidized phospholipids activate PPARalpha in a phospholipase A2-dependent manner. FEBS Lett 471:34-38.

62. Berliner, J. A., and A. D. Watson. 2005. A role for oxidized phospholipids in atherosclerosis. N Engl J Med 353:9-11.

63. Lee, H., W. Shi, P. Tontonoz, S. Wang, G. Subbanagounder, C. C. Hedrick, S. Hama, C. Borromeo, R. M. Evans, J. A. Berliner, and L. Nagy. 2000. Role for peroxisome proliferator-activated receptor alpha in oxidized phospholipid-induced synthesis of monocyte chemotactic protein-1 and interleukin-8 by endothelial cells. Circ Res 87:516-521.

64. Huber, J., A. Furnkranz, V. N. Bochkov, M. K. Patricia, H. Lee, C. C. Hedrick, J. A. Berliner, B. R. Binder, and N. Leitinger. 2006. Specific monocyte adhesion to endothelial cells induced by oxidized phospholipids involves activation of cPLA2 and lipoxygenase. J Lipid Res 47:1054-1062.

65. Bochkov, V. N. 2007. Inflammatory profile of oxidized phospholipids. Thromb Haemost 97:348-354.

66. Mestas, J., and K. Ley. 2008. Monocyte-endothelial cell interactions in the development of atherosclerosis. Trends Cardiovasc Med 18:228-232.

67. Plutzky, J. 2003. The vascular biology of atherosclerosis. Am J Med 115 Suppl 8A:55S-61S.

68. Carmeliet, P., L. Moons, and D. Collen. 1998. Mouse models of angiogenesis, arterial stenosis, atherosclerosis and hemostasis. Cardiovasc Res 39:8-33.

69. Hulten, L. M., H. Lindmark, U. Diczfalusy, I. Bjorkhem, M. Ottosson, Y. Liu,

G. Bondjers, and O. Wiklund. 1996. Oxysterols present in atherosclerotic tissue decrease the expression of lipoprotein lipase messenger RNA in human monocyte-derived macrophages. J Clin Invest 97:461-468.

70. Waddington, E., K. Sienuarine, I. Puddey, and K. Croft. 2001. Identification and quantitation of unique fatty acid oxidation products in human atherosclerotic plaque using high-performance liquid chromatography. Anal Biochem 292:234-244.

71. Berliner, J. 2002. Introduction. Lipid oxidation products and atherosclerosis. Vascul Pharmacol 38:187-191.

72. Dougan, S. K., A. Kaser, and R. S. Blumberg. 2007. CD1 expression on antigen-presenting cells. Curr Top Microbiol Immunol 314:113-141.

73. Terabe, M., J. Swann, E. Ambrosino, P. Sinha, S. Takaku, Y. Hayakawa, D. I. Godfrey, S. Ostrand-Rosenberg, M. J. Smyth, and J. A. Berzofsky. 2005. A nonclassical non-Valpha14Jalpha18 CD1d-restricted (type II) NKT cell is sufficient for down-regulation of tumor immunosurveillance. J Exp Med 202:1627-1633.

74. Beckman, E. M., S. A. Porcelli, C. T. Morita, S. M. Behar, S. T. Furlong, and M. B. Brenner. 1994. Recognition of a lipid antigen by CD1-restricted alpha beta+ T cells. Nature 372:691-694.

75. Thomssen, H., J. Ivanyi, C. Espitia, A. Arya, and M. Londei. 1995. Human CD4-CD8- alpha beta + T-cell receptor T cells recognize different mycobacteria strains in the context of CD1b. Immunology 85:33-40.

76. Tupin, E., A. Nicoletti, R. Elhage, M. Rudling, H. G. Ljunggren, G. K. Hansson, and G. P. Berne. 2004. CD1d-dependent activation of NKT cells aggravates atherosclerosis. J Exp Med 199:417-422.

77. Nakai, Y., K. Iwabuchi, S. Fujii, N. Ishimori, N. Dashtsoodol, K. Watano, T. Mishima, C. Iwabuchi, S. Tanaka, J. S. Bezbradica, T. Nakayama, M. Taniguchi, S. Miyake, T. Yamamura, A. Kitabatake, S. Joyce, L. Van Kaer, and K. Onoe. 2004. Natural killer T cells accelerate atherogenesis in mice. Blood 104:2051-2059.

78. Aslanian, A. M., H. A. Chapman, and I. F. Charo. 2005. Transient role for CD1d-restricted natural killer T cells in the formation of atherosclerotic lesions. Arterioscler Thromb Vasc Biol 25:628-632.

79. Wendt, T., L. Bucciarelli, W. Qu, Y. Lu, S. F. Yan, D. M. Stern, and A. M. Schmidt. 2002. Receptor for advanced glycation endproducts (RAGE) and vascular inflammation: insights into the pathogenesis of macrovascular complications in diabetes. Curr Atheroscler Rep 4:228-237.

80. Eckel, R. H., M. Wassef, A. Chait, B. Sobel, E. Barrett, G. King, M. Lopes-Virella, J. Reusch, N. Ruderman, G. Steiner, and H. Vlassara. 2002. Prevention Conference VI: Diabetes and Cardiovascular Disease: Writing Group II: pathogenesis of atherosclerosis in diabetes. Circulation 105:e138-143.

81. Carmena, R. 2005. Type 2 diabetes, dyslipidemia, and vascular risk: rationale and evidence for correcting the lipid imbalance. Am Heart J 150:859-870.

82. Ginsberg, H. N., and L. S. Huang. 2000. The insulin resistance syndrome: impact on lipoprotein metabolism and atherothrombosis. J Cardiovasc Risk 7:325-331.

83. Goldstein, B. J. 2002. Insulin resistance as the core defect in type 2 diabetes mellitus. Am J Cardiol 90:3G-10G.

84. Brand, K., S. Page, G. Rogler, A. Bartsch, R. Brandl, R. Knuechel, M. Page, C. Kaltschmidt, P. A. Baeuerle, and D. Neumeier. 1996. Activated transcription factor nuclear factor-kappa B is present in the atherosclerotic lesion. J Clin Invest 97:1715-1722.

85. Hajra, L., A. I. Evans, M. Chen, S. J. Hyduk, T. Collins, and M. I. Cybulsky. 2000. The NF-kappa B signal transduction pathway in aortic endothelial cells is primed for activation in regions predisposed to atherosclerotic lesion formation. Proc Natl Acad Sci U S A 97:9052-9057.

86. De Palma, R., and J. Gorski. 1995. Restricted and conserved T-cell repertoires involved in allorecognition of class II major histocompatibility complex. Proc Natl Acad Sci U S A 92:8836-8840.

87. Greenspan, P., E. P. Mayer, and S. D. Fowler. 1985. Nile Red: a selective fluorescent stain for intracellular lipid droplets. J Cell Biol 100:965-973.

88. Honda, H. M., N. Leitinger, M. Frankel, J. I. Goldhaber, R. Natarajan, J. L. Nadler, J. N. Weiss, and J. A. Berliner. 1999. Induction of monocyte binding to endothelial cells by MM-LDL: role of lipoxygenase metabolites. Arterioscler Thromb Vasc Biol 19:680-686.

89. Rogers, L., S. Burchat, J. Gage, M. Hasu, M. Thabet, L. Willcox, T. A. Ramsamy, and S. C. Whitman. 2008. Deficiency of invariant V alpha 14 natural killer T cells decreases atherosclerosis in LDL receptor null mice. Cardiovasc Res 78:167-174.

90. Pidkovka, N. A., O. A. Cherepanova, T. Yoshida, M. R. Alexander, R. A. Deaton, J. A. Thomas, N. Leitinger, and G. K. Owens. 2007. Oxidized phospholipids induce phenotypic switching of vascular smooth muscle cells in vivo and in vitro. Circ Res 101:792-801.

91. Subbanagounder, G., J. W. Wong, H. Lee, K. F. Faull, E. Miller, J. L. Witztum, and J. A. Berliner. 2002. Epoxyisoprostane and epoxycyclopentenone phospholipids regulate monocyte chemotactic protein-1 and interleukin-8 synthesis. Formation of these oxidized phospholipids in response to interleukin-1beta. J Biol Chem 277:7271-7281.

92. De Libero, G., and L. Mori. 2007. Structure and biology of self lipid antigens. Curr Top Microbiol Immunol 314:51-72.

93. Yeh, M., N. Leitinger, R. de Martin, N. Onai, K. Matsushima, D. K. Vora, J. A. Berliner, and S. T. Reddy. 2001. Increased transcription of IL-8 in endothelial cells is differentially regulated by TNF-alpha and oxidized phospholipids. Arterioscler Thromb Vasc Biol 21:1585-1591.

94. Kyriakakis, E., M. Cavallari, J. Andert, M. Philippova, C. Koella, V. Bochkov, P. Erne, S. B. Wilson, L. Mori, B. C. Biedermann, T. J. Resink, and G. De Libero. Invariant natural killer T cells: linking inflammation and

neovascularization in human atherosclerosis. Eur J Immunol 40:3268-3279.

95. Chiappori, F., I. Merelli, L. Milanesi, and E. Rovida. Exploring the role of the phospholipid ligand in endothelial protein C receptor: a molecular dynamics study. Proteins 78:2679-2690.

96. Benlagha, K., A. Weiss, A. Beavis, L. Teyton, and A. Bendelac. 2000. In vivo identification of glycolipid antigen-specific T cells using fluorescent CD1d tetramers. J Exp Med 191:1895-1903.

97. Matsuda, J. L., O. V. Naidenko, L. Gapin, T. Nakayama, M. Taniguchi, C. R. Wang, Y. Koezuka, and M. Kronenberg. 2000. Tracking the response of natural killer T cells to a glycolipid antigen using CD1d tetramers. J Exp Med 192:741-754.

98. Kawano, T., J. Cui, Y. Koezuka, I. Toura, Y. Kaneko, K. Motoki, H. Ueno, R. Nakagawa, H. Sato, E. Kondo, H. Koseki, and M. Taniguchi. 1997. CD1d-restricted and TCR-mediated activation of valpha14 NKT cells by glycosylceramides. Science 278:1626-1629.

99. Rauch, J., J. Gumperz, C. Robinson, M. Skold, C. Roy, D. C. Young, M. Lafleur, D. B. Moody, M. B. Brenner, C. E. Costello, and S. M. Behar. 2003. Structural features of the acyl chain determine self-phospholipid antigen recognition by a CD1d-restricted invariant NKT (iNKT) cell. J Biol Chem 278:47508-47515.

100. Barral, P., P. Polzella, A. Bruckbauer, N. van Rooijen, G. S. Besra, V. Cerundolo, and F. D. Batista. CD169(+) macrophages present lipid antigens to

mediate early activation of iNKT cells in lymph nodes. Nat Immunol 11:303-312.

Vita

[redacted]

At the author’s request, and with the approval of the graduating institution, the Acknowledgements and Vita sections of this dissertation have been redacted to protect the author’s privacy.